Chromosome dynamics and genomic instablity in neuroblastoma. Three genomic pillars: MYCN amplification, numerical and structural changes.

Lundberg, Gisela

2012

Chromosome dynamics and genomic instability in Neuroblastoma

Three genomic pillars; MYCN, numerical and structural changes

LUND
UNIVERSITY

Gisela Lundberg

AKADEMISK AVHANDLING

som med vederbörligt tillstånd av Medicinska fakulteten för avläggande av doktorsexamen i ämnet Laboratoriemedicin med inriktning klinisk genetik kommer att offentligen försvaras i Segerfalkssalen Biomedicinskt Centrum, Lund, torsdagen den 16 maj 2011, kl. 09.00.

Fakultetsopponent:

Michael D. Hogarty

MD, Associate Professor

Division of Oncology/Children's Hospital of Philadelphia, USA

Organization	Document name
LUND UNIVERSITY Department Of Clinical Genetics Lund University Hospital SE-221 85 Lund	DOCTORAL DISSERTATION Date of issue 2012-11-15
Author(s) Gisela Lundberg	Sponsoring organization The Swedish Children's Cancer Foundation, the Swedish Cancer Society, the Swedish Research Council, the Swedish Medical Society, the Lund University Hospital Donation Funds, the Gunnar Nilsson Cancer Foundation, the Crafoord Foundation, the Erik-Philip Sörensen Foundation, the Lundgren Foundation, the Schyberg Foundation and the Medical Faculty at Lund University.

Title and subtitle

Chromosome dynamics and genomic instability in Neuroblastoma
Three genomic pillars: *MYCN* amplification, numerical and structural changes

Abstract

In this thesis, the main focus has been on the childhood cancer neuroblastoma, one of the most common and lethal childhood tumours. Neuroblastoma has througout the years continued to be a clinical and biological enigma.

Our first focus was on one of the most important biological risk factors in neuroblastoma -- amplification of the oncogene *MYCN* in the tumour cells. Because amplified *MYCN* typically reside in ring-formed chromatin structures lacking centromeres (so-called double minutes, DMs) it remained unknown for a long time how the amplified sequences were maintained in the growing tumour. We could show that *MYCN*-carrying DMs in neuroblastoma cells translocate from the nuclear interior to the periphery at the interphase-prophase transition and that they are preferentially anchored to human chromosomes at sites adjacent to the telomeres, resulting in a random segregation pattern of DMs to post-mitotic neuroblastoma cells. Furthermore, by making human/murine hybrids we showed that DMs do not bind to specific positional elements in human chromosomes. Our data explain the vast intercellular variety of *MYCN* copy number in neuroblastoma.

Moving on from here, in our next study we found that telomeres without detectable TTAGGG-repeats were associated with *MYCN* amplification and the generation of chromosomal breakage-fusion bridge cycles and could confirm that *MYCN* amplification was associated with reduced tumour telomere length *in vivo*. We also found a possible association between poor survival and elongated telomeres, which needs to be studied further.

Our third pillar was that of whole chromosome changes, with a focus on intratumoural diversity. We demonstrated a previously unreported high degree of intercellular variation in chromosome copy number and found indications that loss of chromosomes from a tetraploid state is a major route towards this prominent intra-tumour genomic diversity in aneuploid neuroblastomas.

Taken together, these studies suggest that neuroblastoma genomes are highly plastic, which may to some extent explain the poor response to oncological treatment for some of these tumours.

Key words
Neuroblastoma, *MYCN*, telomeres, chromosomal instability

Classification system and/or index terms (if any)

Supplementary bibliographical information	Language English
ISSN and key title 1652-8220	ISBN 978-91-87189-48-7
Recipient´s notes	Number of pages 134 Price Security classification

Distribution by (name and address)

Chromosome dynamics and genomic instability in neuroblastoma

Three genomic pillars: *MYCN* amplification, numerical and structural changes

Gisela Lundberg

Section of Clinical Genetics

Department of Laboratory Medicine

2012

LUND
UNIVERSITY

Faculty of Medicine Doctoral Dissertations Series 2012:85
ISBN 978-91-87189-48-7
ISSN 1652-8220

Tryckt i Sverige av Media-Tryck, Lunds universitet
Lund 2012

To my boys Leo & David

TABLE OF CONTENTS

ORIGINAL ARTICLES

This thesis is based on the following articles, which will be referred to in the text by their Roman numerals.

I. Binomial mitotic segregation of *MYCN*-carrying double minutes in neuroblastoma illustrates the role of randomness in oncogene amplification. Lundberg G, Rosengren A, Jin Y, Stewénius H, Stewénius Y, Påhlman S, Gisselsson D. *PLoS ONE* 2008, (8):e3099

II. Alternative lengthening of telomeres and enhanced chromosomal instability in aggressive non-*MYCN* amplified neuroblastomas. Lundberg G, Sehic D, Länsberg J-K, Øra I, Frigyesi A, Castel V, Navarro S, Piqueras M, Martinsson T, Noguera R, Gisselsson D. *Genes, Chromosomes and Cancer* 2011, 50:250-262

III. Intratumoural diversity of chromosome copy number in neuroblastoma mediated by on-going chromosome loss from a polyploid state. Lundberg G, Jin Y, Sehic D, Øra I, Gisselsson D. Manuscript submitted

ABBREVIATIONS

ALT	alternative lengthening of telomeres
APBs	ALT-associated PML bodies
CIN	chromosomal instability
DDR	DNA damage response
DMs	double minutes
DOPA	dihydroxyphenylalanine
HSRs	homogeneously staining regions
LDH	lactic dehydrogenase
MIBG	metaiodobenzylguanidine
NB	neuroblastoma
NSE	neuron specific enolase
PML	promyelocytic leukemia nuclear bodies
SNS	sympathetic nervous system
VMA	vanillylmandelic acid

PREFACE

Neuroblastoma (NB) is a clinically challenging childhood cancer. It is the most common solid extracranial paediatric tumour and is extremely heterogenous in its clinical and biological features. At one extreme there are tumours that regress spontaneously, and on the other extreme tumours that will not respond to any treatment and eventually kill the patient. Is it really just one disease?

The aim of this thesis was to increase our knowledge of three genomic subtypes of NB i.e. those characterized by *MYCN* amplification, structural aberrations and numerical chromosome changes, respectively.

This thesis is divided into four sections. The first is about the disease NB, which is the major topic of my three original articles. The second is about the oncogene *MYCN* which is the topic of the first article. The third is about telomeres and structural aberrations, the focus of the second article, and finally the fourth section is about numerical changes which are being dealt with in the third paper.

INTRODUCTION

Neuroblastoma

NB is the most frequently occurring extracranial solid tumour in children, with an incidence of approximately 15-20 cases per year in Sweden. [1] It is the fourth most common malignancy of childhood, preceded only by leukaemia, CNS tumours and lymphomas. Despite many advances during the past four decades, it has remained an enigmatic challenge to clinical and pre-clinical scientists. [2]

NB is an embryonal tumour thought to develop from an incompletely committed precursor cell, derived from neural-crest tissues. [3,4] With origin from the ectoderm, one of three germ layers, neural crest cells undergo extensive differentiation and migration and are the origin of a wide range of cells. Included in these are the neurons and glia cells creating the sensory, sympathetic, and parasympathetic nervous systems. These regions of neural crest can be divided into four main functional domains, of which the trunk neural crest gives rise to two populations of cells. One population is designated to become melanocytes and the second form the dorsal root ganglia, wherefrom those more ventrally form the sympathetic ganglia, adrenal medulla, and the nerves surrounding the aorta. [5] Given the evidence supporting the central importance of the neural crest, it is often considered in

addition to the ectoderm, endoderm, and mesoderm, as a fourth germ layer. [6]

NB belongs to the small, blue, round cell tumours of childhood. Other such tumours include non-Hodgkin lymphoma, primitive neuroectodermal tumours and undifferentiated soft tissue sarcoma (rhabdomyosarcoma). More than one third of cases (36%) are diagnosed in children younger than 1 year. Approximately 80 % of cases are diagnosed in children younger than 4 years, and 97% are diagnosed by age 10 years.[7] NB is mainly occurring sporadically, with only 1-2% of cases thought to be familial.[8] NB can arise anywhere along the sympathetic nervous system, with the majority occurring in the adrenal medulla. Tumour metastases to the orbit may cause ptosis and tumour extension into the spinal column may cause cord compression, with resulting paralysis. NBs typically metastasize also to regional lymph nodes and to the bone marrow. NB may in addition metastasize to the liver, particularly in patients with stage MS (metastatic disease in children younger than 18 months) tumours, in whom involvement can be extensive; however, transient and complete regression often occurs with a wait and see approach.

Most NB patients present with abdominal symptoms such as fullness and/or distension. Upon physical examination a non-tender, firm irregular abdominal mass, that crosses the midline, is often palpated. Approximately 65 % of NBs occur in the abdomen and most of these in the adrenal gland. Typically children with disseminated disease are very sick and have systemic manifestations, such as weight loss, failure to

thrive and bone pain whereas children with localized disease are asymptomatic. NB thus has diverse clinical features because of its variable sites of origin, a propensity to metastasise to many distant sites as well as, regular secretion of hormones and may present as a paraneoplastic syndrome. [9]

Many low-stage NBs are encapsulated and can be surgically excised with little risk of complications,[10,11] while high-stage tumours can infiltrate local organ structures, surround critical nerves and vessels and are often unresectable at the time of diagnosis.[12-15] Obtaining a tumour biopsy is of utmost importance, as histological evidence of a small round blue cell neuroblastic tumour with corresponding immunohistochemical features is required for diagnosis and genetic tests on biopsy material are required for risk stratification. Laboratory studies consists of general studies such as complete blood count, i.e. red/white blood cells and platelets, coagulation studies as well as specific laboratory studies such as metabolic tumour by-products (DOPA and VMA) and non-specific tumour markers such as NSE, LDH and ferritin that are useful markers during or after treatment. Imaging studies are recommended in all infants and children with abdominal masses. The standard diagnostic modalities are ultrasonography, ^{123}I-MIBG (metaiodobenzylguanidine) scan, for which a small amount of radioactive iodine (^{123}I), linked to the noradrenaline analogue MIBG, is injected and an overview of the body is visualized through scintigraphy several hours later, and CT or MRI. Bone marrow aspirates are routinely performed since it is a common site for metastasis.

The staging of NB is a delicate task and the staging systems are revised with increasing knowledge. The International neuroblastoma Stage System (INSS)[16] was an improvement of the Evans system [17] and has been the most frequently used system worldwide during the last decades. The INSS is a post- surgical staging system and is evaluated as follows:

- Stage 1: Localized tumour confined to the area of origin.
- Stage 2A: Unilateral tumour with incomplete gross resection; identifiable ipsilateral and contralateral lymph node negative for tumour.
- Stage 2B: Unilateral tumour with complete or incomplete gross resection; with ipsilateral lymph node positive for tumour; identifiable contralateral lymph node negative for tumour.
- Stage 3: Tumour infiltrating across midline with or without regional lymph node involvement; or unilateral tumour with contralateral lymph node involvement; or midline tumour with bilateral lymph node involvement.
- Stage 4: Dissemination of tumour to distant lymph nodes, bone marrow, bone, liver, or other organs except as defined by Stage 4S.
- Stage 4S: Age <1 year with localized primary tumour as defined in Stage 1 or 2A and 2B, with dissemination limited to liver, skin, or bone marrow (less than 10 % of nucleated bone marrow cells are tumour cells and a negative MIBG scan).

The INSS is not suitable for the pre-treatment risk classification and therefore the International Neuroblastoma Risk Groups' task force

(INRG)[18] has developed a new staging system more based on imaging rather than that of the extent of surgical resection:

- ❖ Stage L1: Localized tumour without image-defined risk factors, and confined to one body compartment.
- ❖ Stage L2: Localized disease with one or more image-defined risk factors.
- ❖ Stage M: Distant metastatic disease.
- ❖ Stage MS: Metastatic disease "special", where MS is equivalent to stage 4S.

The new risk stratification is based on the new INRGSS i.e. age (dichotomized at 18 months), tumour grade, *MYCN* amplification, unbalanced 11q aberration, and ploidy.

INRG Stage	Age (months)	Histologic Category	Grade of Tumor Differentiation	*MYCN*	11q Aberration	Ploidy	Pretreatment Risk Group
L1/L2		GN maturing; GNB intermixed					A Very low
L1		Any, except GN maturing or GNB intermixed		NA			B Very low
				Amp			K High
L2	< 18	Any, except GN maturing or GNB intermixed		NA	No		D Low
					Yes		G Intermediate
	≥ 18	GNB nodular; neuroblastoma	Differentiating	NA	No		E Low
					Yes		H Intermediate
			Poorly differentiated or undifferentiated	NA			
				Amp			N High
M	< 18			NA		Hyperdiploid	F Low
	< 12			NA		Diploid	I Intermediate
	12 to < 18			NA		Diploid	J Intermediate
	< 18			Amp			O High
	≥ 18						P High
MS	< 18			NA	No		C Very low
					Yes		Q High
				Amp			R High

GN-ganglioneuroma, GNB- ganglioneuroblastoma, NA-not applicable, Amp-amplified

It is well known that somatic chromosomal changes in neoplastic cells contribute to tumour development and some of these changes are of

great importance to predict prognosis. [19-26] Examples of prognostic indicators based on genetics in NB are loss of heterozygosity for chromosome arm 1p, 11q loss of heterozygosity, gain of the 17q arm and amplification of the *MYCN* oncogene. [27-31]

A significant proportion of tumours (>10%) undergo complete spontaneous regression in the absence of or with minimum therapeutic intervention.[32] The incidence of spontaneous regression in NB is between 10 and 100 times greater than that for any other human cancer, and is the disease most commonly observed in small children (< 18 months). Surgery is mainly used to manage low-grade NBs whereas at more advanced stages, treatment includes months of high dose chemotherapy, surgery, radiation therapy and is followed by autologous stem cell rescue, and in some cases immunotherapy and high doses of retinoic acid. Radiation therapy is used in the treatment of high-risk patients during the consolidation phase or as palliative care for pain reduction. Novel targeted agents are under development and some have just entered the clinic such as *ALK* inhibitors and immunotherapy with GD_2. [33,34] The survival of high-risk groups, e.g. stage 4 patients, is only approximately 30%. [35]

NB, despite many advances in the understanding of its biological diversity and developmental molecular pathways, has remained a dreadful disease in young children. At the same time, its fascinating multiplicity of clinical and biological phenotypes has attracted the attention of an ever growing number of pre-clinical and clinical scientists. It can be expected that our combined efforts inevitably will

lead to an understanding of the molecular pathways governing whether the disease will progress to malignity or regress without any interventions from the clinicians. This knowledge eventually will hopefully provide the platform from which new diagnostic tools can be developed and from which the design of patient-oriented and new types of therapies can be attempted. The ultimate goal is to more precisely assign patients to appropriate treatment with the use of an approach based on molecular genetics. [36]

MYCN

About 30 years ago, the *MYCN* gene was found to be amplified in neuroblastomas. [37,38] Amplified *MYCN* is a major prognostic factor in localised neuroblastoma and is also included in the INSS[16] as well as the INRG. [39] Amplification of *MYCN* is associated with advanced stages of disease and unfavourable biological outcome.[38,40] *MYCN* is also associated with poor outcome in otherwise favourable NB groups such as stages I–III and infants. [41-45] Therefore, the status of the *MYCN* gene is routinely determined from NB samples obtained at diagnosis to assist in therapy planning. [41,46,47] Because of the dramatic degree of *MYCN* amplification and consequent overexpression in a subset of aggressive neuroblastomas, it should be an attractive therapeutic target. [48-51] The proportion of tumours with amplified *MYCN* is about 20% whilst most established cell lines are amplified, with variations in frequency between different studies. [52]

NB karyotypes frequently reveal the cytogenetic hallmarks of gene amplification and the chromosomal localization of amplified *MYCN* as intrachromosomal in the form of homogenously staining regions (HSRs) or as episomal double minutes (DMs). [37,53] *MYCN* is situated at the p-arm of chromosome 2, but when amplified it sojourns in these DMs or HSRs. Amplification of the gene can surpass 400 copies and other genes (*ALK*, *DDX1* and *NAG*) have been found to be co-amplified with it. But *MYCN* is the only gene consistently amplified from this locus. [54]

The physiological role of the *MYCN* gene is to function as a transcription factor which in turn provides instructions for making a protein that plays an important role in the development of tissues and organs during embryogenesis. Studies in animals suggest that this protein is necessary for normal development of the limbs, heart, kidneys, nervous system, digestive system, and lungs. [55-59] *MYCN* is part of the MYC family of oncogenes.[59] It encodes multiple transcription factors that, when overexpressed, lead to deregulated growth, proliferation and apoptosis. [2,60-62]

Germline mutations or a deletion of the *MYCN* gene causes the Feingold syndrome.[63] The Feingold syndrome is characterized by a combination of congenital anomalies such as digital anomalies (shortening of the 2nd and 5th middle phalanx of the hand, clinodactyly of the 5th finger, syndactyly of toes 2-3 and/or 4-5, thumb hypoplasia), microcephaly, facial dysmorphism (short palpebral fissures and micrognathia), gastrointestinal atresias (primarily esophageal and/or duodenal), and mild to moderate learning disability.

Weiss and colleagues [64] created a transgenic mouse model of NB, with *MYCN* expression driven in adrenergic cells by the tyrosine hydroxylase promoter (TH-MYCN mouse). Genomic changes in neuroblastomas arising in TH-MYCN mice closely parallel the genomic changes found characteristically in human tumours.[65] Thus, the TH-MYCN mouse model appears to be a tractable model to study neuroblastoma development, progression and therapy.

ALK and *MYCN*

ALK is an oncogene whose mutations can be both genetic and acquired. In familial NB it has quite recently been shown that the *ALK* gene is mutated in up to 80 % of the cases. [8,66] *ALK* is a tyrosine kinase receptor important in neural differentiation, proliferation, and survival. Its role in malignant transformation is thought to arise from rearrangements of 2p23–24, the *MYCN* region, and result in essential kinase activity. *ALK* can also be mutated at so called hotspots, such as R1275Q and F1174L, in up to 12% of non-familial NBs, [67] with the latter mutation being the most common and associated with resistance to crizotinib, an *ALK*-inhibitor.[68] Co-expression of the *ALK* (F1174L) mutation and *MYCN* in mice leads to more aggressive NB with higher penetrance and increased mortality than either one does alone. [69]

Telomeres and structual chromosomal aberrations

Chromosome abnormalities can be subdivided into two different types: numerical and structural. They are not mutually exclusive and they often coexist. Numerical aberrations, aneuploidy, refer to whole chromosome changes, either having too many or too few, whilst structural abnormalities are changes that alter the content of chromosomes. Structural changes are mainly deletions, insertions, inversions and translocations. Structural abnormalities may occur spontaneously, or they may be induced by agents, such as chemicals, ionizing radiation, viral infections or a failure to protect chromosome ends.

The ends of linear chromosomes, the telomeres, consist in humans of 5'-TTAGGG-3' repeats that adopt a specific chromatin structure. The DNA at the telomeres is mostly double-stranded with a single-stranded terminal 3'-overhang of the G-rich strand. The telomere repeat sequence can fold back on itself with the G-rich tail invading the telomeric duplex DNA to form a telomere loop (t-loop).[70] This specific DNA structure is recognized by shelterin proteins, including TRF1, TRF2, POT1, RAP1, TIN2 and TPP1.[71] This nucleoprotein complex protects the chromosome end from being recognized as a DNA double-strand break (DSB) and prevents triggering a DNA damage response (DDR). Due to the end-replication problem, the ends of linear chromosomes shorten with every cell division. Upon reaching a critical telomere length, DDR factors, such as TP53, induce replicative senescence, cell

cycle arrest or apoptosis.[72] Telomeres also prevent inappropriate DNA repair reactions, such as ligation of one end to another.[73] Accordingly, the number of cell divisions should become limited, and this represents an important tumour suppressor mechanism.[73]

Cancer cells circumvent this constraint to gain an unlimited proliferation potential by acquiring a telomere maintenance mechanism.[74] In about 85% of human cancers, telomere maintenance is achieved by reactivation of telomerase, a reverse transcriptase that synthesizes telomeric repeats but is normally only active in embryonic and adult stem cells.[75] Telomerase has two essential components, the RNA component hTERC (human telomerase RNA component) and a catalytic subunit hTERT (human telomerase reverse transcriptase).[76] Some cancer types extend the telomeres in the absence of telomerase activity by the alternative lengthening of telomeres (ALT) pathway that operates via DNA repair and recombination processes.[77] Cancer cells that use the ALT pathway exhibit distinct phenotypes such as heterogeneous telomeres and specialised promyelocytic leukaemia (PML) nuclear foci called ALT-associated PML bodies (APBs). [78] APBs are unique to ALT cells as they are not present in normal or telomerase-positive cells.[79] Despite these telomere maintenance mechanisms a large number of tumours exhibit globally shortened telomeres, triggering end-to-end chromosome fusions, which in turn may cause complex structural changes through breakage-fusion-bridge cycles.[80]

Chromosomal instability and numerical changes

The association between aneuploidy and cancer is an old story. Chromosome number changes were first associated with tumours in the late 19th century. In 1890, David Hansemann examined tissue sections from epithelial tumours and discovered cells that were going through multipolar divisions as well as bipolar asymmetric divisions of chromosomes.[81] A few years later, Theodor Boveri suggested that aneuploidy, abnormal numbers of chromosomes, causes cancer. He compared defects in sea urchin embryos that had gone through multipolar divisions and proposed that a ‘‘certain abnormal chromatin constitution’’, regardless of how it originated, ‘‘would result in the origin of a malignant tumour”.[82] The consequence of chromosomal instability (CIN) is aneuploidy but the line between aneuploidy and CIN was blurred in these early studies because tools were not available to discriminate between aneuploidy (a state that describes the cellular karyotype) and CIN (increased rates of chromosome missegregation). This distinction is important because aneuploidy can arise in different ways; however, the fact that the majority of aneuploid tumours have chromosome numbers within the range of diploid cells i.e. 40–60 chromosomes indicates that the accumulation of chromosome imbalances generated by the sequential loss and gain of single chromosomes through CIN may be the most common pathway to aneuploidy. [83]

In the modern era, different classes of structural cytogenetic changes – chromosomal translocations, deletions, and amplifications – have all

been shown to have causal roles in tumour development. Yet whether whole chromosome aberrations, aneuploidy, causes or is a consequence of cancer, as originally suggested, has remained a controversial issue. At one extreme, it has been suggested that aneuploidy is the sole cause of cancer, as it is commonly observed in many human tumours.[84,85] At the other end of the spectrum is the view that aneuploidy is simply a consequence of cell division errors in rapidly dividing tumour cells. These extremes are, most probably, not mutually exclusive.[86] Aneuploidy could have a causal role early in the development of some tumours, but in the mature tumour, on-going changes in the karyotype could mainly be due to errors in cell division.[87,88] Likewise, aneuploidy could passively accompany mutations that cause transformation early, but play a key role in generating a metastatic phenotype later in the disease.

Different lines of evidence now make a compelling case for aneuploidy being a discrete chromosome mutation event that contributes to malignant transformation and the progression process. First, precise assesment of chromosome aneuploidy in several primary tumours with *in situ* hybridization and comparative genomic hybridization techniques have revealed that specific chromosome aneusomies correlate with distinct tumour phenotypes.[89] Second, aneuploid tumour cell lines and *in vitro* transformed rodent cells have been reported to display an elevated rate of chromosome instability, thereby indicating that aneuploidy is a dynamic chromosome mutation event associated with transformation of cells. Third, and most important, a number of mitotic genes regulating chromosome segregation have been found mutated in

human cancer cells, implicating such mutations in induction of aneuploidy in tumours.[90,91]

THE PRESENT INVESTIGATIONS

Genetic markers have been used for decades to provide prognostic information in NBs. Several structural chromosome aberrations have been associated with a poor outcome, including *MYCN* amplification and several deletions such as 1p, 3p, 4p, and 11q and gain of 17q.[27] In contrast to di- or tetra-ploidy triploidy is usually associated with a good outcome. [92]

Albeit such genomic imbalances appear to be important for NB pathogenesis and progression, surprisingly little is known about the mechanisms leading up to them. Some of the most crucial questions from the perspective of a cytogeneticist are: How do so the many copies of *MYCN* in DMs and HSR first arise? Because DMs are episomes typically lacking centromere sequences, how are they transported through the cell cycle? And how do structural aberrations in NB arise? Do they have an association with telomere disturbances, as have complex structural changes in adult tumours? If so, does structural chromosome instability have a role in tumour progression per se? And finally, how do the numerical changes dominating the near triploid low-risk infant NBs arise? Maybe their origin could provide a clue to why patients with this genetic signature do relatively well. The aim of this thesis was to shed some light on these issues.

Aims of the original studies included in this thesis

I. To characterise the cell cycle dynamics of *MYCN* containing double minutes (DMs) in NB cells and assess to what extent their behaviour is similar to that inferred by studies in other model systems with DMs; to deduce the statistical principles of DM segregation, and to investigate the topography of DM binding sites on human chromosomes.

II. To assess the biological role of telomere-dependent chromosome instability in NB cells. To assess experimentally whether quantification of telomere length and/or telomere-dependent genomic instability can be used for improved risk stratification of children with NB.

III. To analyse the variation in whole chromosome aberrations within neuroblastomas and to create algorithms to model the process leading up to aneuploidy in this tumour.

Materials and Methods

Patient material and cell lines

For the present studies frozen tumour material was obtained from the biobanks of the Departments of Clinical Genetics and Human Genetics at Lund University (Lund, Sweden) and the Academic Medical Centre (Amsterdam, the Netherlands). Formalin-fixed paraffin-embedded tissue blocks were obtained from the Department of Pathology at Skåne Regional and University Laboratories, Lund, Sweden. Complementary samples were obtained from a tissue micro array (TMA), from the Department of Human Genetics, Academic Medical Centre in Amsterdam. Another 12 samples were obtained from TMAs from the Department of Pathology, Valencia Medical School.

Only tumours classified as primary NBs were included, after having undergone histopathological review. All patients were treated according to the European protocol active at the time. The follow-up time ranged from 91 days (dead of the disease) up to 18 years. Written consent was given by the parents for documentation, biological studies and analysis of medical data. The study was approved by the ethics review board of the participating institutes.

Established NB cell lines, SK-N-AS, SK-N-FI, SK-N-SH and GI-MEN, were obtained from LGC Standards (Teddington, UK) and DSMZ (Braunschweig, Germany). The NB cell-lines CHP-212 and LA-N-5,

the neuroepithelioma cell-line MC-IX, and mouse 3T3 cells were obtained from the American Type Culture Collection.

Fluorescence *in situ* hybridization (FISH)

FISH is a laboratory technique for detecting and locating a specific DNA sequence on a chromosome. The technique relies on exposing chromosomes to a small DNA sequence called a probe that has a fluorescent molecule attached to it. The probe sequence binds to its complementary sequence on chromosome spreads or interphase nuclei.

FISH provided us with a way to visualize and map the genetic material in an individual tumour cells, including specific genes or portions of genes. Centromeric repeat probes are generated from repetitive sequences found in the middle of each chromosome. We have used these probes to determine whether cells have the correct number of chromosomes. These probes can also be used in combination with "locus specific probes" to determine whether a cell is missing genetic material from a particular chromosome.

Immunofluoroscence

Immunofluorescence is a technique allowing the visualization of a specific protein/antigen in cells or tissue sections by binding to a specific antibody chemically conjugated with a fluorescent dye, such as fluorescein isothiocyanate (FITC). There are two major types of immunofluorescence staining methods: 1) direct immunofluorescence staining in which the primary antibody is labelled with fluorescence

dye, and 2) indirect immunofluorescence staining in which a secondary antibody labelled with fluorochrome is used to recognize a primary antibody. Immunofluorescence staining can be performed on cells fixed on slides and tissue sections. Immunofluorescence stained samples are examined under a fluorescence microscope or confocal microscope.

Single nucleotide polymorphism (SNP) arrays

Single nucleotide polymorphisms, frequently called SNPs, are the most common type of genetic variation among people. Each SNP represents a difference in a nucleotide. Here is one example: replacement of the nucleotide guanine (G) with the nucleotide adenine (A). SNPs occur normally throughout everybody's DNA. There are approximately 10 million SNPs in the human genome, with occurrence every 300 nucleotide in average. Most commonly, these variations are found in the introns e.g. between genes. They can act as biological markers, helping us to locate genes that are associated with disease. If a SNP occur within a gene or in a regulatory region near a gene, they may play a more direct role in disease by affecting the gene's function. Most SNPs don't have any effect of an individual's health.

SNP array methodology is a method by which the status (e.g. heterozygosity, homozygosity and allelic loss) of millions of SNPs in a DNA sample can be analysed in the same experiment. SNP array data present two different data tracks; the log ratio which is the total copy number on a logarithmic scale, and the B allele frequency (BAF) which visualizes the relative presence of each of the two alternative

nucleotides at each SNP locus profiled. If the sample is diploid, a locus with two identical copies will appear with a log ratio value close to 0, and a BAF value of either 0 (homozygous genotype AA) or 1 (homozygous genotype BB) or 0.5 (heterozygous genotype AB). From these SNP array data, different genomic aberrations (gains, losses, copy number-neutral events) can be interpreted in tumour samples.[93] Cancer genomes often show multiple complex rearrangements such as a single nucleotide mutation to gains, amplifications, insertions or deletions of genes or fragments, as well as whole-genome duplications.[94,95] Most of these changes can be detected and analysed in detail by SNP array methodology. However, this approach will fail to detect genomis rearrangements that do not disturb the allelic balance, such as balanced translocations and pure polyploidization. Furthermore, genomes in cancer often show intratumour heterogeneity, which may reduce the sensitivity of the analysis and lead to difficulties in interpretation. However, algoritms have now been developed that may assist in the analysis of tumours consisting of multiple clones.[96,97]

Results and Discussion

Article I

MYCN amplification is the strongest biological negative predictor in NB known so far. However, because extra MYCN copies in NB cells are frequently carried by episomal DMs lacking centromeric sequences, it has remained a mystery how they are maintained through cell division. The purpose of Article I was to determine how *MYCN*- carrying DMs are maintained thorough mitosis in NB cells. In summary, we showed that these DMs translocate from the nuclear interior to its periphery at transition from interphase to prophase. Throughout cell division they were preferentially located adjacent to the telomere repeat sequences of the chromosomes throughout cell division. However, disruption of the telomere nucleoprotein complex by telomerase inhibition did not affect DM segregation at cell division, indicating that intact telomeric repeats are not a key of importance to DM maintenance. When hybrid cells were constructed by fusion of mouse T3T cells with the NB cell line CHP-212 there was migration from human to murine chromatin, indicating that DMs do not bind to human-specific positional elements in chromosomes. We also showed that DMs segregated in a binomial-like random fashion during cell division, and that DM copy-number distribution in NB cells could be mathematically simulated by a bionomial distribution at segregation, combined with positive proliferative selection for cells with high *MYCN* copy numbers. The positive selective value of high *MYCN* copy number was also

confirmed experimentally by colony-forming assay, showing astrong growth-advantage for NB cells with high DM (*MYCN)* copy-numbers, compared to NB cells with lower copy-numbers.

Taken together, this study showed that *MYCN*-carrying DMs in NB are retained through mitosis by attaching to regular chromosomes and that this type of segregation is highly disordered, in turn explaining why *MYCN* copy number may be highly diverse among cells within the same tumour.

Article II

Apart from *MYCN* amplification, several segmental aberrations, most prominently 11q deletion, have shown to predict prognosis in NB. Complex structural aberrations in several adult tumour types have been shown to result from telomere length abnormalities, but to what extent such were present in NB and what significance they may have was relatively unknown at the beginning of our second study. In Article II our aim was to assess the relationship between telomere length alterations in NB and clinico-biological parameters. For each tumour, telomere fluorescence intensity values obtained by quantitative FISH on NB cells were compared to those of surrounding non-neoplastic cells in formalin-fixed paraffin-embedded material. Each NB cell population was classified by Student's *t*-test and Mann-Whitney *U*-test as either having longer, shorter or similar telomere lengths compared to that of non-neoplastic cells from the same patient. The results revealed 10

tumours having longer, 12 having unchanged and 28 having shorter telomeres than that of the normal tissue. Survival analyses according to Kaplan-Meier identified two sub-groups with poor outcome. One was having decreased tumour telomere length and *MYCN* amplification, and another showed increased tumour telomere length in the absence of *MYCN* amplification. Tumour cells with increased telomere length showed a high frequency of APBs, indicating that telomere elongation was dependant on the ALT pathway. Most tumour biopsies and cell lines exhibited an elevated rate of anaphase bridges, suggesting telomere-dependant chromosomal instability. This was more prevalent in tumours with increased telomere length showing that ALT mechanisms fail to stabilize the genome completely. In cell lines, we found anaphase bridging and TTAGGG-negative chromosome ends predominantly present in those with MYCN amplification, with *MYCN* sequences present in bridges, indicating that telomere-dependant instability may have a role in recombination of such amplicons.

In summary, this study showed that telomere length abnormalities are common in NBs and may be related to instablility in chromosome structure as well as associated with clinical outcome.

Article III

A subset of NBs with favourable prognosis is characterized by multiple extra chromosomes (trisomies and tetrasomies) resulting in chromosome numbers at the hyperdiploid-triploid level. Again the

mechanism behind this peculiar chromosomal patter is unknown. The aim of the third study was to assess intra-tumour genetic variation in NBs with a focus on such whole-chromosome changes and also to form hypothesis regarding their mechanism of origin. We first used SNP array data from primary NBs to quantify the degree of genetic intra-tumour diversity with respect to structural/segmental and numerical chromosome aberrations. The structural aberrations showed a high degree of intratumour diversity, indicative of continuous chromosomal remodelling. In contrast, numerical aberrations were typically confined to the same cell population stratum in each tumour. However, a comparison between aneuploidy NBs and normal fibroblast cells showed a considerably higher degree of whole chromosome copy number diversity in NB than in normal cells. Prominent copy number diversity was also found in cell populations grown from single NB cells, supporting that aneuploidy is an on-going process. Mathematical modelling indicated that loss of chromosomes from a tetraploid state was more likely to explain the pattern of aneuploidy in NB than other mechanisms reported in cancer cells. This was supported by experimental findings of a high frequency of chromosome lagging at anaphase in parallel topolyploidisation events in growing NB cells, as shown by time-lapse imaging.

In summary, this study showed that numerical aberrations in NB may show vast cell-to-cell differences, and that this is an ongoing process in many tumours.

Conclusion

The main focus of this thesis has been on three genomic pillars within the childhood tumour neuroblastoma. Our first focus was on one of the most important biological risk factors in neuroblastoma the oncogene *MYCN*. We could show that *MYCN*-carrying DMs in NB cells translocate from the nuclear interior to the periphery at the interphase-prophase transition and that they are preferentially located adjacent to the telomeres as well as that they segregate randomly. Furthermore we showed that DMs do not bind to specific positional elements in human chromosomes by making human/murine hybrids. We could explain the vast intercellular variety of *MYCN* copy number in NB. Moving on from here, in our next study we found that telomeres without detectable TTAGGG-repeats was associated with *MYCN* amplification and the generation of chromosomal breakage-fusion bridge cycles and could confirm that *MYCN* amplification was associated with reduced tumour telomere length (TTL) *in vivo*. We also found a possible association between poor survival and elongated telomeres, which needs to be studied further. Our third pillar was that of whole chromosome changes, with a focus on intratumoural diversity. We demonstrated a previously unreported high degree of intercellular variation in chromosome copy number and found indications that loss of chromosomes from a tetraploid state is a major route towards this prominent intra-tumour genomic diversity in aneuploid NBs. Taken together, these studies suggest that NB genomes are highly plastic, which may to some extent explain the poor response to oncological treatment for some of these tumours.

FUTURE PERSPECTIVES

NB continues to be an enormous clinical and biological enigma, despite so many scientists working with this tumour type. My sincere hope is that this thesis will shred a little light on the three different subjects I've assessed. Advances in our understanding of the fundamental genomic alterations that are associated with varying tumour behaviour and patient outcome has hopefully moved us closer to the goal of precise prognostication based on molecular analysis of patient-specific and tumour-specific variables, such as my study on telomere length.

Unfortunately we are not quite there yet. The patient material accessible was small and our studies need confirmation in larger patient cohorts in unbiased studies. There are many more aspects to assess in the field of genomic instability in NB, such as finding out how frequent ALT is in NB. Could it possibly be used as part of an assay for prognostication? As when it comes to the whole chromosome changes the intriguing part is why do the triploid tumours have a better clinical outcome, albeit they are expressing such a chromosomal instability?

SVENSK SAMMANFATTNING

Neuroblastom är den vanligaste solida tumören, utanför hjärnan, hos små barn och finns nästan inte alls hos vuxna. Varje år insjuknar mellan femton och tjugo barn i Sverige, de flesta före två års ålder. Överlevnaden har ökat de senaste tjugo åren men är fortfarande på låga nivåer för de mer aggressiva formerna.

Neuroblastom uppstår i det sympatiska nervsystemet. Därför är binjurarna en vanlig utgångspunkt för neuroblastom i buken. Sjukdomen kallas ibland för den stora imitatören då den kan ta många olika skepnader. Att man upptäcker sjukdomen kan ibland bero på att barnet blir röntgat för någon annan sjukdom, eller att man upptäcker en knöl i magen.

De stillsammare varianterna av neuroblastom, ofta de minsta barnens sjukdom, ger ofta inga direkta symptom emedan de mera aggressiva formerna kan ta sig uttryck av diarréer, skelettsmärtor, blodbrist och att barnet får mycket ont i kroppen. På grund av sitt ursprung utsöndrar tumören ofta stresshormon och därav blir barnet oroligt och magerlagt.

De mindre aggressiva varianterna av sjukdomen botas ofta med enbart kirurgi men de mer aggressiva formerna kräver såväl kirurgi som cellgiftsbehandlingar, strålning, stamcellstransfusioner, höga doser A-

vitamin (som får de sista tumörcellerna att mogna eller dö ut) samt biologisk behandling.

Barn som har haft någon av de mer aggressiva formerna, och därav tuffare behandlingarna, har senare i livet ökad risk för en sekundär cancer och kan få komplikationer som hormonrubbningar, sterilitet, hörselnedsättningar samt ökad risk för neurologiska och psykologiska förändringar.

Neuroblastomceller uppvisar i regel många förändringar i arvsmassan som tros ha stor betydelse för sjukdomens utveckling. De vanligaste är ett ökat antal kopior av en gen som heter *MYCN*, att delar av kromosomer fattas eller finns i för många kopior alternativt att hela kromosomer finns i ökat antal eller saknas. Inom den här avhandlingen har jag studerat dessa tre olika hörnstenar i neuroblastom för att bättre förstå hur sjukdomen utvecklas och väcka tankar om nya angreppspunkter för behandling.

I den första artikeln som är en del av avhandlingen har vi tittat på hur *MYCN* rör sig igenom cellcykeln. Frågan var om de band till ändarna av kromosomerna, telomererna, med hjälp av några för människan specifika ämnen. Vi kunde genom vår studie visa att *MYCN*-inbindningen inte är specifikt för människan utan att de extra kopiorna av genen kan flytta sig över artgränserna. Detta visade vi genom att i laboratoriet slå samman mänskliga tumörceller med musceller. Vidare kunde vi visa att *MYCN* rör sig genom cellcykeln från de centrala delarna av cellkärnan till de mer perifera delarna, alltid i närheten av

telomererna. Vi kunde också matematiskt åskådligöra hur fördelningen av *MYCN* till de nya dottercellerna går till i cellcykeln.

I den andra artikeln låg fokus på telomererna. Vi tittade på hur långa de var i tumörer jämfört omkringliggande normal vävnad. Vi kunde på så vis påvisa två distinkta patientgrupper som hade en mycket dålig prognos, de med korta telomerer och *MYCN* amplifiering samt en grupp med långa telomerer.

I det tredje arbetet låg fokus på kopietalet av hela kromosomer i tumörerna. Vi visade att det inte är samma kopietal av kromosomer i alla tumörceller i samma tumörer. Vi analyserade också genetiskt kloner från enskilda tumörceller och kunde på det sättet visa att förändringen i kromosomtalet är en pågående process – att tumören fortsatte få nya förändringar över tid. Vi gjorde också en matematisk modell för hur denna process sker.

ACKNOWLEDGEMENT

I wish to express my deepest gratitude and appreciation to:

My supervisor **David Gisselsson Nord**, for believing in me and guiding me through on this marvellous trip. For, almost, always being there with your amazing knowledge your pep talks and great scientific discussions. For introducing me to the fantastic world of science. Thank you!
My co-supervisors; **Ingrid Øra**, for always being cheerful and helpful and introducing me to the clinic. **Sven Påhlman**, for you delightful comments and bright ideas. **Fredrik Mertens**, for always giving support when needed.

To all newcomers within the group of childhood cancers **Linda**, **Jenny**, **Daniel** and **Anders**.

To all former and present PhD students with whom I've spent so little space and so much time ☺; **Ylva Stewenius**, **Karolin Hansén Nord**, **Emily Möller**, **Josef Davidsson**, **Henrik Lilljebjörn**, **Helena Ågerstam**, **Hammurabi Bartuma**, **Kristina Karrman**, **Nils Hansen**, **Linda Olsson**, **Setareh Safavi** and **Elsa Arbajian**.

To **Anette Welin** without whom this department would come to a complete standstill!

To the technical staff, present and former, who has helped me so much, with a special thanks to ***Linda Magnusson***, as well as **Andrea Bigolav**, **Carin Lassen**, **Jenny Nilsson**, **Marianne Rissler** and **Bodil Strömbäck**.

To the former head of the department **Felix Mitelman**, for creating such inspired atmosphere to work in.

To all PI and senior scientists at the department; **Bertil Johansson**, **Kajsa Pålsson**, **Thoas Fioretes** and **Anna Andersson**.

To all senior staff of the Department of Clinical Genetics; **Mia Soller**, **Ulf Kristoffersson**, **Samuel Gebre-Mehdin**, **Catarina Lundin** and **Nina Larsson**.

To our Journal Club, for great discussions; **Susanne** and **Charles**.

To my wonderful friends from "Skånefika"; **Anette**, **Annica**, **Gabriella** and **Sanna**, this thesis would never have been accomplished without you guys! I survived thanks to you.

To my fantastic and loving parents, **Kerstin & John, for** always being there

To my wonderful boys **Leo & David**, I love you.

REFERENCES

1. http://192.137.163.49/sdb/can/resultat.aspx. The Swedish cancer registry.

2. Brodeur GM. Neuroblastoma: biological insights into a clinical enigma. *Nat Rev Cancer.* Mar 2003;3(3):203-216.

3. Hoehner JC, Gestblom C, Hedborg F, Sandstedt B, Olsen L, Pahlman S. A developmental model of neuroblastoma: differentiating stroma-poor tumors' progress along an extra-adrenal chromaffin lineage. *Lab Invest.* Nov 1996;75(5):659-675.

4. Schulte JH, Lindner S, Bohrer A, et al. MYCN and ALKF1174L are sufficient to drive neuroblastoma development from neural crest progenitor cells. *Oncogene.* Apr 9 2012.

5. Gilbert S. *Developmental Biology*. 6th ed: Sinauer Associates; 2000.

6. Hall BK. The neural crest as a fourth germ layer and vertebrates as quadroblastic not triploblastic. *Evol Dev.* Jan-Feb 2000;2(1):3-5.

7. London WB, Castleberry RP, Matthay KK, et al. Evidence for an age cutoff greater than 365 days for neuroblastoma risk group stratification in the Children's Oncology Group. *J Clin Oncol.* Sep 20 2005;23(27):6459-6465.

8. Mosse YP, Laudenslager M, Longo L, et al. Identification of ALK as a major familial neuroblastoma predisposition gene. *Nature.* Oct 16 2008;455(7215):930-935.

9. Bourdeaut F, de Carli E, Timsit S, et al. VIP hypersecretion as primary or secondary syndrome in neuroblastoma: A retrospective study by the Societe Francaise des Cancers de l'Enfant (SFCE). *Pediatr Blood Cancer.* May 2009;52(5):585-590.

10. Nitschke R, Smith EI, Shochat S, et al. Localized neuroblastoma treated by surgery: a Pediatric Oncology Group Study. *J Clin Oncol.* Aug 1988;6(8):1271-1279.

11. Strother DR, London WB, Schmidt ML, et al. Outcome after surgery alone or with restricted use of chemotherapy for patients with low-risk neuroblastoma: results of Children's Oncology Group study P9641. *J Clin Oncol.* May 20 2012;30(15):1842-1848.

12. Hara J. Development of treatment strategies for advanced neuroblastoma. *Int J Clin Oncol.* Jun 2012;17(3):196-203.

13. De Corti F, Avanzini S, Cecchetto G, et al. The surgical approach for cervicothoracic masses in children. *J Pediatr Surg.* Sep 2012;47(9):1662-1668.

14. Castel V, Tovar JA, Costa E, et al. The role of surgery in stage IV neuroblastoma. *J Pediatr Surg.* Nov 2002;37(11):1574-1578.

15. Shorter NA, Davidoff AM, Evans AE, Ross AJ, 3rd, Zeigler MM, O'Neill JA, Jr. The role of surgery in the management of stage IV neuroblastoma: a single institution study. *Med Pediatr Oncol.* May 1995;24(5):287-291.

16. Brodeur GM, Pritchard J, Berthold F, et al. Revisions of the international criteria for neuroblastoma diagnosis, staging, and response to treatment. *J Clin Oncol.* Aug 1993;11(8):1466-1477.

17. Evans AE, D'Angio GJ, Randolph J. A proposed staging for children with neuroblastoma. Children's cancer study group A. *Cancer.* Feb 1971;27(2):374-378.

18. Monclair T, Brodeur GM, Ambros PF, et al. The International Neuroblastoma Risk Group (INRG) staging system: an INRG Task Force report. *J Clin Oncol.* Jan 10 2009;27(2):298-303.

19. Duker NJ. Chromosome breakage syndromes and cancer. *Am J Med Genet.* Oct 30 2002;115(3):125-129.

20. Fix A, Lucchesi C, Ribeiro A, et al. Characterization of amplicons in neuroblastoma: high-resolution mapping using DNA microarrays, relationship with outcome, and identification of overexpressed genes. *Genes Chromosomes Cancer.* Oct 2008;47(10):819-834.

21. Fordyce CA, Heaphy CM, Bisoffi M, et al. Telomere content correlates with stage and prognosis in breast cancer. *Breast Cancer Res Treat.* Sep 2006;99(2):193-202.

22. Fraga MF, Ballestar E, Villar-Garea A, et al. Loss of acetylation at Lys16 and trimethylation at Lys20 of histone H4 is a common hallmark of human cancer. *Nat Genet.* Apr 2005;37(4):391-400.

23. Gisselsson D, Lundberg G, Ora I, Hoglund M. Distinct evolutionary mechanisms for genomic imbalances in high-risk and low-risk neuroblastomas. *J Carcinog.* 2007;6:15.

24. Haber M, Bordow SB, Haber PS, Marshall GM, Stewart BW, Norris MD. The prognostic value of MDR1 gene expression in primary untreated neuroblastoma. *Eur J Cancer.* Oct 1997;33(12):2031-2036.

25. Hanahan D, Weinberg RA. Hallmarks of cancer: the next generation. *Cell.* Mar 4 2011;144(5):646-674.

26. Isidoro A, Martinez M, Fernandez PL, et al. Alteration of the bioenergetic phenotype of mitochondria is a hallmark of breast, gastric, lung and oesophageal cancer. *Biochem J.* Feb 15 2004;378(Pt 1):17-20.

27. Attiyeh EF, London WB, Mosse YP, et al. Chromosome 1p and 11q deletions and outcome in neuroblastoma. *N Engl J Med.* Nov 24 2005;353(21):2243-2253.

28. Brodeur GM, Sekhon G, Goldstein MN. Chromosomal aberrations in human neuroblastomas. *Cancer.* Nov 1977;40(5):2256-2263.

29. Rubie H, Delattre O, Hartmann O, et al. Loss of chromosome 1p may have a prognostic value in localised neuroblastoma: results of the French NBL 90 Study. Neuroblastoma Study Group of the Societe Francaise d'Oncologie Pediatrique (SFOP). *Eur J Cancer.* Oct 1997;33(12):1917-1922.

30. Savelyeva L, Corvi R, Schwab M. Translocation involving 1p and 17q is a recurrent genetic alteration of human neuroblastoma cells. *Am J Hum Genet.* Aug 1994;55(2):334-340.

31. Schleiermacher G, Bourdeaut F, Combaret V, et al. Stepwise occurrence of a complex unbalanced translocation in neuroblastoma leading to insertion of a telomere sequence and late chromosome 17q gain. *Oncogene.* May 5 2005;24(20):3377-3384.

32. Hero B, Simon T, Spitz R, et al. Localized infant neuroblastomas often show spontaneous regression: results of the prospective trials NB95-S and NB97. *J Clin Oncol.* Mar 20 2008;26(9):1504-1510.

33. La Madrid AM, Campbell N, Smith S, Cohn SL, Salgia R. Targeting ALK: a promising strategy for the treatment of non-small cell lung cancer, non-Hodgkin's lymphoma, and neuroblastoma. *Target Oncol.* Sep 12 2012.

34. Yu AL, Gilman AL, Ozkaynak MF, et al. Anti-GD2 antibody with GM-CSF, interleukin-2, and isotretinoin for neuroblastoma. *N Engl J Med.* Sep 30 2010;363(14):1324-1334.

35. de Cremoux P, Jourdan-Da-Silva N, Couturier J, et al. Role of chemotherapy resistance genes in outcome of neuroblastoma. *Pediatr Blood Cancer.* Mar 2007;48(3):311-317.

36. Flahaut M, Muhlethaler-Mottet A, Martinet D, et al. Molecular cytogenetic characterization of doxorubicin-resistant neuroblastoma cell lines: evidence that acquired multidrug resistance results from a unique large amplification of the 7q21 region. *Genes Chromosomes Cancer.* May 2006;45(5):495-508.

37. Schwab M, Alitalo K, Klempnauer KH, et al. Amplified DNA with limited homology to myc cellular oncogene is shared by human neuroblastoma cell lines and a neuroblastoma tumour. *Nature.* Sep 15-21 1983;305(5931):245-248.

38. Seeger RC, Brodeur GM, Sather H, et al. Association of multiple copies of the N-myc oncogene with rapid progression of neuroblastomas. *N Engl J Med.* Oct 31 1985;313(18):1111-1116.

39. Cohn SL, Pearson AD, London WB, et al. The International Neuroblastoma Risk Group (INRG) classification system: an INRG Task Force report. *J Clin Oncol.* Jan 10 2009;27(2):289-297.

40. Brodeur GM, Seeger RC, Schwab M, Varmus HE, Bishop JM. Amplification of N-myc in untreated human neuroblastomas correlates with advanced disease stage. *Science.* Jun 8 1984;224(4653):1121-1124.

41. Look AT, Hayes FA, Shuster JJ, et al. Clinical relevance of tumor cell ploidy and N-myc gene amplification in childhood neuroblastoma: a Pediatric Oncology Group study. *J Clin Oncol.* Apr 1991;9(4):581-591.

42. Tonini GP, Boni L, Pession A, et al. MYCN oncogene amplification in neuroblastoma is associated with worse prognosis, except in stage 4s: the Italian experience with 295 children. *J Clin Oncol.* Jan 1997;15(1):85-93.

43. Katzenstein HM, Bowman LC, Brodeur GM, et al. Prognostic significance of age, MYCN oncogene amplification, tumor cell ploidy, and histology in 110 infants with stage D(S) neuroblastoma: the pediatric oncology group experience--a pediatric oncology group study. *J Clin Oncol.* Jun 1998;16(6):2007-2017.

44. Bagatell R, Rumcheva P, London WB, et al. Outcomes of children with intermediate-risk neuroblastoma after treatment stratified by MYCN status and tumor cell ploidy. *J Clin Oncol.* Dec 1 2005;23(34):8819-8827.

45. Schneiderman J, London WB, Brodeur GM, Castleberry RP, Look AT, Cohn SL. Clinical significance of MYCN amplification and

ploidy in favorable-stage neuroblastoma: a report from the Children's Oncology Group. *J Clin Oncol.* Feb 20 2008;26(6):913-918.

46. Schwab M. MYCN in neuronal tumours. *Cancer Lett.* Feb 20 2004;204(2):179-187.

47. Ambros PF, Ambros IM. Pathology and biology guidelines for resectable and unresectable neuroblastic tumors and bone marrow examination guidelines. *Med Pediatr Oncol.* Dec 2001;37(6):492-504.

48. Tonelli R, Purgato S, Camerin C, et al. Anti-gene peptide nucleic acid specifically inhibits MYCN expression in human neuroblastoma cells leading to cell growth inhibition and apoptosis. *Mol Cancer Ther.* May 2005;4(5):779-786.

49. Pession A, Tonelli R. The MYCN oncogene as a specific and selective drug target for peripheral and central nervous system tumors. *Curr Cancer Drug Targets.* Jun 2005;5(4):273-283.

50. Bell E, Chen L, Liu T, Marshall GM, Lunec J, Tweddle DA. MYCN oncoprotein targets and their therapeutic potential. *Cancer Lett.* Jul 28 2010;293(2):144-157.

51. Nara K, Kusafuka T, Yoneda A, Oue T, Sangkhathat S, Fukuzawa M. Silencing of MYCN by RNA interference induces growth inhibition, apoptotic activity and cell differentiation in a neuroblastoma cell line with MYCN amplification. *Int J Oncol.* May 2007;30(5):1189-1196.

52. Buechner J, Einvik C. N-myc and non-coding RNAs in neuroblastoma. *Mol Cancer Res.* Aug 30 2012.

53. Kohl NE, Kanda N, Schreck RR, et al. Transposition and amplification of oncogene-related sequences in human neuroblastomas. *Cell.* Dec 1983;35(2 Pt 1):359-367.

54. Stock C, Bozsaky E, Watzinger F, et al. Genes proximal and distal to MYCN are highly expressed in human neuroblastoma as visualized by comparative expressed sequence hybridization. *Am J Pathol.* Jan 2008;172(1):203-214.

55. Terrile M, Bryan K, Vaughan L, et al. miRNA expression profiling of the murine TH-MYCN neuroblastoma model reveals similarities with human tumors and identifies novel candidate miRNAs. *PLoS One.* 2011;6(12):e28356.

56. Dominguez-Frutos E, Lopez-Hernandez I, Vendrell V, et al. N-myc controls proliferation, morphogenesis, and patterning of the inner ear. *J Neurosci.* May 11 2011;31(19):7178-7189.

57. Smith KN, Singh AM, Dalton S. Myc represses primitive endoderm differentiation in pluripotent stem cells. *Cell Stem Cell.* Sep 3 2010;7(3):343-354.

58. Kuwahara A, Hirabayashi Y, Knoepfler PS, et al. Wnt signaling and its downstream target N-myc regulate basal progenitors in the developing neocortex. *Development.* Apr 2010;137(7):1035-1044.

59. Ravasi T, Suzuki H, Cannistraci CV, et al. An atlas of combinatorial transcriptional regulation in mouse and man. *Cell.* Mar 5 2010;140(5):744-752.

60. Neri F, Zippo A, Krepelova A, Cherubini A, Rocchigiani M, Oliviero S. Myc regulates the transcription of the PRC2 gene to control the expression of developmental genes in embryonic stem cells. *Mol Cell Biol.* Feb 2012;32(4):840-851.

61. Anderson PD, McKissic SA, Logan M, et al. Nkx3.1 and Myc crossregulate shared target genes in mouse and human prostate tumorigenesis. *J Clin Invest.* May 1 2012;122(5):1907-1919.

62. Pelengaris S, Khan M. The many faces of c-MYC. *Arch Biochem Biophys.* Aug 15 2003;416(2):129-136.

63. Marcelis CL, Hol FA, Graham GE, et al. Genotype-phenotype correlations in MYCN-related Feingold syndrome. *Hum Mutat.* Sep 2008;29(9):1125-1132.

64. Weiss WA, Aldape K, Mohapatra G, Feuerstein BG, Bishop JM. Targeted expression of MYCN causes neuroblastoma in transgenic mice. *EMBO J.* Jun 2 1997;16(11):2985-2995.

65. Hackett CS, Hodgson JG, Law ME, et al. Genome-wide array CGH analysis of murine neuroblastoma reveals distinct genomic aberrations which parallel those in human tumors. *Cancer Res.* Sep 1 2003;63(17):5266-5273.

66. Azarova AM, Gautam G, George RE. Emerging importance of ALK in neuroblastoma. *Semin Cancer Biol.* Oct 2011;21(4):267-275.

67. Kelleher FC, McDermott R. The emerging pathogenic and therapeutic importance of the anaplastic lymphoma kinase gene. *Eur J Cancer.* Sep 2010;46(13):2357-2368.

68. Voena C, Chiarle R. The battle against ALK resistance: successes and setbacks. *Expert Opin Investig Drugs.* Aug 25 2012.

69. Berry T, Luther W, Bhatnagar N, et al. The ALK(F1174L) mutation potentiates the oncogenic activity of MYCN in neuroblastoma. *Cancer Cell.* Jul 10 2012;22(1):117-130.

70. Blackburn EH. The molecular structure of centromeres and telomeres. *Annu Rev Biochem.* 1984;53:163-194.

71. Palm W, de Lange T. How shelterin protects mammalian telomeres. *Annu Rev Genet.* 2008;42:301-334.

72. Purvis JE, Karhohs KW, Mock C, Batchelor E, Loewer A, Lahav G. p53 dynamics control cell fate. *Science.* Jun 15 2012;336(6087):1440-1444.

73. Peuscher MH, Jacobs JJ. DNA-damage response and repair activities at uncapped telomeres depend on RNF8. *Nat Cell Biol.* Sep 2011;13(9):1139-1145.

74. Donate LE, Blasco MA. Telomeres in cancer and ageing. *Philos Trans R Soc Lond B Biol Sci.* Jan 12 2011;366(1561):76-84.

75. Chan SR, Blackburn EH. Telomeres and telomerase. *Philos Trans R Soc Lond B Biol Sci.* Jan 29 2004;359(1441):109-121.

76. Zvereva MI, Shcherbakova DM, Dontsova OA. Telomerase: structure, functions, and activity regulation. *Biochemistry (Mosc).* Dec 2010;75(13):1563-1583.

77. Chung I, Osterwald S, Deeg KI, Rippe K. PML body meets telomere: The beginning of an ALTernate ending? *Nucleus.* May 1 2012;3(3):263-275.

78. Henson JD, Neumann AA, Yeager TR, Reddel RR. Alternative lengthening of telomeres in mammalian cells. *Oncogene.* Jan 21 2002;21(4):598-610.

79. Reddel RR, Bryan TM, Colgin LM, Perrem KT, Yeager TR. Alternative lengthening of telomeres in human cells. *Radiat Res.* Jan 2001;155(1 Pt 2):194-200.

80. Gisselsson D, Jonson T, Petersen A, et al. Telomere dysfunction triggers extensive DNA fragmentation and evolution of complex chromosome abnormalities in human malignant tumors. *Proc Natl Acad Sci U S A.* Oct 23 2001;98(22):12683-12688.

81. Hansemann D. *Arch. Pathol. Anat. Phys. Klin. Med* 1891;119:299-326.

82. Boveri T. Zur Frage der Entstehung maligner Tumoren. *Verlag von Gustav Fischer.* 1914.

83. Holland AJ, Cleveland DW. Losing balance: the origin and impact of aneuploidy in cancer. *EMBO Rep.* Jun 2012;13(6):501-514.

84. Li L, McCormack AA, Nicholson JM, et al. Cancer-causing karyotypes: chromosomal equilibria between destabilizing aneuploidy and stabilizing selection for oncogenic function. *Cancer Genet Cytogenet.* Jan 1 2009;188(1):1-25.

85. Duesberg P, Rasnick D. Aneuploidy, the somatic mutation that makes cancer a species of its own. *Cell Motil Cytoskeleton.* Oct 2000;47(2):81-107.

86. Thompson SL, Compton DA. Chromosomes and cancer cells. *Chromosome Res.* Apr 2011;19(3):433-444.

87. Thompson SL, Compton DA. Chromosome missegregation in human cells arises through specific types of kinetochore-microtubule attachment errors. *Proc Natl Acad Sci U S A.* Nov 1 2011;108(44):17974-17978.

88. Charlebois BD, Kollu S, Schek HT, Compton DA, Hunt AJ. Spindle pole mechanics studied in mitotic asters: dynamic distribution of spindle forces through compliant linkages. *Biophys J.* Apr 6 2011;100(7):1756-1764.

89. Brown JA, Alcaraz A, Takahashi S, Persons DL, Lieber MM, Jenkins RB. Chromosomal aneusomies detected by fluorescent in situ hybridization analysis in clinically localized prostate carcinoma. *J Urol.* Oct 1994;152(4):1157-1162.

90. Michor F, Iwasa Y, Vogelstein B, Lengauer C, Nowak MA. Can chromosomal instability initiate tumorigenesis? *Semin Cancer Biol.* Feb 2005;15(1):43-49.

91. Nowak MA, Komarova NL, Sengupta A, et al. The role of chromosomal instability in tumor initiation. *Proc Natl Acad Sci U S A.* Dec 10 2002;99(25):16226-16231.

92. Brodeur GM, Nakagawara A. Molecular basis of clinical heterogeneity in neuroblastoma. *Am J Pediatr Hematol Oncol.* May 1992;14(2):111-116.

93. Van Loo P, Nilsen G, Nordgard SH, et al. Analyzing cancer samples with SNP arrays. *Methods Mol Biol.* 2012;802:57-72.

94. Stratton MR, Campbell PJ, Futreal PA. The cancer genome. *Nature.* Apr 9 2009;458(7239):719-724.

95. Balmain A, Gray J, Ponder B. The genetics and genomics of cancer. *Nat Genet.* Mar 2003;33 Suppl:238-244.

96. Staaf J, Lindgren D, Vallon-Christersson J, et al. Segmentation-based detection of allelic imbalance and loss-of-heterozygosity in cancer cells using whole genome SNP arrays. *Genome Biol.* 2008;9(9):R136.

97. Lindgren D, Hoglund M, Vallon-Christersson J. Genotyping techniques to address diversity in tumors. *Adv Cancer Res.* 2011;112:151-182.

I

OPEN ACCESS Freely available online

PLoS one

Binomial Mitotic Segregation of *MYCN*-Carrying Double Minutes in Neuroblastoma Illustrates the Role of Randomness in Oncogene Amplification

Gisela Lundberg[1], Anders H. Rosengren[2], Ulf Håkanson[3], Henrik Stewénius[4], Yuesheng Jin[1], Ylva Stewénius[1], Sven Påhlman[5], David Gisselsson[1,6]*

1 Department of Clinical Genetics, Lund University Hospital, Lund, Sweden, **2** Department of Clinical Sciences Malmö, Lund University, Lund, Sweden, **3** The Nanometer Structure Consortium, Division of Solid State Physics, Lund University, Lund, Sweden, **4** Department of Mathematics, Lund University, Lund, Sweden, **5** Department of Molecular Medicine, Malmö, Lund University, Lund, Sweden, **6** Department of Pathology, Lund University Hospital, Lund, Sweden

Abstract

Background: Amplification of the oncogene *MYCN* in double minutes (DMs) is a common finding in neuroblastoma (NB). Because DMs lack centromeric sequences it has been unclear how NB cells retain and amplify extrachromosomal *MYCN* copies during tumour development.

Principal Findings: We show that *MYCN*-carrying DMs in NB cells translocate from the nuclear interior to the periphery of the condensing chromatin at transition from interphase to prophase and are preferentially located adjacent to the telomere repeat sequences of the chromosomes throughout cell division. However, DM segregation was not affected by disruption of the telosome nucleoprotein complex and DMs readily migrated from human to murine chromatin in human/mouse cell hybrids, indicating that they do not bind to specific positional elements in human chromosomes. Scoring DM copy-numbers in ana/telophase cells revealed that DM segregation could be closely approximated by a binomial random distribution. Colony-forming assay demonstrated a strong growth-advantage for NB cells with high DM (*MYCN*) copy-numbers, compared to NB cells with lower copy-numbers. In fact, the overall distribution of DMs in growing NB cell populations could be readily reproduced by a mathematical model assuming binomial segregation at cell division combined with a proliferative advantage for cells with high DM copy-numbers.

Conclusion: Binomial segregation at cell division explains the high degree of *MYCN* copy-number variability in NB. Our findings also provide a proof-of-principle for oncogene amplification through creation of genetic diversity by random events followed by Darwinian selection.

Citation: Lundberg G, Rosengren AH, Håkanson U, Stewénius H, Jin Y, et al. (2008) Binomial Mitotic Segregation of *MYCN*-Carrying Double Minutes in Neuroblastoma Illustrates the Role of Randomness in Oncogene Amplification. PLoS ONE 3(8): e3099. doi:10.1371/journal.pone.0003099

Editor: Beth Sullivan, Duke University, United States of America

Received July 14, 2008; **Accepted** August 8, 2008; **Published** August 29, 2008

Funding: This study was supported by the Swedish Children's Cancer Foundation, the Swedish Cancer Society, the Swedish Research Council, the Swedish Medical Society, the Lund University Hospital Donation Funds, the Gunnar Nilsson Cancer Foundation, the Crafoord Foundation, the Erik-Philip Sörensen Foundation, the Lundgren Foundation, and the Medical Faculty at Lund University. The funders had no role in study design, data collection and analysis, decision to publish, or preparation of the manuscript.

Competing Interests: The authors have declared that no competing interests exist.

* E-mail: david.gisselsson@med.lu.se

Introduction

Neuroblastomas (NB) are tumours of the sympathetic nervous system, occurring predominantly in early childhood and accounting for 8–10% of all paediatric cancers. One of the most important prognostic markers in NB is amplification of the oncogene *MYCN*, which is observed in ≈30% of NB [1]. Amplification of *MYCN* is associated with advanced stages of disease and the 3-year event-free survival of tumours with *MYCN* amplification is <20% [2]. The MYCN protein forms a heterodimer with MAX. This protein complex functions as a transcriptional activator, the targets of which include *ODC*, *MCM7*, and *MDR1* [3,4]. The activation of these genes leads to progression through the G1 phase of the cell cycle. Conversely, transcriptional repression of *MYCN*, or *MYCN* copy-number elimination, leads to growth-arrest, senescence and apoptosis of NB cells [5–7]. Cytogenetically, *MYCN* amplicons are typically carried either in extrachromosomal double minute (DMs) or in intrachromosomal homogeneously staining regions (HSRs). Under *in vitro* conditions HSR is the most common manifestation of *MYCN* amplification, whereas in fresh NB biopsies the amplicons are typically carried by DMs [8]. DMs are composed of circular DNA, up to only a few million base pairs in size, containing no centromere and no telomere [9]. DMs typically replicate only once during S-phase [10]. Because DMs lack centromeric sequences it has remained unclear how they segregate through mitosis and, consequently, how they are maintained and amplified in a growing NB cell population. However, recent elegant studies of the colorectal cancer model COLO322 have shown that DMs can move through mitosis by binding close to the termini of human chromosomes [11,12]. The aims of the present study were (1) to characterise the cell cycle dynamics of DMs in NB cells and assess to which extent their behaviour is similar to

that inferred by studies in other model systems, (2) to deduce the statistical principles of DM segregation, and (3) to investigate the topography of DM binding sites on human chromosomes. Based on our findings, we finally sought to assess whether unequal segregation of DMs to daughter cells at mitosis could play a mechanistic role in *MYCN* gene amplification by generating cell populations with heterogeneous DM copy-numbers on which Darwinian principles could be imposed.

Results

Cell cycle dynamics of DMs

To locate DMs in relation to chromosomes through the cell cycle, *MYCN* amplicons in the two NB cell lines CHP-212 and SK-N-AS were detected by combined fluorescence in situ hybridization (FISH) and beta-tubulin immunofluorescence using epifluorescence microscopy (Figure 1A–F). As a comparison, we also analysed neuroepithelioma MC-IX cells carrying *MYC* amplification in DMs. In >85% of the analysed interphase cells (>1000 cells/cell line scored), DMs were distributed evenly in the nucleus. The remaining nuclei either exhibited DMs restricted to the nuclear periphery (10–14%) or a preferential localisation of DMs to nuclear membrane protrusions or micronuclei (<1%). In contrast, prometaphase and metaphase cells (>100 cells/cell line scored) invariably showed DMs only at the periphery of the prometaphase rosette/metaphase plate. At anaphase, the DMs in all three cell lines remained at the periphery of the chromosome poles and were typically (>90% of DMs) located at, or adjacent to, the termini of the chromosomes (>50 cells/cell line scored). This configuration was also observed in telophase cells. DMs that had detached from the chromosomes were not included in the analyses; these consisted of <10% of observed DMs.

In order to characterize the mitotic distribution of DMs during the cell cycle in three dimensions, we then performed confocal microscopy of mitotic and interphase cells in the three cell lines (>20 mitotic cells and >10 interphase cells scored in each line). DMs were classified as peripherally located if the corresponding FISH signals overlapped with the chromatin border as assessed by DRAQ5 counterstaining (Figs. 1G–K). From prometaphase through telophase, 100% of DMs were located peripherally, close to the chromosome termini. In contrast, <20% of DMs in interphase cells located peripherally, while the remaining DMs were distributed at locations not overlapping with the outer chromatin border. This fluctuation in distribution between interphase and mitosis was observed in all the cell lines, without any significant difference between them in the fraction peripheral DMs at interphase or mitosis.

The mitotic location of DMs adjacent to chromosome termini prompted us to investigate whether DMs co-localized with telomeric repeat sequences in LA-N-5 and CHP-212. Co-hybridization with *MYCN* and TTAGGG-sequence probes assessed by epifluorescence microscopy showed that approximately 80% of *MYCN* signals overlapped with signals from telomeric repeats in mitotic cells from prometaphase through telophase (Figure 1L–N). In contrast, <10% of *MYCN* signals in interphase nuclei typically overlapped with TTAGGG repeat signals. As a comparison, co-hybridization with *MYCN* and pan-centromeric (alpha-satellite sequence) probes was also performed in LA-N-5 and CHP-212. On average, only 4% and 6% of *MYCN* signals, respectively, overlapped with centromere signals in mitotic cells and interphase cells (range 0–13% and 0–16%, respectively; 60 cells analyzed per cell line).

To validate our fluorescence microscopy data by an additional method, we performed further analysis of DM topography in mitotic CHP-212 cells by combined atomic force microscopy (AFM) and FISH. AFM is a well established technique in material sciences, making it possible to map surface topography with nanometre resolution. Superimposition of FISH images and AFM topography plots made it possible to establish the location of single and clustered DMs with high precision in three dimensions and confirmed the peripheral localisation of DMs at mitosis (Figure 2). Approximately half of the totally 50 DMs analysed were located on the surface of chromosomes, corresponding to peaks of approximately 200 nm in the AFM surface plots. The other DMs were located in grooves between chromosomes. In interphase cells, there was no clear correlation between DMs and surface features by AFM (data not shown). Taken together, our FISH and AFM data thus indicated that DMs underwent repeated topographical fluctuations during the cell cycle, moving rapidly from locations in the nuclear interior at interphase to positions adjacent to the telomeres at prometaphase, where they remained through telophase to finally drift back into the interior of the newly formed interphase nucleus.

Statistical distribution of DMs at mitosis

We then attempted to assess the statistical distribution of DMs between daughter cells by scoring the DM copy-numbers in opposite ana-telophase poles. To evaluate whether scoring by two-dimensional microscopic analysis was a sufficiently precise method for this, we first scored DMs, detected by *MYCN* or *MYC* probes, in 30 interphase cells from each of CHP-212, LA-N-5, and MC-IX, both by serial confocal sections (3D; 1 AU pinhole) and a single wide confocal section (2D; >5 AU pinhole). The average difference in DM copy number per cell by 2D analysis compared to 3D analysis was very low in each cell line up to a copy-number of approximately 100 (3.4–3.9% of the total DM copy-number; Figure 3A–C). Based on this, we then scored DM copy-number by epifluorescence microscopy in ana- and telophase cells, identified by cross-labelling with beta-tubulin (Figure 3D; 100 cells scored in CHP-212, 100 in LA-N-5, and 50 in MC-IX). Plotting of copy-number data revealed a similar pattern in the three cell lines. An identical DM copy-number in two opposite daughter poles was very rare, but the interpolar differences in copy number were typically small and there was a positive correlation in copy-number between opposite poles ($r = 0.53$ in LA-N-5, $r = 0.92$ in CHP-212, $r = 0.94$ in MC-IX; $p<0.05$ for all). Our data could readily be approximated by assuming binomial distribution of DMs at mitosis, with a probability of 50% for an individual DM to segregate into each daughter cell (Figure 3E–F). In CHP-212 and MC-IX only 2% of cell divisions deviated significantly ($P<0.01$) from such a binomial distribution, whereas in LA-N-5, 10% deviated from this distribution.

To assess whether the rare mitoses with a non-binomial DM segregation pattern were reflected by corresponding copy-number heterogeneity in growing cell populations, single cells were then isolated from each cell line and expanded to monoclonal colonies, in which DM copy-numbers were scored in individual cells by interphase-FISH. In total, 20 colonies from each cell line were analysed. With few exceptions, the colonies showed modal DM copy-numbers similar to those of the original cultures. In order not to overestimate the number of cells with copy-numbers produced by a non-binomial distribution, cells that deviated in >20 DM copies from each clone's modal value (outlier cells) were tested against a hypothetical binomial segregation, using the cell with the DM copy-number closest to its own as its presumed post-mitotic sister cell. It has been shown that DMs separate into single minutes during G1-phase [15] and it could therefore not be excluded that outlier cells with higher copy-numbers than a specific colony's modal value represented cells where the DMs had just separated

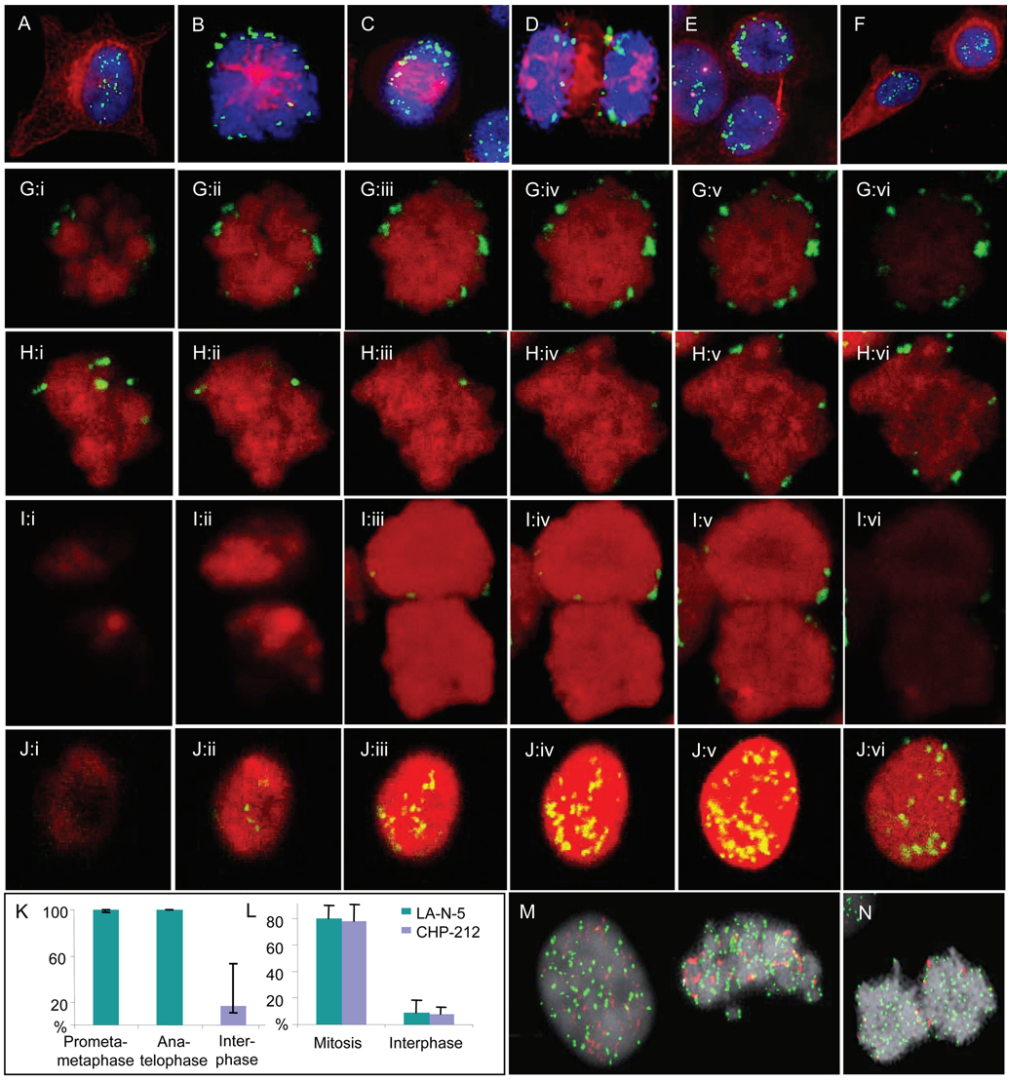

Figure 1. Fluorescence microscopy. All figures are from CHP-212. **A–F.** Combined immunofluorescence (IF) for beta tubulin (red), fluorescence in situ hybridisation (FISH) with a *MYCN* probe (green), and chromatin counterstaining by DAPI (blue) shows translocation of DMs to the periphery of the chromosome rosette at transition from interphase (A) to prometaphase (B); the peripheral localisation is maintained through metaphase (C), anaphase (D) and telophase (E), after which DMs again transfer to interior positions in the nucleus (F). **G–J.** Serial confocal optical sections **(i–vi)** corroborate the peripheral positions of DMs (green) at prometaphase (G), metaphase (H), and telophase (I), in contrast to a more central localisation at interphase (J); chromatin is counterstained by DRAQ5 (red). **K.** Proportion of peripheral DMs at prometa/metaphase, ana/telophase, and interphase; error bars denote standard deviation. **L.** The proportion of DM (*MYCN*) signals overlapping with telomeric TTAGGG-repeat signals at mitosis and interphase, respectively, in LA-N-5 and CHP-212. **M–N.** FISH for telomeric TTAGGG sequences (green) and *MYCN* (red) shows more frequent overlapping of signals for telomeres and DMs at metaphase (M, right) and telophase (N), compared to interphase (M, left).
doi:10.1371/journal.pone.0003099.g001

into single-minutes, leading to a duplication of the actual DM copy-numbers. Therefore, only outlier cells with copy-numbers below each colony's modal copy-number were tested. Using this approach, cells with copy-numbers not consistent with binomial segregation were found in 2–6 monoclonal colonies from each cell line (Supplementary Figure S1). Using the total number of cells in

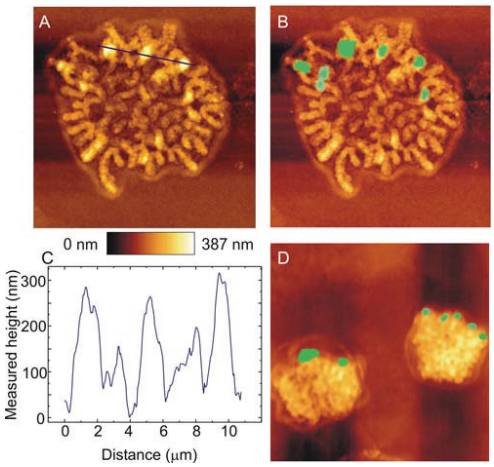

Figure 2. Atomic force microscopy. A. Atomic force microscopy of a CHP-212 prometaphase cell. **B.** Superimposition of MYCN fluorescence in situ hybridisation (FISH) signals allows localisation of DMs in the AFM image. **C.** Surface plot of the segment indicated by a blue line in A shows that DMs correspond to surface peaks of approximately 200 nm. **D.** Superimposed AFM and FISH images show peripheral location of DMs in a late telophase cell. Surface height is shown by the heat map and surface dimensions are indicated by scale bars corresponding to 2 μm in A, B and D.
doi:10.1371/journal.pone.0003099.g002

each colony to calculate the minimum number of cell divisions that occurred during colony-formation, the frequency of non-binomial DM segregations were approximately 3% (3/88) in CHP-212, 2% (2/100) in MC-IX, and 8% (6/73) in LA-N-5. These values were consistent with the data from direct analysis of ana- and telophase cells, also showing a higher frequency of non-binomial segregation in LA-N-5 (10%) compared to CHP-212 (2%) and MC-IX (2%). Hence, even though non-binomial distributions were rare in the three cell lines, they were sufficiently frequent to generate cells with a DM copy-number strongly deviating from the modal value of the cell population.

Non-binomial distribution occurs through clustering at high DM copy numbers

One potential explanation of non-binomial DM segregation is detachment of multiple DMs at anaphase, leading to a decreased number of DMs in one of the daughter cells. Further image analysis of the ana- and telophase cells with non-binomial segregation showed that these cells rarely exhibited DMs that detached from the chromosomes, and no more than 4 DMs were observed to be detached in any single cell. This argued against loss of DMs through micronucleus formation as a mechanism for non-binomial segregation. However, the ana- and telophase cells with a non-binomial DM distribution had a higher median DM copy-number than those with a binomial distribution (median 74 vs. 40; $P<0.0001$ Mann-Whitney test; two-sided; pooled data from the three cell lines). Based on this, we selected 10 ana-telophases with a DM copy-number >50 from each cell line for a detailed analysis by confocal microscopy. This showed that all of the totally 30 analyzed ana-telophases exhibited at least one cluster of DMs at or adjacent to the chromosome termini (Figure 4A and B). The precise number of DMs in each cluster could not be determined at the obtained resolution level, but each cluster appeared to contain at least 5 DMs. In contrast, only approximately one third of ana-telophase cells with 50 or fewer DMs contained clusters, typically containing only two or three DMs.

Previous studies have shown that gamma radiation exposure induces clustering of DMs as well as elimination of DMs through micronucleation [16]. To evaluate whether non-binomial DM distribution could be promoted by radiation-induced clustering of DMs, we subjected CHP-212 cells to ionising radiation (2 Gy and 4 Gy) prior to *MYCN* FISH detection in ana-and telophase cells. Analysis of the DMs that remained attached to chromosomes, often arranged in clusters, indeed showed an elevated frequency of segregations deviating ($P<0.01$) from the binomial distribution compared to unexposed cells, 2% after 0 Gy, 22% after 2 Gy and 24% after 4 Gy (Figure 4C). Although copy-number estimation could be expected to be more error-prone in these mitoses, with many clustered DMs, our collected data thus indicated that clustering of DMs could be one cause of deviations from the binomial distribution at high DM copy-numbers.

DM frequency distributions can be modelled by selection imposed on the binomial distribution

Early studies of DMs in tumour bulk populations by chromosome banding have indicated that their overall copy-number distribution conforms neither to a binomial nor to a Poisson distribution [14]. Assessment of the DM copy-number distribution in metaphase spreads by FISH in CHP-212, LA-N-5, MC-IX and in primary cultures from two fresh neuroblastoma samples revealed a skewed non-binomial ($P<0.01$; Chi Square test) distribution in all samples, with a tail towards higher copy-numbers (Figure 5A and Supplementary Figure S2). These findings were similar to the distribution previously described in the SEWA-model [14], suggesting a uniform principle behind DM frequency distribution in different cell systems.

It has been well established that a high *MYCN*-copy number corresponds to elevated levels of *MYCN* expression [17–19], which in turn results in increased cellular proliferation [2,20–22]. Accordingly, when a colony formation assay was performed for CHP-212, the *MYCN* copy-number by interphase FISH was found to be significantly higher in colony-forming than in single cells (Figure 5B; >20 colonies and >100 single cells evaluated). Thus, proliferative advantages existed, at least *in vitro*, for cells with a high number of DMs, compared to those with a low number. On the other hand, cells with very high (>200 DMs) were extremely rare in our model systems, indicating some degree of selection against cells with an extremely high DM copy-number. Based on this, we hypothesized that cells with a higher DM copy-number would divide more frequently up to a certain copy-number level, where the selection pressure would continuously shift to become less favourable (Figure 6A). A simple algorithm applying these criteria on a model in which DMs segregated in a binomial fashion at mitosis reproduced the skewed frequency distribution observed in our cell lines and tumour biopsies when clonal growth from a single cell containing one DM was simulated (Figure 6B–C). Thus, a very simple model of Darwinian selection superimposed on binomial distribution of DMs at cell division was capable of explaining the frequency distribution of DMs, including a minority cell population with high *MYCN* copy numbers.

DMs are not irreversibly bound to positionally stable chromosome elements

Since DMs were localized very close to telomeres during mitosis, we investigated to what extent the mitotic segregation of

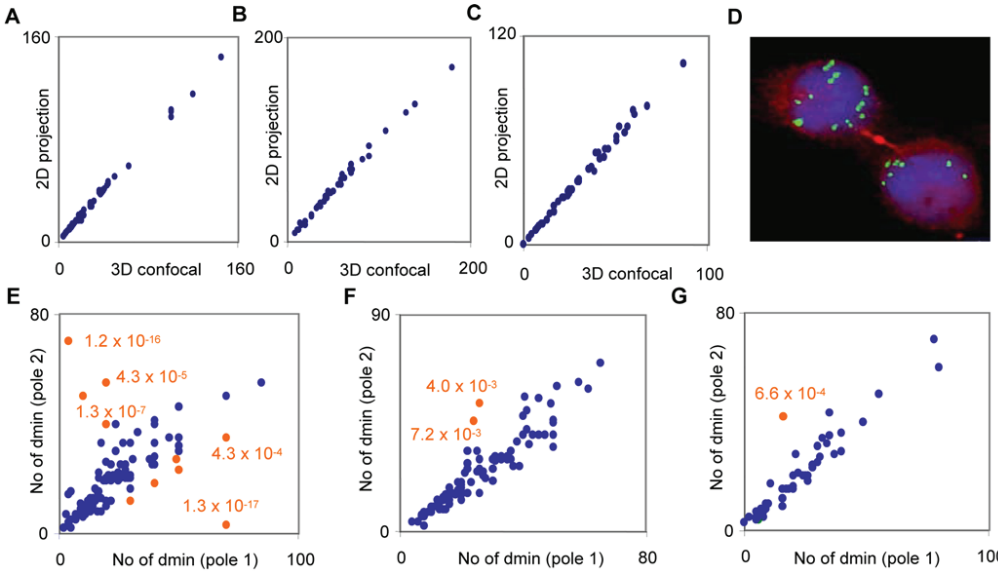

Figure 3. Statistics of DM segregation. A–C. DM copy-numbers in interphase nuclei obtained by scoring 1 μm confocal optical sections (three-dimensional, 3D) plotted against the copy-number obtained by scoring a projected (two-dimensional, 2D) image in LA-N-5 (A), CHP-212 (B) and MC-IX (C). **D.** Segregation of 7 and 10 DMs, respectively, to each daughter cell at telophase, shown by IF for beta tubulin (red) and FISH for *MYCN* (green). **E–G.** DM copy-numbers in ana/telophase poles typically follow a binomial distribution (blue data points) in LA-N-5 (E), CHP-212 (F), and MC-IX (G); ana-telophase cells significantly ($p<0.01$) deviating from the binomial distribution are denoted by orange data points.
doi:10.1371/journal.pone.0003099.g003

DMs was dependent on telomere stability. Neuroblastoma cell lines invariably express telomerase [23], which is believed to be crucial for stabilizing telomere length in transformed cells [24,25]. To shorten telomeres to a critical length and disrupt telosome function, we treated CHP-212 cells for 14 days with the telomerase inhibitor MST-312 [26,27]. MST-312 has been shown to inhibit telomerase activity by 47–66% in our culture system [28]. As expected, MST-312 treatment resulted in a significant shortening of telomeres as determined by quantitative FISH with peptide nucleic acid probes against TTAGGG-repeats (Figure 7A). Increased frequencies of chromosome termini without detectable TTAGGG-sequences were also observed, corresponding to critically short, potentially unstable telomeres (Figure 7B–D). Accordingly, MST-312 treated cells showed an elevated frequency of anaphase bridges compared to untreated CHP-212 cells (Figure 7E–F), indicating that telomere shortening induced global chromosomal instability in this cell line. However, when *MYCN*-FISH was performed on MST-312 treated ana-telophase cells, there was no difference in the number of cells deviating from a binomial distribution of DMs (Figure 7G), nor was there an

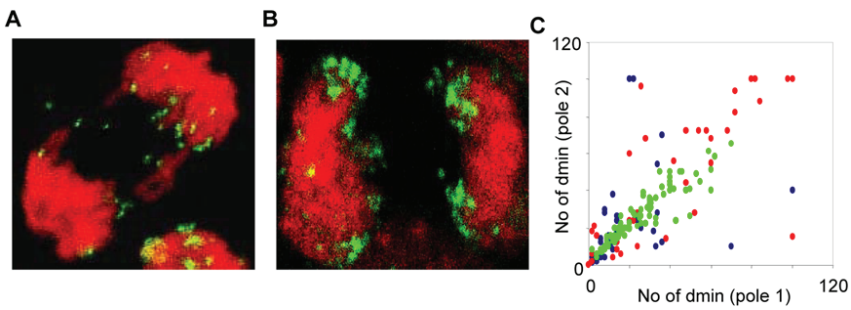

Figure 4. Clustering of DM at high copy-number. A–B. Clustering of DMs at cell division is less frequent in cells with lower (A) than with higher (B) DM copy-number, here exemplified by two anaphase cells. **C.** DM copy-numbers in CHP-212 ana/telophase poles prior to irradiation (green data points), after irradiation with 2 Gy (red data points), and after irradiation with 4 Gy (blue data points).
doi:10.1371/journal.pone.0003099.g004

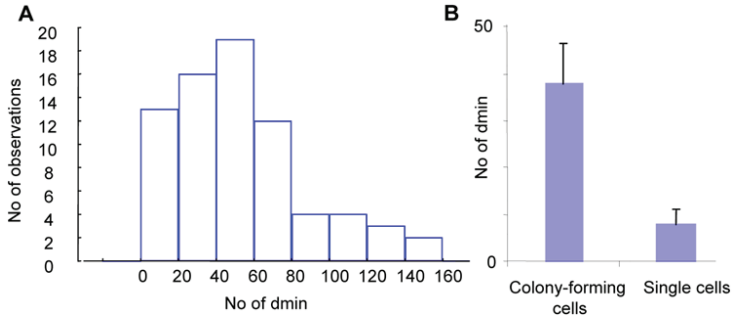

Figure 5. DM copy-number distributions in bulk populations. A. The frequency distribution of DM copy-numbers in near-diploid metaphase cells in LA-N-5 is skewed and differs from a normal distribution. **B.** Median DM-copy numbers in colony-forming compared to non-colony forming CHP-212 cells; error bars denote 25th and 75th percentiles.
doi:10.1371/journal.pone.0003099.g005

increase in the frequency of DMs that had detached from the chromosomes (one detached DM each in 2/50 cells after MST-312 treatment). Thus, DM segregation did not seem dependent on binding to functional telomeres in human chromosomes.

To further assess whether DMs were bound to any other positionally stable structures on human chromosomes, we used cell fusion by polyethylene glycol to create NB/mouse (CHP-212/3T3) hybrid nuclei. Human- and mouse- specific repetitive DNA sequences and *MYCN*-carrying DMs were then detected by triple colour FISH in these hybrid cells. Hybrid nuclei were obtained in approximately 1:60 cells. In all the 50 analysed hybrid nuclei, murine and human chromosome domains could be readily distinguished by our FISH strategy (Figure 7H). In these nuclei, 36–76% of DMs were located in murine chromosome domains and there was no difference in the number of DMs located in human domains compared to mouse domains (Figure 7I). In the few mitotic hybrid cells that were observed, DMs attached both to murine and human chromosomes (Figure 7J). Thus, DMs were free to relocate to murine chromosome domains in interspecies hybrid nuclei, indicating that they do not bind irreversibly to a specific positional element on human chromosomes.

Discussion

MYCN amplification is the strongest biological predictor of outcome in NB patients [1]. It has previously been shown that *MYCN* copy-numbers can be highly heterogeneous in NB cell populations. Such genetic heterogeneity may reflect different tumour clones and its role is believed to be under-recognized and underestimated in neuroblastoma biology [29]. In spite of this, the mechanisms behind clonal variability have been little investigated in NB cells. It is known from earlier studies that the DMs typically carrying *MYCN* copies *in vivo* do not separate at anaphase, but remain as double circles until G1-phase [14,15,30]. Evidently, a random distribution of DMs at the metaphase-anaphase transition would readily explain clonal variability [18], but whether the events governing DM distribution to daughter cells are really random had not previously been tested experimentally. Furthermore, the randomness function best approximating the behaviour of DMs had not been determined.

In the present study, we show that DMs in NB cells exhibit a regular topographic fluctuation during the cell cycle, translocating rapidly from the nuclear interior to the periphery of the prometaphase rosette at the initiation of cell division, attaching close to the telomeric repeat sequences. For the vast majority of DMs, this attachment was retained from prometaphase through telophase. After reconstitution of the interphase chromatin structure, the DMs relocated to the nuclear interior, possibly to occupy positions at the periphery of chromosome territories [18], separate to single minutes during G1-phase [15], and replicate in S-phase [30] as described. Our findings are highly consistent with previous descriptions of DM behaviour in non-NB model systems, including the human COLO322 [12,31] and the murine SEWA cell lines [14]. Thus our description of the mitotic topography of DMs mainly serves to confirm that previously suggested models of DM behaviour at cell division are applicable to NB. In contrast, our findings regarding the statistical distribution of DMs are novel and confirm a long held suspicion of the origin of oncogene copy-number heterogeneity.

We showed that the skewed frequency distributions of DM copy-number could be modelled by combining binomial mitotic segregation with a selection pressure favouring cells with a higher DM copy-number up to a certain level. The binomial distribution is the discrete probability distribution of the numbers in a sequence of n independent events, each of which yields one out of two possible outcomes with the probability p. In the context of DM segregation, n corresponds to the DM copy-number at metaphase. Because we assumed that each DM was equally likely to segregate to one of the daughter cells as to the other, p was set to 0.5. Our finding that DM copy-numbers can be described by a simple binomial distribution has at least three implications for the evolution of *MYCN* amplicons in NB cells: (1) *MYCN*-copies in DMs segregate independently of each other in a random fashion up to a certain copy-number level. (2) When this level has been reached, the random binomial model is no longer applicable; our experimental data indicate that this level is determined by the copy-number at which DMs start to interact with each other to form clusters, presumably because of the spatial restrictions of the mitotic figures. (3) The modal DM copy-number in the tumour cell population reflects the number of *MYCN*-copies conferring the greatest proliferative advantage under these cells' specific growth conditions. In the established cell lines and tumours used in the present study, this number varied between 25 and 50 DMs.

We cannot completely exclude that non-binomial segregation of clustered DMs also has a role in generating the skewed frequency distribution found in tumour bulk populations. However, non-binomial segregations were relatively rare in our material.

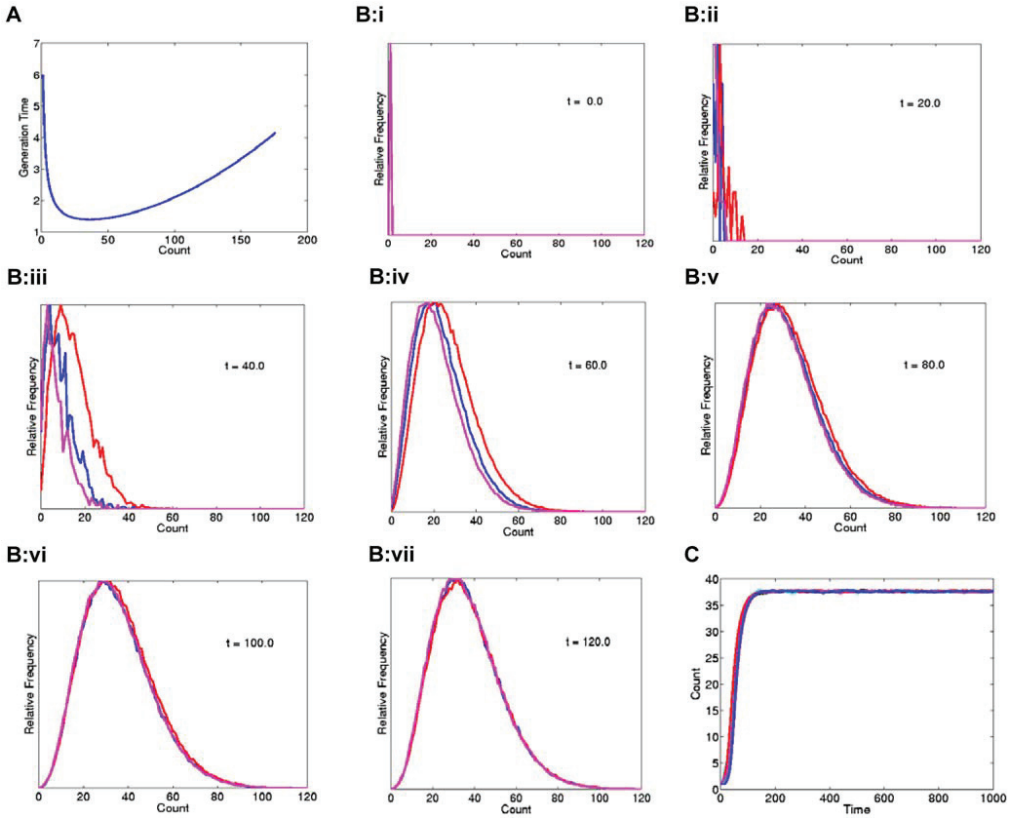

Figure 6. Mathematical modelling. A. Cellular generation time described as a continuous function of the DM-copy number count, with longer generation times for cells with low as well as extremely high DM copy-numbers. Each simulation was initiated with a single cell starting with a DM count equal to 1 at time zero. Cells with 36 DMs have the shortest generation time in the present model, while cells with fewer or extremely high DM-copy numbers proliferate more slowly. **B.** Convergence towards a skewed distribution for three modelled cell populations (purple, red, and blue curves). **C.** The equilibrium DM modal numbers for all populations correspond to the copy-number resulting in the shortest generation time in A (n = 36).

doi:10.1371/journal.pone.0003099.g006

Furthermore, they would be more likely to generate discrete sub-populations at non-modal copy-numbers rather than a continuous, skewed distribution. Our findings do not unequivocally explain the negative selection pressure at higher DM copy-numbers, although it points to clustering as a cause of non-binomial segregation at high copy-numbers. Such mitotic clustering should cause dramatic shifts in *MYCN*-copy number after cell division, potentially leading to dysregulation of *MYCN*-dependent intracellular signalling systems and apoptosis [32]. Nevertheless, our mathematical model is supported by several studies showing that *MYCN* amplification confers a proliferative advantage [5,33–35], and also by our own finding of a higher DM copy number among colony-forming CHP-212 cells compared to non-colony forming cells.

Our findings do not explain the molecular mechanisms underlying the topographical fluctuation of DMs during the cell cycle. The co-localisation of DMs and telomeric TTAGGG-repeats at mitosis could suggest that DMs bind to parts of the telosome multiprotein complex. However, disruption of telomere stability by telomere shortening induced by MST-312 failed to perturb the binomial segregation of DMs at cell division. Even though our studies do not fully exclude that DMs bound to the telomeres that remained intact after telomerase inhibition, our data speak against a specific interaction between DMs and the telosome complex. This was further supported by the finding that not all DMs co-localised with telomere repeats at cell division and also by our confocal microscopy and AFM images showing that several DMs were localised to interstitial segments close to the termini, rather than to the termini *per se*. A previous study has demonstrated that DMs are typically located at the periphery of folded chromosome territories in interphase nuclei [18]. It is possible that the centripetal force acting on centromeres during formation of the prometaphase rosette results in a centrifugal movement of DMs relative to the chromosomes as DMs do not interact with the mitotic spindle. The peripheral translocation of

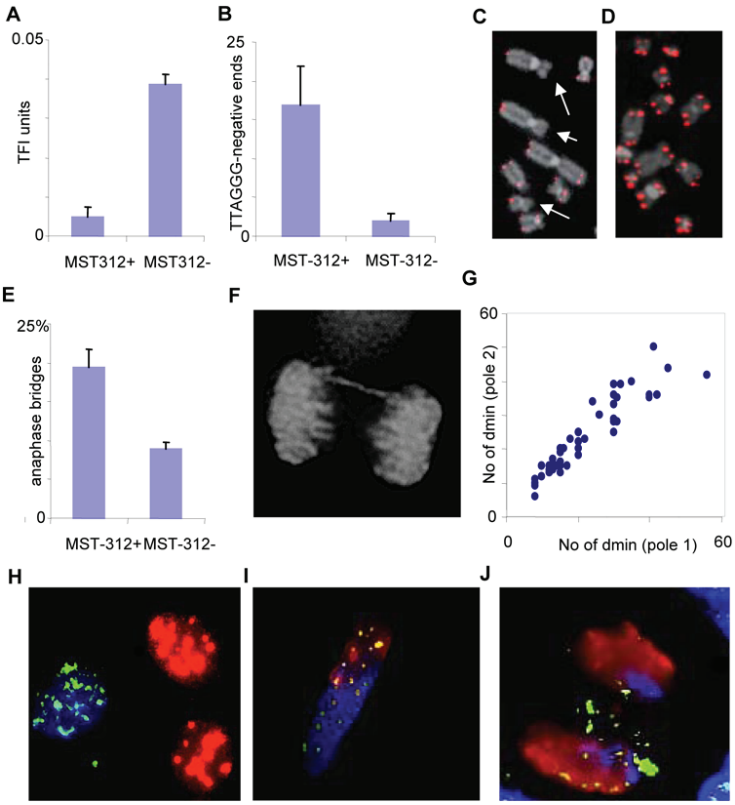

Figure 7. DMs do not bind to telomeres or other specific positional elements. A–B. Mean telomere length (A) assessed by arbitrary telomere fluorescence intensity (TFI) units and dysfunctional telomeres identified as the mean number of TTAGGG-negative chromosome termini (B) in CHP-212 cells exposed (MST312+) and not exposed (MST312-) to a telomerase inhibitor; errors bars denote standard deviations. **C–D.** A higher number of TTAGGG-negative chromosome termini (arrows) are observed by FISH after telomerase inhibition (C), compared to CHP-212 cells not exposed to the MST-312 inhibitor (D). **E–F.** Elevated frequency of anaphase bridging after MST-312 treatment. **G.** The DM distribution between telophase poles does not deviate from a binomial distribution after telomere dysfunction was induced by telomerase inhibition ($P>0.01$ for all data points). **H–J.** Co-hybridisation with mouse Cot-1 DNA (red), human Cot-1 DNA (blue) and human *MYCN* (green) probes readily distinguishes between the nuclei of co-cultured murine 3T3 and human CHP-212 cells (H); this labelling protocol also differentiates between murine and human chromatin domains in a murine/human hybrid nucleus (I) and in an anaphase cell (J) where some DMs have migrated into the murine chromatin domains (green-yellow in I and J).
doi:10.1371/journal.pone.0003099.g007

DMs at prometaphase formation would then be caused by DMs sliding longitudinally along the chromosomes as the interphase chromosome territories condense at prometaphase and are pulled centrally by the spindle fibres. Our findings are consistent with those of a previous study, based on the COLO322 cell line, showing that DMs were repelled from the spindle poles while they attached to the chromosome periphery [11]. Disrupting microtubule organization eliminated such peripheral localization of DMs in this model system, but it did not affect their association with chromosomes, indicating that a microtubule-mediated antipolar force would be responsible for the mitotic fluctuation of DMs. Together with our data, these findings imply that unspecific, weak biophysical forces cause the attachment of DMs to chromosomes during mitosis. This is supported by our finding that DMs could move freely in the interphase nuclei of interspecies hybrids.

The present study is one of a few showing a specific mechanism causing genetic heterogeneity by random events, which in turn can form the substrate for selection according to Darwinian principles, ultimately leading up to oncogene amplification and an increased proliferation of tumour cells. Furthermore, by clarifying the statistical principles of *MYCN* amplicon segregation, we have now acquired a precise standard against which the effects of potential anti-neuroblastoma drugs acting through *MYCN* amplicon elimination can be compared. The mechanisms by which DMs bind to chromosomes in NB clearly need to be studied further, particularly as the molecules participating in this attachment would be attractive therapeutic targets. If the binding of DMs to chromosomes could be efficiently, and specifically, inhibited, this could be an efficient way of eliminating *MYCN* amplicons from NB cells, thus causing growth reduction and apoptosis [5–7]. The

present study may provide a first step in identifying target proteins for such drugs, implicating weak biophysical forces rather then covalent attachments and binding to broadly distributed chromosome bio-molecules rather than specific binding to the telosome nucleoprotein complex.

Materials and Methods

Cell lines and cell culture

The study was reviewed and approved by the Ethics Review Board at Lund University Hospital, Sweden. The NB cell-lines CHP-212 and LA-N-5, the neuroepithelioma cell-line MC-IX, and mouse 3T3 cells were obtained from the American Type Culture Collection. Chromosome preparations from NB tumour biopsies and bone marrow infiltrates were obtained from the Department of Clinical Genetics in Lund. Cell culturing, harvest and chromosome preparation for FISH were according to standard methods [36]. All cells were cultured in DMEM:F12 1:1 supplemented with 10% foetal bovine serum and antibiotics. Single-cell clones were made from trypsinized single cell suspensions and plated in collagen- and fibronectin-coated chamber slides (5,000–10,000 cells/slide). Attaching cells were cultured for two weeks under standard conditions. The analysis was limited to colonies with a circular growth pattern, growing separate from other colonies, in order to avoid scoring colonies originating from different cells. Cell lines subjected to ionizing radiation were harvested for analysis 5–10 after irradiation, when mitotic figures were first visible by microscopic inspection.

FISH analysis

DMs were detected by single-copy probes for *MYCN* and *MYC* (Abbott Molecular Inc., Des Plaines, IL) and telomeric repeat sequences by fluorescein-conjugated $(CCCTAA)^3$ peptide nucleic acid probes as described [37]. Human and murine DNA sequences were identified by hybridisation with Cy3-labelled mouse Cot-1 and biotin-Cy5-labelled human Cot-1, respectively (Invitrogen, Stockholm, Sweden). The number of DMs was calculated manually in digital images acquired by a CCD camera coupled to an epi-fluorescence microscope. For combined immunofluoroscence and FISH, cells were fixed in $-20^{\circ}C$ methanol for 5–10 minutes and air-dried. Slides were then rehydrated in PBS containing 1% bovine serum albumin (BSA) for at least 30 min. Beta-tubulin was detected by the monoclonal antibody TUB2.1 (Sigma-Aldrich, St. Louis, MO), conjugated to Cy3, diluted 1:100 in 1% BSA/PBS and incubated with the target cells for 60 min at room temperature. After incubation, target cells were washed twice in 1% BSA/PBS and antibody conjugation was fixed by immersion in 1% formaldehyde for 5 min. After washing in PBS and dehydration in ethanol, FISH was performed by standard protocols without prior enzymatic pre-treatment.

Confocal microscopy

Cells were fixed according to Solovei et al. [18]. Confocal images were obtained on a Zeiss LSM 510 META system with an inverted Zeiss Axiovert 100 M microscope and LSM 510 META software version 3.2 (Carl Zeiss, Jena, Germany). FITC was excited with the 488 nm line of a krypton-argon laser and emission was collected through a Plan-Fluar 100x/1.45 NA objective using a band-pass 505–550 nm filter. DRAQ5-labelled chromatin (Biostatus Ltd, Shepshed, UK) was excited by the 633 nm line of a helium-neon laser and emission was collected using a band-pass 644.5–719.4 filter. The pinhole was adjusted to 1 AU (Airy units) when acquiring confocal images and set to 5 AU or above for two-dimensional images.

Combined AFM and FISH

Combined AFM and optical microscopy investigations were performed using a JPK Nanowizard II AFM with the JPK Life Science stage mounted on an inverted optical microscope (Nikon TE2000-U; JPK Instruments AG, Berlin, Germany). For all measurements, a Nikon CFI Plan Apo VC 60x, 1.40 DIC oil immersion objective was used. For epi-fluorescence a mercury light source was used in combination with standard filter blocks: DAPI (Ex 340-380nm, DM 400nm, BA 435-485nm), TRITC (Ex 540/25nm, DM 505nm, Em 605/55nm). A standard CCD camera was used for the digital imaging acquisition. Prior to AFM imaging, the samples were inspected by phase contrast microscopy to locate the regions of interest as well as for precise location of the AFM tip. The cantilever was placed above the selected region using the positioning screws on the stage before approaching the tip to the sample surface. For AFM imaging, standard noncontact cantilevers were used in intermittent contact mode to reduce the lateral forces during scanning. The scan speeds were typically 0.3–0.5 Hz when acquiring images with 512×512 pixels. AFM and FISH images were superimposed using AdobePhotoshop.

Interspecies cell hybrids

Cytoplasmic membrane fusion was achieved in sub-confluent cultures containing CHP-212 and 3T3 cells at equal proportions by washing in serum-free medium, followed by treatment with 50% polyethylene glycol (PEG 6000, BDH Chemicals Ltd., Poole, UK) for 2 min. PEG-treated cells and untreated control cultures were then grown in DMEM:F12 1:1 supplemented with 10% foetal bovine serum and antibiotics for 3–4 days before harvest.

Telomerase inhibition

The MST-312 telomerase inhibitor (Calbiochem/EMD Biosciences, Madison, WI) was diluted in DMSO and used at a noncytotoxic concentration of 1.0 μmol/L (25). To maintain a stable concentration of MST-312, the medium was changed every third day. Cultures exposed only to DMSO were cultured in parallel as controls. Colony formation assay was done by plating 10 000 cells on chamber slides. The rate of population doubling was measured by colony formation assay at regular intervals with colonies defined as groups of >10 cells.

Mathematical modelling

The time between divisions for a cell with n DMs was set to $1+10/(1+n)+n\hat{}2/10000$, where the term 1 was the lower limit of the inter-mitotic time, and the term $10/(1+n)$ simulated the growth advantage of cells with high DM copy-numbers. $1/(n+1)$ was used instead of $1/n$ so that cells with 0 DMs would obtain a finite time to the next division. The term $n\hat{}2/10000$ was used to simulate a penalty on cells with very high DM counts. After each mitotic cycle, the n for each cell was doubled and then distributed randomly according to a binomial function between the two daughter cells. To keep computations limited we capped the cell population at 100,000 by random deletion. Each simulation was initiated with a single cell starting with a DM count equal to 1 at time zero. Matlab (MathWorks, Kista, Sweden) programming was used to simulate the growth of each population according to these rules.

Supporting Information

Figure S1 Single cell colonies. DM interphase copy-number distributions in single-cell-derived colonies from LA-N-5, CHP-212, and MC-IX. Scored interphase nuclei correspond to red and grey circles, respectively, of which only the former were included

in the statistical analysis (see text). Variations in DM copy-number that were not explained ($P<0.01$) by a binomial distribution are marked by arrows.
Found at: doi:10.1371/journal.pone.0003099.s001 (0.57 MB TIF)

Figure S2 DM copy-numbers. The DM frequency distribution in near-diploid metaphase cells in the CHP-212 and MC-IX cell lines, and in biopsies from one primary NB (Patient 1), and one bone marrow NB metastasis (Patient 2). Similar to SK-N-5, the distributions are skewed towards higher copy-numbers and differ from a normal distribution ($P<0.01$; Chi Square Test).
Found at: doi:10.1371/journal.pone.0003099.s002 (0.10 MB TIF)

Author Contributions

Conceived and designed the experiments: GL UH HS SP DG. Performed the experiments: GL AR UH HS YJ YS DG. Analyzed the data: GL AR UH HS DG. Contributed reagents/materials/analysis tools: SP. Wrote the paper: GL DG.

References

1. Seeger RC, Brodeur GM, Sather H, Dalton A, Siegel SE, et al. (1985) Association of multiple copies of the N-myc oncogene with rapid progression of neuroblastomas. N Engl J Med 313: 1111–1116.
2. Brodeur GM (2003) Neuroblastoma: biological insights into a clinical enigma. Nat Rev Cancer 3: 203–216.
3. Norris MD, Bordow SB, Haber PS, Marshall GM, Kavallaris M, et al. (1997) Evidence that the MYCN oncogene regulates MRP gene expression in neuroblastoma. Eur J Cancer 33: 1911–1916.
4. Shohet JM, Hicks MJ, Plon SE, Burlingame SM, Stuart S, et al. (2002) Minichromosome maintenance protein MCM7 is a direct target of the MYCN transcription factor in neuroblastoma. Cancer Res 62: 1123–1128.
5. Narath R, Ambros IM, Kowalska A, Bozsaky E, Boukamp P, et al. (2007) Induction of senescence in MYCN amplified neuroblastoma cell lines by hydroxyurea. Genes Chromosomes Cancer 46: 130–142.
6. Tonelli R, Purgato S, Camerin C, Fronza R, Bologna F, et al. (2005) Anti-gene peptide nucleic acid specifically inhibits MYCN expression in human neuroblastoma cells leading to cell growth inhibition and apoptosis. Mol Cancer Ther 4: 779–786.
7. Yaari S, Jacob-Hirsch J, Amariglio N, Haklai R, Rechavi G, et al. (2005) Disruption of cooperation between Ras and MycN in human neuroblastoma cells promotes growth arrest. Clin Cancer Res 11: 4321–4330.
8. Moreau LA, McGrady P, London WB, Shimada H, Cohn SL, et al. (2006) Does MYCN amplification manifested as homogeneously staining regions at diagnosis predict a worse outcome in children with neuroblastoma? A Children's Oncology Group study. Clin Cancer Res 12: 5693–5697.
9. Barker PE (1982) Double minutes in human tumor cells. Cancer Genet Cytogenet 5: 81–94.
10. Barker PE, Drwinga HL, Hittelman WN, Maddox AM (1980) Double minutes replicate once during S phase of the cell cycle. Exp Cell Res 130: 353–360.
11. Kanda T, Otter M, Wahl GM (2001) Mitotic segregation of viral and cellular acentric extrachromosomal molecules by chromosome tethering. J Cell Sci 114: 49–58.
12. Kanda T, Wahl GM (2000) The dynamics of acentric chromosomes in cancer cells revealed by GFP-based chromosome labeling strategies. J Cell Biochem Suppl Suppl 35: 107–114.
13. Levan A, Levan G (1978) Have double minutes functioning centromeres? Hereditas 88: 81–92.
14. Levan G, Mandahl N, Bregula U, Klein G, Levan A (1976) Double minute chromosomes are not centromeric regions of the host chromosomes. Hereditas 83: 83–90.
15. Deng X, Zhang L, Zhang Y, Yan Y, Xu Z, et al. (2006) Double minute chromosomes in mouse methotrexate-resistant cells studied by atomic force microscopy. Biochem Biophys Res Commun 346: 1228–1233.
16. Schoenlein PV, Barrett JT, Kulharya A, Dohn MR, Sanchez A, et al. (2003) Radiation therapy depletes extrachromosomally amplified drug resistance genes and oncogenes from tumor cells via micronuclear capture of episomes and double minute chromosomes. Int J Radiat Oncol Biol Phys 55: 1051–1065.
17. Schneiderman J, London WB, Brodeur GM, Castleberry RP, Look AT, et al. (2008) Clinical significance of MYCN amplification and ploidy in favorable-stage neuroblastoma: a report from the Children's Oncology Group. J Clin Oncol 26: 913–918.
18. Solovei I, Kienle D, Little G, Eils R, Savelyeva L, et al. (2000) Topology of double minutes (dmins) and homogeneously staining regions (HSRs) in nuclei of human neuroblastoma cell lines. Genes Chromosomes Cancer 29: 297–308.
19. Stock C, Bozsaky E, Watzinger F, Poetschger U, Orel L, et al. (2008) Genes proximal and distal to MYCN are highly expressed in human neuroblastoma as visualized by comparative expressed sequence hybridization. Am J Pathol 172: 203–214.
20. Brodeur GM, Seeger RC, Schwab M, Varmus HE, Bishop JM (1984) Amplification of N-myc in untreated human neuroblastomas correlates with advanced disease stage. Science 224: 1121–1124.
21. Stallings RL (2007) Origin and functional significance of large-scale chromosomal imbalances in neuroblastoma. Cytogenet Genome Res 118: 110–115.
22. Tsuda T, Obara M, Hirano H, Gotoh S, Kubomura S, et al. (1987) Analysis of N-myc amplification in relation to disease stage and histologic types in human neuroblastomas. Cancer 60: 820–826.
23. Choi LM, Kim NW, Zuo JJ, Gerbing R, Stram D, et al. (2000) Telomerase activity by TRAP assay and telomerase RNA (hTR) expression are predictive of outcome in neuroblastoma. Med Pediatr Oncol 35: 647–650.
24. Oshimura M, Barrett JC (1997) Multiple pathways to cellular senescence: role of telomerase repressors. Eur J Cancer 33: 710–715.
25. Smith LL, Coller HA, Roberts JM (2003) Telomerase modulates expression of growth-controlling genes and enhances cell proliferation. Nat Cell Biol 5: 474–479.
26. Seimiya H, Oh-hara T, Suzuki T, Naasani I, Shimazaki T, et al. (2002) Telomere shortening and growth inhibition of human cancer cells by novel synthetic telomerase inhibitors MST-312, MST-295, and MST-1991. Mol Cancer Ther 1: 657–665.
27. Seimiya H, Sawada H, Muramatsu Y, Shimizu M, Ohko K, et al. (2000) Involvement of 14-3-3 proteins in nuclear localization of telomerase. EMBO J 19: 2652–2661.
28. Jin Y, Stewenius Y, Lindgren D, Frigyesi A, Calcagnile O, et al. (2007) Distinct mitotic segregation errors mediate chromosomal instability in aggressive urothelial cancers. Clin Cancer Res 13: 1703–1712.
29. Thorner PS, Ho M, Chilton-MacNeill S, Zielenska M (2006) Use of chromogenic in situ hybridization to identify MYCN gene copy number in neuroblastoma using routine tissue sections. Am J Surg Pathol 30: 635–642.
30. Itoh N, Shimizu N (1998) DNA replication-dependent intranuclear relocation of double minute chromatin. J Cell Sci 111(Pt 22): 3275–3285.
31. Kanda T, Sullivan KF, Wahl GM (1998) Histone-GFP fusion protein enables sensitive analysis of chromosome dynamics in living mammalian cells. Curr Biol 8: 377–385.
32. Tang XX, Zhao H, Kung B, Kim DY, Hicks SL, et al. (2006) The MYCN enigma: significance of MYCN expression in neuroblastoma. Cancer Res 66: 2826–2833.
33. del Carmen Mejia M, Navarro S, Pellin A, Ruiz A, Castel V, et al. (2002) Study of proliferation and apoptosis in neuroblastoma. Their relation with other prognostic factors. Arch Med Res 33: 466–472.
34. Paffhausen T, Schwab M, Westermann F (2007) Targeted MYCN expression affects cytotoxic potential of chemotherapeutic drugs in neuroblastoma cells. Cancer Lett 250: 17–24.
35. Schweigerer L, Breit S, Wenzel A, Tsunamoto K, Ludwig R, et al. (1990) Augmented MYCN expression advances the malignant phenotype of human neuroblastoma cells: evidence for induction of autocrine growth factor activity. Cancer Res 50: 4411–4416.
36. Gisselsson D (2001) Refined characterisation of chromosome aberrations in tumours by multicolour banding and electronic mapping resources. Methods Cell Sci 23: 23–28.
37. Lansdorp PM, Verwoerd NP, van de Rijke FM, Dragowska V, Little MT, et al. (1996) Heterogeneity in telomere length of human chromosomes. Hum Mol Genet 5: 685–691.

II

GENES, CHROMOSOMES & CANCER 50:250–262 (2011)

Alternative Lengthening of Telomeres—An Enhanced Chromosomal Instability in Aggressive Non-*MYCN* Amplified and Telomere Elongated Neuroblastomas

Gisela Lundberg,[1]* Daniel Sehic,[1] John-Kalle Länsberg,[2] Ingrid Øra,[2,3] Attila Frigyesi,[4] Victoria Castel,[5] Samuel Navarro,[6] Marta Piqueras,[6] Tommy Martinsson,[7] Rosa Noguera,[6] and David Gisselsson[1,8]

[1]Department of Clinical Genetics, Lund University, University and Regional Laboratories, Skåne University Hospital, Lund, Sweden
[2]Department of Paediatric Oncology and Haematology, Skåne University Hospital, Lund, Sweden
[3]Department of Human Genetics, Academic Medical Center, Amsterdam, The Netherlands
[4]Department of Anaesthesiology and Intensive Care, Skåne University Hospital, Lund, Sweden
[5]Pediatric Oncology Service, La Fe Hospital, Valencia, Spain
[6]Department of Pathology, Medical School, University of Valencia, Valencia, Spain
[7]Department of Clinical Genetics, Gothenburg University, Gothenburg, Sweden
[8]Department of Pathology, Skåne University and Regional Laboratories, Lund, Sweden

Telomere length alterations are known to cause genomic instability and influence clinical course in several tumor types, but have been little investigated in neuroblastoma (NB), one of the most common childhood tumors. In the present study, telomere-dependent chromosomal instability and telomere length were determined in six NB cell lines and fifty tumor biopsies. The alternative lengthening of telomeres (ALT) pathway was assayed by scoring ALT-associated promyelocytic leukemia (PML) bodies (APBs). We found a reduced probability of overall survival for tumors with increased telomere length compared to cases with reduced or unchanged telomere length. In non-*MYCN* amplified tumors, a reduced or unchanged telomere length was associated with 100% overall survival. Tumor cells with increased telomere length had an elevated frequency of APBs, consistent with activation of the ALT pathway. The vast majority of tumor biopsies and cell lines exhibited an elevated rate of anaphase bridges, suggesting telomere-dependent chromosomal instability. This was more pronounced in tumors with increased telomere length. In cell lines, there was a close correlation between lack of telomere-protective TTAGGG-repeats, anaphase bridging, and remodeling of oncogene sequences. Thus, telomere-dependent chromosomal instability is highly prevalent in NB, and may contribute to the complexity of genomic alterations as well as therapy resistance in the absence of *MYCN* amplification and in this tumor type.

INTRODUCTION

Neuroblastoma (NB) is one of the most common childhood tumors. It is the most frequent solid tumor of infancy, becoming less prevalent in each succeeding year of age (London et al., 2005). NB has a diverse pattern of somatic chromosome changes, of which some closely correlate to clinical features. Among the genomic changes known to be associated with poor outcome are amplification of the *MYCN* gene (Brodeur et al., 1984), loss of heterozygosity in chromosome arms 1p (Brodeur et al., 1977) and 11q (Srivatsan et al., 1991), and gain of sequences from 17q (Attiyeh et al., 2005). It remains to be shown by what mechanism somatic chromosome changes occur in NB. It is known from previous studies of other tumor types that shortened dysfunctional telomeres in neoplastic cells can trigger chromosome changes (Artandi et al., 2000; Gisselsson et al., 2001). Telomeres are composed of tandem repeats of TTAGGG sequences ending in a 3′single-strand overhang, forming a T-loop at the end of human chromosomes (de Lange, 2005). They thereby protect chromosomes from end-to-end fusions, provide a mechanism for replication of linear DNA, and limit the replicative life span of somatic cells (Chan and Blackburn, 2004). Chromosome ends with strongly reduced telomere lengths compromise the ability of cells to

Supported by: Swedish Children's Cancer Foundation, the Swedish Cancer Society, the Swedish Research Council, the Swedish Medical Society, the Lund University Hospital Donation Funds, the Gunnar Nilsson Cancer Foundation, the Crafoord Foundation, the Erik-Philip Sörensen Foundation, the Lundgren Foundation, the Schyberg Foundation, and the Medical Faculty at Lund University.

*Correspondence to: Gisela Lundberg, Department of Clinical Genetics, Lund University Hospital, SE 221 85 Lund, Sweden. E-mail: gisela.lundberg@med.lu.se

Received 20 July 2010; Accepted 30 November 2010

DOI 10.1002/gcc.20850

Published online 14 January 2011 in Wiley Online Library (wileyonlinelibrary.com).

continue cell division and are prone to fusion with each other through nonhomologous end-joining (Capper et al., 2007). The resulting dicentric chromosomes stabilize telomere-free ends but are likely to break in mitosis and initiate cycles of chromosomal breakage-fusion-bridge events in cells with abrogated DNA-damage response (McClintock, 1938). This type of genome instability has been associated with the accumulation of genetic changes such as deletions, unbalanced translocations, and amplifications in cancer cells. Telomere length alterations have also been associated with clinical outcome in several hematological neoplasms, e.g., myelodysplastic syn-dromes (Ohyashiki et al., 1999), acute myeloid leukemia (Swiggers et al., 2006), and chronic lymphocytic leukemia (Bechter et al., 1998), as well as in solid tumors such as breast cancer (Fordyce et al., 2006), prostate cancer (Donaldson et al., 1999), nonsmall cell lung cancer (Frias et al., 2008), and Ewing sarcoma (Avigad et al., 2007).

With regard to NB, early studies by Hiyama et al., (Hiyama et al., 1992) suggested that a reduction of telomeric repeats correlated to advanced stages of disease and poor prognosis. On the other hand, more extensive studies by the same group as well as another team have recently indicated that long or unchanged telomere length in NB cells compared with a patient's normal white blood cells are predictive of a poor outcome in high-risk patients, whereas short telomeres are associated with an favorable outcome (Ohali et al., 2006; Onitake et al., 2009). In light of this, additional corroborative studies of the correlation between telomere length and clinical course would be valuable. In addition, it remains unclear how telomere length is regulated in NB. Previous studies were unable to show any clear association between telomere length and expression/activity of the telomerase enzyme, indicating that telomere elongation in NB occurs through an alternative route (Onitake et al., 2009). Finally, the consequence of telomere length dysregulation on genomic stability in NB has not been addressed in previous studies. The aim of the present study was to investigate further the telomere alterations in NB, and to assess how these correlate to clinical outcomes and to explore whether telomere length alterations are associated with an increased formation rate of structural chromosome alterations. We also evaluated the presence of the alternative lengthening of telomeres (ALT) pathway in NB.

MATERIALS AND METHODS

Patients and Tissue Samples

Formalin-fixed paraffin-embedded tissue blocks were obtained from the Department of Pathology at Lund University Hospital, Lund, Sweden. Only tumors classified as primary neoplasms were included, after having undergone histopathological review. In total, 34 tumors from Lund University Hospital were found sufficient for telomere length analysis, with a minimum of 50 NB and 30 non-neoplastic, mainly endothelium and occasionally stroma cells, assessable cell nuclei present in the biopsy. For quantitative fluorescence *in situ* hybridization (Q-FISH) 3.5–4 μm sections were cut from the paraffin blocks and applied to positively charged slides (DAKO, Glostrup, Denmark). Complementary samples were obtained from a tissue micro array (TMA), from the Department of Human Genetics, Academic Medical Center in Amsterdam, but here only four out of forty-four tumor samples had a sufficient number of non-neoplastic cells to be included in the study. Another 12 samples fulfilling the criteria for inclusion were obtained from TMAs from the Department of Pathology, Valencia Medical School. The patients were classified according to the International NB Staging System (Brodeur et al., 1993) and divided into clinical-genetic risk groups as follows:

- Low-risk: Stage 1, any age, with or without *MYCN*-amplification; stage 2a/2b, any age without *MYCN*-amplification; stage 4S, <18 months, without *MYCN*-amplification
- Intermediate-risk: Stage 3, any age without *MYCN*-amplification; stage 4, age <18 months without *MYCN*-amplification
- High-risk: stage 2a, 2b, 3 and 4, any age and *MYCN*-amplification

All patients were treated according to the European protocol active at the time and stage of their disease. The follow-up time ranged from 12 days (dead of disease) to 15 years. Written consent was given by the parents for documentation, biological studies, and analysis of medical data. The study was approved by the ethics review boards of the participating institutes.

Cell Lines and Cell Culture

The human NB cell-lines SH-SY5Y, SK-N-BE (2C), IMR32, CHP-212, and SK-N-FI were originally obtained from the American Type Culture

Collection. LA-N-5 has been established by Dr. Robert Seeger, Children's Hospital, Los Angeles. Cell culture, harvest, and chromosome preparation for fluorescence *in situ* hybridization (FISH) from cultured cells were according to standard methods (Gisselsson et al., 2001). Telomeric TTAGGG repeats were visualized in cultured cells by FISH with fluorescein-conjugated $(CCCTAA)_3$ peptide nucleic acid probes (DAKO, Glostrup, Denmark), and the number of negative chromosome termini was scored in metaphase cells of the lowest ploidy level. Although a negative terminus may still contain up to 500 bp of TTAGGG repeat sequences, this method has previously been shown to yield a valid assessment of the protective capacity of telomeres (Gisselsson et al., 2001). In normal fibroblasts, taken from the forearm dermis on a volunteering healthy male, used as controls, the number of TTAGGG-negative ends was 0–1 per metaphase cell. To determine the frequency of telomere fusion events, a pan-alpha satellite probe was used (Cambio, Cambridge, United Kingdom). The *MYCN* copy-number was evaluated by FISH with custom-labeled probes (Vysis/Abbott Molecular, Des Plaines, Illinois), according to standard procedures (Gisselsson et al., 2001). A finding of more than nine copies of this gene was scored as genomic amplification, including continuously fluorescence-positive chromosome segments corresponding to >9 copies (Ambros and Ambros, 2001).

Assessment of Relative Telomere Length in Tissue Sections

Slides with tissue sections were preheated in an oven at 65°C for at least 10 min to melt the paraffin. They were then deparaffinised in xylene for 2 × 5 min, followed by hydration through a graded ethanol series, followed by washing in deionized water. The slides were then immersed in 100 mM Tris/EDTA pH 7.0 at 95°C for 15 min, followed by washing in deionized water and PBS with 0.05% Tween 20 (PBST). The samples were dehydrated in a graded ethanol series, after which the telomere probe was applied. Tissue sections were covered with a coverslip and the edges were cemented with rubber glue. The probe and target nuclei were then codenaturated on a hot plate at 84°C for 4 minutes, after which the slides were placed in a humidified chamber for 2 hr at room temperature. Stringency washing was in 70% formamide/10 mmoL/Tris, pH 7.5 for 2 × 15 min. The slides were drained and stained with DAPI at 1:10,000 dilution of 5 mg/ml stock solution, rinsed with PBST and water and mounted with ProLong antifade (Invitrogen Molecular Probes, Carlsbad, California). For each case the same optimized exposure settings were used throughout the biopsy, for both neoplastic and non-neoplastic endothelial and stromal cells. Images were captured with a charged-coupled device camera coupled to an epifluorescence microscope and the Cytovision software (Applied Imaging International, Newcastle, United Kingdom). 2-D images were taken using the *z*-stack with 10 planes at 0.350 μm. All telomere length measurements were made without prior knowledge of clinical data. Relative telomere lengths were assessed by fluorescence quantifications as described (Meeker et al., 2002), using the ImageJ telometer plug- in (http://bui2.win.ad.jhu.edu/telometer). This method has previously been validated as a stable method (Poon et al., 1999; Meeker et al., 2002; Ferlicot et al., 2003; O'sullivan et al., 2004).

Combined Telomere and Promyelocytic Leukemia Body Detection

Paraffin sections were deparaffinized twice in xylene for 5 minutes each, in absolute ethanol for 5 minutes, and in 95% ethanol for 3 minutes. A pressure heater (BIOCARE, Decloaking Chamber DC2002 CE, Concord, California, USA) was used for heat-induced epitope retrieval (HIER) and was filled with 500 ml distilled water. Slides were placed in a plastic chamber filled with enough retrieval buffer solution (S2367, DAKO) to cover the tissue on each slide. HIER was preformed at 120°C for 20–30 min and with cool down for at least 20 min. Slides were then washed with PBS for 5 minutes and dehydrated in 70%, 85%, and absolute ethanol for 1 min each. The telomere probe (K5326, DAKO) was added to the slides and covered with rubber-glued cover slips. Probe and target DNA were codenatured for 4 min and incubated for 2 hr at room temperature in the dark. The samples were washed with rinse solution 3 (K5326, DAKO) for 1 min and washed with wash solution 4 (K5326, DAKO) at 40°C for 5 min. Slides were then washed with PBS for 5 min and blocked with 1% milk powder in PBS for 30 min at room temperature. The promyelocytic leukemia (PML) primary antibody (abcam, ab53773, Cambridge, United Kingdom; diluted 1/100 in blocking solution) was added to the slides and incubated for 1 hr at room temperature,

followed by washing in block solution for 5 min. Anti rabbit secondary antibodies labeled with FITC (F1262-1ML, SIGMA, Stockholm, Sweden; diluted 1/100 in blocking solution) were added to the slides and incubated for 30 min at room temperature. Slides were washed in block solution for 5 min, PBS for 1 min and dehydrated in 70%, 85%, and absolute ethanol for 1 min each. Slides were then stained with 2% DAPI (0.5 mg/ml) with DABCO, and if needed with Prolong Antifade Kit (P7481, Abcam). Nuclei with ALT-associated PML protein nuclear bodies (APBs) were scored based on focal colocalization of PML protein (FITC) and telomere signal (Cy3). Only nuclei in which the PML signals colocalized with any of the five strongest telomere signals were scored as APB-positive. In each case, scoring was performed on at least 100 PML-positive nuclei. At least 1,000 nuclei in total were studied in each case. To provide negative controls, tissue sections were subjected to the same procedure as described above, but without addition of PML-antibody. Control tissue sections uniformly showed APB-negative nuclei (data not shown). APB-detection in cell lines was performed as for paraffin sections with omission of the deparaffination and epitope retrieval steps. Reproducibility of the APB detection method was evaluated by independent scoring of APBs in of SK-N-BE (2C) and its subline SK-N-BE(2C)X, showing consistent results (mean prevalence 4.7% compared to 5.7%, $P = 0.72$, t test).

Assessment of 1p and 11q Deletions and *MYCN* Amplification by Genome Arrays

For the majority of tumors, 1p and *MYCN* amplification was determined by FISH, according to standard clinical laboratory procedures. For the tumors from Amsterdam, DNA was extracted and analyzed using the Illumina Infinium^{TM} II Bead Chip technology (Illumina, San Diego, California, USA) (Gunderson et al., 2005; Steemers et al., 2006). Intensity values were determined and loaded into Illumina's genotype analysis software, Genome Studio. Segmentation and further data analysis including designation of 1p and *MYCN* amplification were performed with BAF segmentation (Staaf et al., 2008) and analysis in Nexus (Bio Discovery, El Segundo, California, USA).

Analysis of Chromosome Segregation Errors

The frequency of anaphase bridges was determined as previously described (Stewenius et al., 2005). For cell lines, proliferating cells were harvested without Colcemid, washed in PBS for 5 min, fixed in methanol:acetic acid (3:1) for 30 min, air dried, and stained with H&E (HE). For tissue sections, archived H&E -stained slides were used. At least 30 anaphase cells were analyzed in each case. Anaphase bridges were defined as strings of chromatin either connecting the two poles or stretching from one pole in the direction of the other pole and spanning >2/3 of the interpolar distance. The frequency of anaphase bridges was calculated as the ratio between cells exhibiting such bridges and the total number of anaphase cells.

Statistical Analysis

Telomere length was classified as increased, unchanged, or decreased in tumor cells compared with non-neoplatic cells at $P < 0.05$ by Mann-Whitney t test and Student's t test. To increase the stringency of the analysis, both tests had to show a significant difference for a case to be classified as having increased or decreased tumor telomere length (TTL). Fisher's exact test was used for nonparametric tests (STATISTICA version 8.0, StatSoft, Inc. 2008, Tulsa, OK). Survival (Kaplan-Meier, overall) and multivariate (general linear model, tests of between-subjects effects) analyses were made in SPSS for Windows, Rel. 18.0.0. 2008 (SPSS Inc., Chicago, IL). Overall survival was defined as complete remission at the end of the follow-up period. Event-free survival analysis was not performed since the cases with increased TTL either had a complete remission or was dead of the disease (DOD). Cases with *MYCN* amplification and/or 1p loss of heterozygosity were combined into a single group because these changes were concurrent in the majority of cases.

RESULTS

MYCN Amplification Is Rare in Primary Tumors with Long Telomeres

We first analyzed the relative median telomere length in NB cells compared with that of surrounding non-neoplastic cells (stroma and endothelium) in tissue sections from 50 primary NBs, using Q-FISH (Table 1; Figs. 1A and 1B). To evaluate whether our series of patients was representative with respect to clinical outcome, Kaplan-Meier plots according to risk-groups and

TABLE 1. Clinical and Biological Parameters

Case	Pathology[a]	Sex[b]	Age at diagnosis (mo)	TTL	Risk group[c]	Stage	MYCN amplification[d]	1p deletion[d]	Current status[e]
1	NB	F	55	Increased	H	4	–	–	DOD
2	NB	M	3.5	Increased	I	3	–	–	CR
3	NB	F	6.5	Increased	L	2	–	–	CR
4	GNB	F	27	Increased	H	4	–	–	PR
5	NB	M	28	Increased	H	4	–	–	DOD
6	NB	M	63	Increased	H	4	–	–	DOD
7	NB	M	26	Increased	H	4	–	–	DOD
8	NB	F	439	Increased	H	4	–	–	DOD
9	NB	M	24	Increased	H	4	–	–	CR
10	NB	F	80	Increased	I	3	–	+	DOD
11	NB	F	11	Unchanged	L	2B	–	–	PR
12	NB	F	25	Unchanged	I	3	–	–	CR2
13	NB	F	50	Unchanged	H	4	+	+	DOD
14	NB	M	12	Unchanged	I	3	–	–	CR
15	NB	M	0.3	Unchanged	L	I	–	–	CR
16	NB	F	4.0	Unchanged	I	3	–	–	PR
17	NB	M	21	Unchanged	H	4	+	+	DOD
18	NB	F	0.3	Unchanged	L	I	–	–	CR
19	NB	M	9.5	Unchanged	H	4S	+	+	DOD
20	GNB	F	1.5	Unchanged	L	2B	ND	ND	PR
21	NB	F	51	Unchanged	H	4	–	–	DOD
22	NB	F	7.0	Unchanged	I	3	–	–	CR
23	NB	F	16	Decreased	L	I	–	–	CR
24	NB	F	3.0	Decreased	I	4	–	+	CR2
25	NB	M	8.0	Decreased	L	I	–	–	CR
26	NB	F	2.0	Decreased	L	I	–	–	CR
27	NB	F	22	Decreased	H	4	+	+	PD
28	NB	M	24	Decreased	I	3	–	–	CR
29	NB	M	14	Decreased	H	4	+	+	CR2
30	NB	M	6.0	Decreased	I	3	–	–	CR2
31	NB	F	41	Decreased	L	2B	–	–	CR
32	NB	F	7.7	Decreased	L	2B	–	ND	CR
33	GNB	F	13	Decreased	L	I	–	–	CR
34	NB	M	2.0	Decreased	L	2A	–	–	CR
35	GNB	M	58	Decreased	L	2A	–	–	CR
36	NB	M	37	Decreased	H	4	+	–	DOD
37	NB	F	2.0	Decreased	I	4S	–	–	CR
38	NB	M	4.2	Decreased	L	2B	–	–	CR2
39	NB	M	4.0	Decreased	I	3	–	–	CR
40	NB	M	227	Decreased	H	4	+	+	CR
41	NB	F	79	Decreased	H	4	+	+	DOD
42	NB	M	9.0	Decreased	H	3	+	+	CR
43	NB	F	8.0	Decreased	H	4	+	+	CR
44	NB	F	13	Decreased	H	4	+	ND	CR
45	NB	F	27	Decreased	H	4	+	+	CR
46	NB	M	45	Decreased	H	3	+	+	CR
47	NB	F	38	Decreased	L	I	–	–	CR
48	NB	M	4.0	Decreased	H	4	+	+	DOD
49	NB	M	11	Decreased	L	I	–	+	CR
50	NB	F	1.0	Decreased	L	I	–	–	CR

[a]NB, neuroblastoma; GNB, ganglioneuroblastoma.
[b]F, female; M, male.
[c]H, high risk group; I, intermediate risk group; L, low risk group.
[d]+, *MYCN* amplification or 1p deletion; –, no *MYCN* amplification or 1p deletion; ND, not determined.
[e]DOD, dead of disease; PR, partial remmision; CR, complete remission; CR2 complete remission after two treatments; PD, progressive disease.

MYCN/1p status were performed. As expected from multiple previous studies, high-risk classification based on clinical-genetic parameters ($P = 0.00003$; Mantel-Cox log-rank test; Fig. 2A) and the presence of *MYCN*-amplification and/or 1p deletion ($P = 0.012$; Fig. 2B) were associated

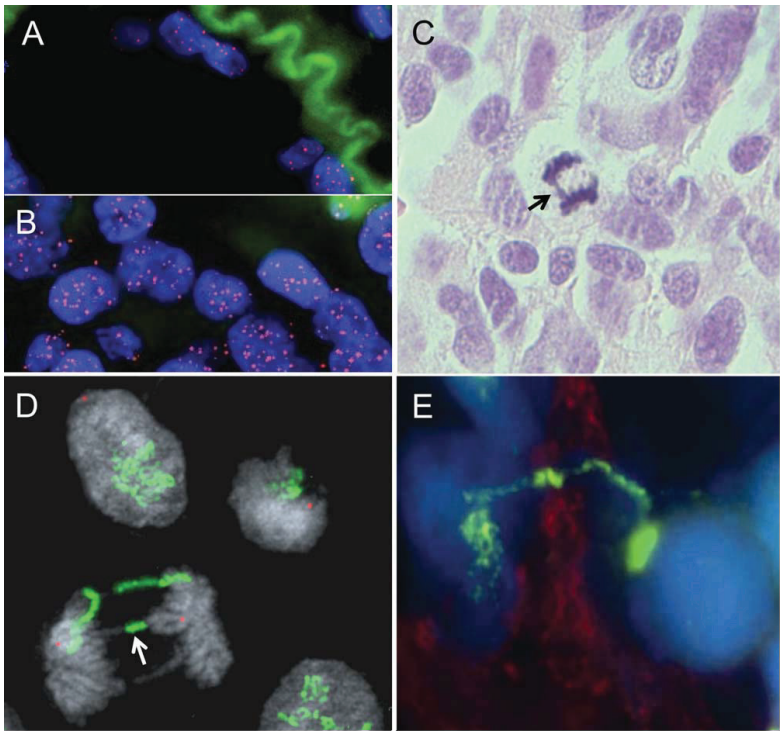

Figure 1. Fluorescence *in situ* hybridization and histological staining. A: Haematoxylin eosin staining of paraffin embedded tissue (case 16; Table 1). B: Telomeres detected by FISH (red) and cell nuclei detected by diaminophenylindol (blue) in a paraffin section from the same case as A. C: Anaphase bridge (arrow) in a paraffin section, stained by haematoxylin and eosin. D: Anaphase bridge (arrow) in SK-NE-BE (2C) containing amplified *MYCN* sequences (green); a chromosome 2 centromere probe is used as an internal control (red). E: A chromatin bridge containing amplified *MYCN* is detected by FISH in a tissue section from a *MYCN* amplified tumor. [Color figure can be viewed in the online issue, which is available at wileyonlinelibrary.com.]

with a low frequency of overall survival, corroborating that our sample was representative. Of the 50 analyzed tumors, 10 had elongated, 28 reduced, and 12 had unchanged TTL compared with non-neoplastic cells in the same biopsies. Strikingly, no cases with *MYCN* amplification and only one case with 1p deletion was found in the group with increased TTL compared with the group of unchanged TTL, which contained three cases of *MYCN* amplification and 1p allelic loss, and the group with reduced TTL which contained 13 cases with *MYCN* amplification and/or 1p deletion. *MYCN* amplification/1p loss was significantly over-represented in the subgroup of cases with reduced TTL, compared with those with increased TTL ($P = 0.03$; Fisher's exact test). There was no significant difference in *MYCN*-status between cases with unchanged TTL and those with increased or decreased TTL.

Telomere Length in Tumors Predicts Survival

Taking all cases into account, patients with increased TTL had a significantly lower rate of overall survival (27% versus 89%) than those having tumors with reduced TTL ($P = 0.013$; Mantel-Cox log-rank test). There was also a significant difference in overall survival between patients with unchanged TTL, compared with the groups with increased and decreased TTL ($P = 0.033$, Fig. 2C). Multivariate analysis showed that TTL was an independent prognostic risk factor for death of disease or progressive disease ($P = 0.012$) together with stage ($P = 1.067 \times 10^{-5}$), *MYCN* status ($P = 0.0019$), allelic loss of 1p ($P = 0.0083$), and age ($P = 0.0012$). Sex was also included in the multivariate analysis but was not an independent prognostic factor ($P = 0.63$). We couldn't find any correlation between age and telomere length, all ages were represented in each group ($r = -0.195$ and $P = 0.087$ one-tailed Spearmann).

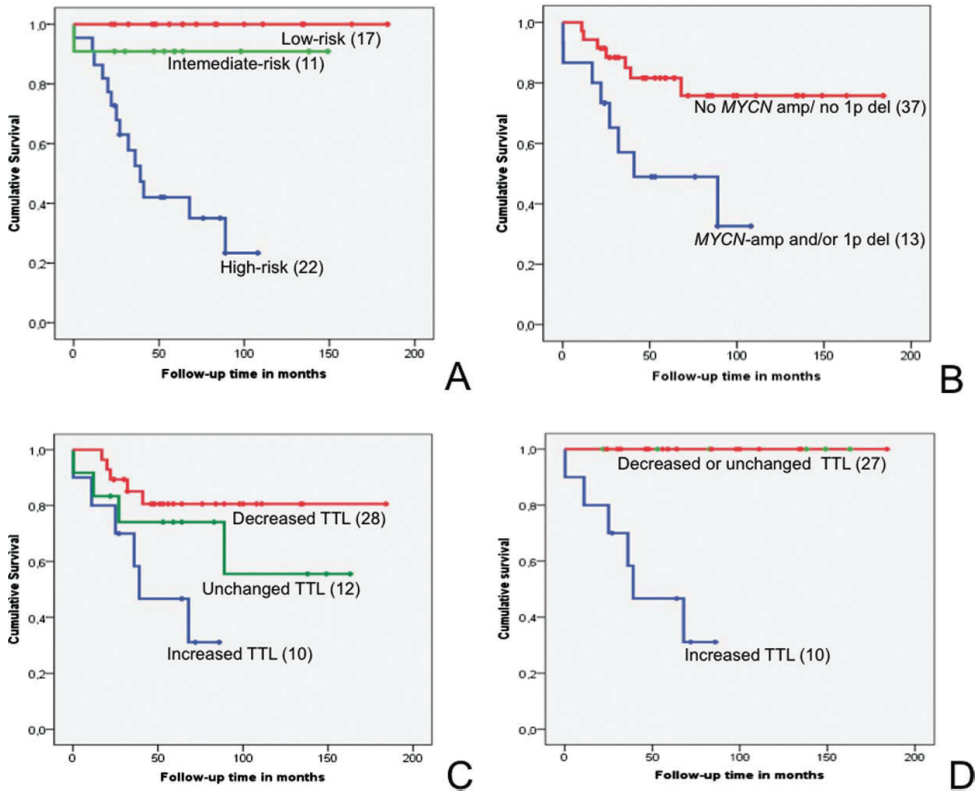

Figure 2. Cumulative survival plots according to Kaplan-Meier. Plus signs indicate censored cases in all categories. A: Survival categorized according to risk-groups, high-risk, 22 patients (blue), intermediate risk, 11 patients (green), and low risk, 17 patients (red). $P = 0.00003$. B: Survival categorized according to the presence and the absence of *MYCN* amplification/1p deletion, respectively. Blue line indicates that *MYCN* amplification and/or 1p deletion is present, 13 patients, and red that *MYCN* amplification and 1p deletion is absent, 37 patients. $P = 0.012$. C: All analyzed tumors categorized according to decreased relative tumor telomere length, 28 patients (TTL; red), unchanged TTL, 12 patients (green) and increased TTL, 10 patients (blue). $P = 0.013$. D: Survival of cases without *MYCN* amplification and 1p deletion having decreased or unchanged TTL, 27 patients (identical survival rates, red line) and increased TTL, 10 patients (blue line). $P = 0.00042$. [Color figure can be viewed in the online issue, which is available at wileyonlinelibrary.com.]

When excluding cases with the two known unfavorable genetic prognostic factors on which information was available in our material, *MYCN*-amplification and 1p deletion, there was a more pronounced difference in overall survival between the groups with increased and decreased TTL, respectively ($P = 0.00042$; Fig. 2D). In fact, of the non-*MYCN* amplified/non-1p deleted patients with decreased or unchanged TTL, overall survival was 100% compared with 27% for those with increased TTL (mean and median follow-up time 95 and 64 months respectively). Because all but one of the patients exhibiting *MYCN* amplification or 1p deletion had unchanged or decreased TTL, the impact of increased TTL in the *MYCN* amplified/1p deleted subgroup of patients could not be evaluated.

ALT in NBs with Increased TTL

By Q-FISH, the variation in telomere length between different chromosome termini was remarkably wide in NB cell nuclei compared with the surrounding non-neoplastic cells (median coefficient of variance 107% in non-neoplastic cells compared to 123% in NB, respectively; $P = 0.01$; Wilcoxon's paired-test). This was particularly pronounced in the subset of tumors with increased TTL, showing coefficients of variance up to 148% between normal cells and tumor cells

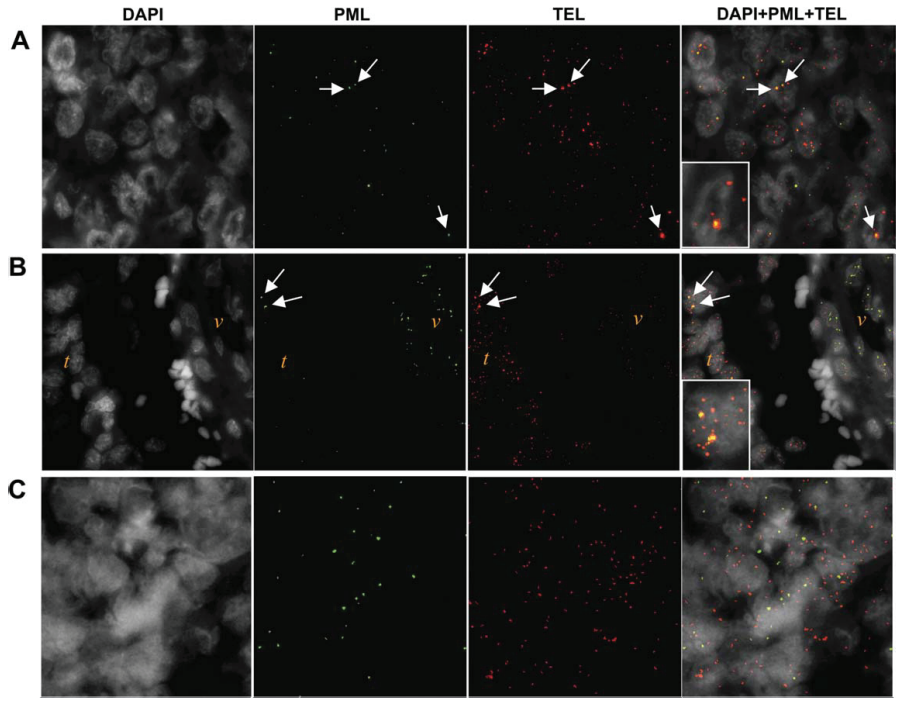

Figure 3. Combined telomere and PML body detection. Separate images are shown for diaminophenylindol nuclear counterstain (DAPI), PML-body immunofluorescence (PML), and telomere repeat fluorescence *in situ* hybridizatin (TEL). Combinatorial labeling is shown in the rightmost column. Alternative lengthening of telomeres (ALT)-associated PML bodies (APBs) are indicated by arrows. A: Representative image of tumor cells in a case with increased TTL (Case 10, Table 1), showing two APB-positive nuclei of which one is shown as an inset in the rightmost image. B: Tumors cells from the same case (t) located adjacent to a blood vessel (v) with surrounding stromal cells in the same case. Note the strong telomere signals in the tumor cells compared to the vascular endothelium and the stromal fibroblasts. Two APB-positive tumor cells are shown as an inset in the leftmost image. C: Representative image of tumor cells in a case with unchanged TTL (Case 19, Table 1) without APB-positive nuclei. [Color figure can be viewed in the online issue, which is available at wileyonlinelibrary.com.]

and up to 400% in individual tumor cells. The high variability in telomere signal intensity in NBs with increased TTL suggested that telomere elongation in these cases could be mediated by ALT, as tumors using this pathway for telomere elongation have previously been shown to exhibit high diversity in the lengths of individual telomeres (Ulaner, 2004). However, intense telomere signals may also be caused by extrachromosomal telomeric aggregates and fusion of telomeres different chromosomes. We therefore chose to further evaluate the presence of ALT, and 12 tumors from which material was still available were subjected to detection of APBs by combined immunofluorescence and FISH (Fig. 3). Because overlapping telomere and PML fluorescence signals resembling true APBs may occur artifactually at two-dimensional tissue analysis, the frequency of APB-positive nuclei was scored using blood vessel cells in tissue sections as a normal reference to estimate the baseline level of APBs. The frequencies of APB-positive nuclei showed extensive variation among the five cases with increased TTL (Fig. 4). Nevertheless, all tumors with increased TTL exhibited a significantly higher APB frequency than the non-neoplastic reference cells ($P < 0.05$; case-by-case comparison, Student's t test). The number of APBs ranged from one to five per nucleus, with no significant difference among the cases with increased TTL. In contrast, neither the cases with reduced nor those with unchanged TTL showed an elevated APB-frequency ($P > 0.16$) compared with the reference cells. Comparison of pooled APB frequencies in each group (increased, reduced, and unchanged TTL) showed a significantly higher frequency of APBs in tumors with increased TTL compared with those with

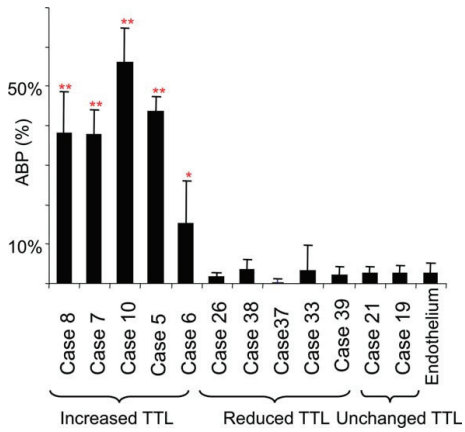

Figure 4. Frequencies of alternative lengthening of telomeres (ALT) associated PML bodies (APBs). Error bars reflect 95% confidence intervals. Single and double asterisks denote significant differences in APB frequency at $P < 0.05$ and $P < 0.0001$, respectively, compared to endothelial cells (Case 10, Table 1). [Color figure can be viewed in the online issue, which is available at wileyonlinelibrary.com.]

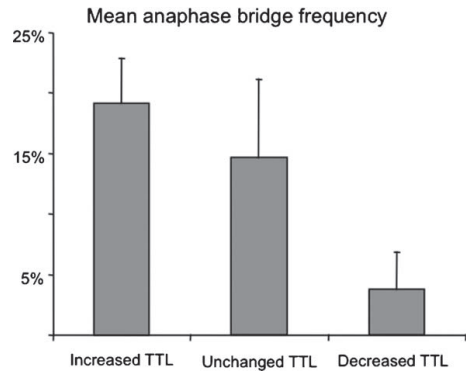

Figure 5. Mean frequency of anaphase bridges scored in tissue sections. Data are from NBs with increased (six cases), unchanged (six cases), and reduced (six cases) tumor telomere length (TTL), respectively. Bars indicate SD.

reduced and unchanged TTL ($P < 1 \times 10^{-22}$), while there as no difference between cases with reduced and unchanged TTL ($P = 0.56$).

Increased Telomere Length Is Associated with Frequent Chromosome Recombination

To assess the relationship between telomere length and structural chromosomal instability due to end-to-end fusions, we then quantified the frequency of anaphase bridging in H&E-stained NB tissue sections. For this, we selected six tumors with increased, decreased, and unchanged TTL, respectively. The reason for including only 18 cases in this analysis was that the remaining cases showed a mitotic rate that was too low for reliable quantification of anaphase bridging (>30 anaphase cells present in each case). As a negative control, mitotic cells in crypts of 10 normal colorectal mucosa samples were used, showing chromatin bridges in <1% of anaphase cells. An elevated rate of chromatin bridges (2%–29%, Fig. 1C) was present in the majority (15/18) of the NB samples. Tumors with increased TTL showed a higher frequency of anaphase bridges compared to those with decreased TTL ($P = 0.0002$; Fig. 5). The group with unchanged TTL showed an intermediate frequency between the other two groups.

Anaphase Bridging in NB Correlates to Telomere Dysfunction

The high frequency of anaphase bridges in tumors with increased TTL was inconsistent with anaphase bridging in NB, being caused by

TABLE 2. Telomere-Dependent Instability in Cell Lines

Cell line	TTAGGG-negative ends median (range)	Anaphase bridges (%)	End-to-end fusions[a] (number of cells)	Telomerase activity[a]
MYCN amplified in homogeneously staining regions				
SK-N-BE (2C)	5 (0–7)	8	16% (5/31)	No
IMR32	2 (1–4)	3	3% (2/30)	Yes
MYCN amplicon in double minute chromatin bodies				
LA-N-5	2 (0-5)	3	3% (1/32)	No
CHP-212	8 (5-11)	17	30% (9/30)	nd[b]
No *MYCN* amplicons present				
SH-SY5Y	2 (0–5)	3	7% (2/30)	Yes
SK-N-FI	2 (0–2)	3	0 (0/30)	No
Fibroblast control				
FI	0.2 (0–1)	<1%	<2% (1/200)	

[a]References: Binz et al., 2005; Narath et al., 2007; Wesbuer, et al., 2010.
[b]Not determined.

an overall reduction in telomere repeat length. The pronounced variability in TTL among cases with increased TTL rather suggested that these tumors contained a high frequency of individual chromosome ends with extremely short telomeres that may cause end-to-end fusions. To substantiate the relationship between reduced length of individual telomeres and anaphase bridging in NB cells, we examined telomere deficiency, and assessed by the number of TTAGGG-negative chromosome ends on metaphase spreads by FISH in six NB cell lines (Table 2). Although a negative chromosome terminus may still contain up to 500 base pairs of TTAGGG repeat sequences, this method has previously been shown to yield a valid assessment of the protective capacity of individual telomeres (Gisselsson et al., 2001). The analysis revealed an elevated number of TTAGGG-negative chromosome ends in all cell lines compared with fibroblasts cultured in parallel.

Similar to the variability in TTL in tumor sections, there was considerable diversity among different cells in most of the cell lines with respect to the number of TTAGGG-negative chromosomes. The diversity was highest in the cell lines, also showing the highest median number of TTAGGG-negative ends i.e., SK-N-BE(2C) and CHP-212. All cell lines also showed an elevated rate of anaphase bridges compared with fibroblasts, again with the highest rates in SK-NE-BE (2C) and CHP-212. Overall, the correlation between the mean number of TTAGGG-negative chromosome ends and the frequency of anaphase bridging was 0.99 (Pearson correlation). Consistent with telomere deficiency giving rise to unstable chromosome termini, there was en elevated prevalence of cells with dicentric chromosomes and telomere fusions in five of the six cell lines compared to fibroblasts, again with the highest frequencies in SK-NE-BE (2C) and CHP-212. Thus, at least *in vitro* there appeared to be a clear connection between telomere length reduction at individual chromosome ends, telomere fusion, and anaphase bridges.

Anaphase Bridging Can Modulate the Structure of *MYCN* Amplicons

Our collective data suggest that some degree of telomere-dependent anaphase bridging was present in the vast majority of NBs. To assess whether breaking-fusion-bridge events could have any impact on known oncogene genome sequences in NB, we assessed the presence of amplified *MYCN* sequences in anaphase bridges in SK-NE-BE (2C), containing *MYCN* amplicons as intrachromosomal homogeneously staining regions (hsr). FISH analysis with a probe for *MYCN* showed that 50% of the anaphase bridges in this cell line contained amplified *MYCN* sequences (Fig. 1D). The two marker chromosomes carrying the amplicons in the SK-NE-BE (2C) stem line exhibited a high frequency of TTAGGG-negative termini for three of its chromosome arms (negative in 45% and 48%, 6% and 56% of scored cells, for p and q arm, respectively). In contrast, the p and q arms of chromosome 1, used as control, lacked detectable TTAGGG-repeats in only 7% and 9% of scored cells ($P < 0.01$ compared with that of *MYCN*-carrying markers; Fisher's exact test). FISH for *MYCN* sequences revealed a considerable heterogeneity in the cytogenetic architecture of the hsr carrying *MYCN* in this cell line, being present in chromosome derivates different than those in the stem line in 44% of 50 analyzed metaphase cells. In contrast, the cell line IMR32, also showing *MYCN* amplified sequences in hsr, but having largely intact telomeres, did not exhibit *MYCN* amplicons in the low number of anaphase bridges found. Furthermore, only 7% of the analyzed cells exhibited different location and/or size of its hsr carrying amplified *MYCN* in this cell line. Thus, defective telomere protection in chromosomes harboring *MYCN* amplicons appeared to be connected to frequent rearrangement of amplicon structure through anaphase bridging. To finally evaluate whether *MYCN*-amplicons were involved in anaphase bridges also *in vivo*, FISH-analyses of anaphase bridges in tissue sections from one of the *MYCN* amplified cases was performed. This revealed that ~10% of the chromatin bridges present between anaphase poles or cell nuclei contained amplified *MYCN* (Fig. 1E), implying that the remodeling of *MYCN* amplicons by anaphase bridging could also occur in primary NB tissue.

DISCUSSION

Previous studies of the role of telomere length and stability in NB have been few and to some extent contradictory. Ohali et al. (2006) as well as Onitake et al. (2009) showed that increased TTL and high levels of telomerase activity are poor prognostic factors. On the other hand, an earlier study by Hiyama et al. (1992) suggested that

decreased TTL was significantly associated with poor prognosis. Our series of patients, in whom telomere length was evaluated, was relatively small but nevertheless representative with respect to risk stratification and the clinical course of patients with *MYCN* amplification/1p deletion. The Q-FISH method used for determining TTL has some notable advantages, such as the need of relatively few cells in comparison with Southern blot based methods, and the fact that it can be used on paraffin embedded tissues. Furthermore, comparison with parallel H&E stained slides allows estimation of telomere length in tumor cells with a high degree of cell-type specificity. On the other hand, there is a risk of bias in the selection of cells if a biopsy is not thoroughly sampled. None the less, several previous studies have shown that Q-FISH can be efficiently used to reliably quantify telomere length in tissue sections (Meeker and Argani, 2004; Feldser et al., 2006; Wise et al., 2009). Using Q-FISH, we found that tumors without *MYCN* amplification and with unchanged or reduced TTL had an excellent outcome compared with that of non-*MYCN* amplified tumors with increased TTL. Our results are thus overall consistent with those of Ohali et al. and Onitake et al., showing that short telomeres in NB cells compared to blood lymphocytes conferred an increased chance of survival (Ohali et al., 2006; Onitake et al., 2009). In contrast, our clinical correlation analysis did not support the conclusions from early work suggesting that a reduction of telomeric repeats are correlated to advanced stages of disease and poor prognosis, possibly because of the fact that non-*MYCN* amplified tumors were not selected for subgroup analysis in that study.

Two distinct groups of NB with poor clinical outcome were identified in the present study. The first consists of cases with *MYCN* amplification, typically showing decreased or unchanged TTL, the second of cases with normal *MYCN* status and with increased TTL. The biological mechanisms underlying this dichotomy remain to be explored. Telomere stabilization can be achieved by human cancer cells by *de novo* synthesis of telomeric DNA by telomerase or by ALT, which is dependent on recombination of telomeres in PML-bodies (Bryan et al., 1997; Draskovic et al., 2009). However, later studies have shown that ALT and telomerase activity may coexist over a prolonged period of time in human cancer cells (Cerone et al., 2001; Guiducci et al., 2001). Furthermore, at least one additional mechanism for immortalization and telomere stabilization may be present in human cells (Brachner et al., 2006). Telomerase activity has previously been shown to be highly variable in NBs with no correlation to telomere length (Onitake et al., 2009). In contrast, the findings of highly variable telomere lengths and a high prevalence of APBs in cases with increased TTL in the present study strongly suggest that the ALT pathway contributes significantly to telomere lengthening also in NB. The generally poor survival of non-*MYCN* amplified cases with increased TTL, in turn, suggests that the telomere length maintenance by the ALT pathway may be an important route to therapy resistance. In this context, it is important to note that increased TTL and ALT did not appear to be associated with a pan-genomic stabilization of telomeres but rather with an increase in the average telomere length, as there was a wide variability in the length of individual telomeres. This suggests that telomere length has a role in NB that may be independent of protection against chromosomal end-to-end fusion.

The mechanism behind aggressive disease in *MYCN* amplified tumors with decreased/unchanged TTL was not addressed by the present study. Onitake et al. reported a similar predominance of *MYCN* amplification in cases with unchanged/shortened telomeres, although no formal statistical analysis was made (Onitake et al., 2009). That study also demonstrated high telomerase activity in *MYCN* amplified tumors. The Myc pathway may directly lead to increased activation of *hTERT* promoter sequences (Wu et al., 1999), even although later studies have shown that increased *hTERT* transcript levels and telomere stabilization may to some extent be dependent on subsequent genomic alterations (Bazarov et al., 2009). It is possible that *MYCN* has a similar capability of *hTERT* activation, explaining the correlation between telomerase activity and amplification of *MYCN*. Similar to the ALT-tumors, *MYCN* amplified tumors exhibited an elevated rate of genomic instability through anaphase bridging in the present study, indicating that telomerase expression failed to stabilize all chromosome ends. It has been shown that *MYCN* binds to and upregulates the *MDM2* promoter (Slack et al., 2005), and *MYCN* amplified cells may override the G1 checkpoint (Bell et al., 2007), thereby bypassing the triggering of DNA damage response normally leading to permanent growth arrest or apoptosis in cells with critically

reduced telomere length. It is thus feasible that *MYCN* amplification allows circumvention of the telomere-dependent checkpoints of cellular replication, allowing further proliferation of cells with short, unstable telomeres. One possible explanation could be that the short telomeres are induced by oxidative stress (von Zglinicki, 2002), much more common in tumors than that of normal cells.

To our knowledge, the present study is the first to demonstrate that extensive telomere dysfunction leading to chromosome fusion and breakage-fusion-bridge cycles can be present in NB cells. Anaphase bridging was not only found in established cell lines but also in tumor tissue from a majority of cases, demonstrating that this type of genomic instability is present also *in vivo*. The breakage-fusion-bridge cycle triggered by telomere shortening and dysfunction is a well-known mechanism behind oncogene amplification in tumors (Bignell et al., 2007; Gisselsson and Hoglund, 2005). Our study shows that this mechanism may remodel the structure of intrachromosomal *MYCN* amplicons in NB cells, as evidenced by a high degree of structural variability of *MYCN*-containing homogeneously staining regions carried in chromosomes with TTAGGG-negative termini and the participation of amplified *MYCN* sequences in anaphase bridges, both in one of the cell lines and in tumor tissue. Our data does not provide any direct evidence for telomere dysfunction being of importance for the origination of *MYCN* amplicons. It is nevertheless possible that dysfunctional telomeres and anaphase bridging have a role in extending low-copy number amplicons and thereby increase gene dosage, as shown in model systems of chemotherapy resistance, where breakage-fusion-bridge cycles have been demonstrated to be key events behind increasing drug tolerance (Coquelle et al., 1997). Our findings in NB are largely similar to studies of osteosarcomas, which have shown that the ALT mechanism is associated with a high-frequency of TTAGGG-negative ends, dicentric chromosomes, and breakage-fusion-bridge cycles, and that the presence of ALT is linked to an unfavorable prognosis (Scheel et al., 2001; Ulaner et al., 2003).

As a conclusion, the present study shows that telomere-dependent chromosome instability is highly prevalent in NB and may contribute to clonal evolution through the remodeling of oncogenic sequences. We also show that *in situ* quantification of telomere length identifies two distinct groups with poor survival, one with elongated TTL mediated by ALT and one with reduced TTL and *MYCN* amplification. Our results prompt further studies of the prognostic impact and genetic correlations of telomere length and activation of the ALT pathway in NB, possibly within the framework of clinical trial protocols.

REFERENCES

Ambros PF, Ambros IM. 2001. Pathology and biology guidelines for resectable and unresectable neuroblastic tumors and bone marrow examination guidelines. Med Pediatr Oncol 37:492–504.

Artandi SE, Chang S, Lee SL, Alson S, Gottlieb GJ, Chin L, DePinho RA. 2000. Telomere dysfunction promotes non-reciprocal translocations and epithelial cancers in mice. Nature 406: 641–645.

Attiyeh EF, London WB, Mossé YP, Wang Q, Winter C, Khazi D, McGrady PW, Seeger RC, Look AT, Shimada H, Brodeur GM, Cohn SL, Matthay KK, Maris JM. 2005. Chromosome 1p and 11q deletions and outcome in neuroblastoma. N Engl J Med 353:2243–2253.

Avigad S, Naumov I, Ohali A, Jeison M, Berco GH, Mardoukh J, Stark B, Ash S, Cohen IJ, Meller I, Kollender Y, Issakov J, Yaniv I. 2007. Short telomeres: A novel potential predictor of relapse in Ewing sarcoma. Clin Cancer Res 13:5777–5783.

Bazarov AV, Hines WC, Mukhopadhyay R, Beliveau A, Melodyev S, Zaslavsky Y, Yaswen P. 2009. Telomerase activation by c-Myc in human mammary epithelial cells requires additional genomic changes. Cell Cycle 8:3373–3378.

Bechter OE, Eisterer W, Pall G, Hilbe W, Kuhr T, Thaler J. 1998. Telomere length and telomerase activity predict survival in patients with B cell chronic lymphocytic leukemia. Cancer Res 58:4918–4922.

Bell E, Lunec J, Tweddle DA. 2007. Cell cycle regulation targets of MYCN identified by gene expression microarrays. Cell Cycle 6:1249–1256.

Bignell GR, Santarius T, Pole JC, Butler AP, Perry J, Pleasance E, Greenman C, Menzies A, Taylor S, Edkins S, Campbell P, Quail M, Plumb B, Matthews L, McLay K, Edwards PA, Rogers J, Wooster R, Futreal PA, Stratton MR. 2007. Architectures of somatic genomic rearrangement in human cancer amplicons at sequence-level resolution. Genome Res 17:1296–1303.

Binz N, Shalaby T, Rivera P, Shin-ya K, Grotzer MA. 2005. Telomerase inhibition, telomere shortening, cell growth suppression and induction of apoptosis by telomestatin in childhood neuroblastoma cells. Eur J Cancer 41:2873–2881.

Brachner A, Sasgary S, Pirker C, Rodgarkia C, Mikula M, Mikulits W, Bergmeister H, Setinek U, Wieser M, Chin SF, Caldas C, Micksche M, Cerni C, Berger W. 2006. Telomerase- and alternative telomere lengthening-independent telomere stabilization in a metastasis-derived human non-small cell lung cancer cell line: Effect of ectopic hTERT. Cancer Res 66:3584–3592.

Brodeur GM, Sekhon G, Goldstein MN. 1977. Chromosomal aberrations in human neuroblastomas. Cancer 40:2256–2263.

Brodeur GM, Seeger RC, Schwab M, Varmus HE, Bishop JM. 1984. Amplification of N-myc in untreated human neuroblastomas correlates with advanced disease stage. Science 224:1121–1124.

Brodeur GM, Pritchard J, Berthold F, Carlsen NL, Castel V, Castelberry RP, De Bernardi B, Evans A, Favrot M, Hedborg F. 1993. Revisions of the international criteria for neuroblastoma diagnosis, staging, and response to treatment. J Clin Oncol 11: 1466–1477.

Bryan TM, Englezou A, Dalla-Pozza L, Dunham MA, Reddel RR. 1997. Evidence for an alternative mechanism for maintaining telomere length in human tumors and tumor-derived cell lines. Nat Med 3:1271–1274.

Capper R, Britt-Compton B, Tankimanova M, Rowson J, Letsolo B, Man S, Haughton M, Baird DM. 2007. The nature of telomere fusion and a definition of the critical telomere length in human cells. Genes Dev 21:2495–2508.

Cerone MA, Londono-Vallejo JA, Bacchetti S. 2001. Telomere maintenance by telomerase and by recombination can coexist in human cells. Hum Mol Genet 10:1945–1952.

Chan SR, Blackburn EH. 2004. Telomeres and telomerase. Philos Trans R Soc Lond B Biol Sci 359:109–121.
Coquelle A, Pipiras E, Toledo F, Buttin G, Debatisse M. 1997. Expression of fragile sites triggers intrachromosomal mammalian gene amplification and sets boundaries to early amplicons. Cell 89:215–225.
de Lange T. 2005. Shelterin: The protein complex that shapes and safeguards human telomeres. Genes Dev 19:2100–2110.
Donaldson L, Fordyce C, Gilliland F, Smith A, Feddersen R, Joste N, Moyzis R, Griffith J. 1999. Association between outcome and telomere DNA content in prostate cancer. J Urol 162:1788–1792.
Draskovic I, Arnoult N, Steiner V, Bacchetti S, Lomonte P, Londono-Vallejo A. 2009. Probing PML body function in ALT cells reveals spatiotemporal requirements for telomere recombination. Proc Natl Acad Sci U S A 106:15726–15731.
Feldser D, Strong MA, Greider CW. 2006. Ataxia telangiectasia mutated (Atm) is not required for telomerase-mediated elongation of short telomeres. Proc Natl Acad Sci U S A 103:2249–2251.
Ferlicot S, Youssef N, Feneux D, Delhommeau F, Paradis V, Bedossa P. 2003. Measurement of telomere length on tissue sections using quantitative fluorescence *in situ* hybridization (Q-FISH). J Pathol 200:661–666.
Fordyce CA, Heaphy CM, Bisoffi M, Wyaco JL, Joste NE, Mangalik A, Baumgartner KB, Baumgartner RN, Hunt WC, Griffith JK. 2006. Telomere content correlates with stage and prognosis in breast cancer. Breast Cancer Res Treat 99:193–202.
Frías C, García-Aranda C, De Juan C, Morán A, Ortega P, Gómez A, Hernando F, López-Asenjo JA, Torres AJ, Benito M, Iniesta P. 2008. Telomere shortening is associated with poor prognosis and telomerase activity correlates with DNA repair impairment in non-small cell lung cancer. Lung Cancer 60:416–425.
Gisselsson D, Hoglund M. 2005. Connecting mitotic instability and chromosome aberrations in cancer—Can telomeres bridge the gap? Semin Cancer Biol 15:13–23.
Gisselsson D, Jonson T, Petersen A, Strombeck B, Dal Cin P, Hoglund M, Mitelman F, Mertens F, Mandahl N. 2001. Telomere dysfunction triggers extensive DNA fragmentation and evolution of complex chromosome abnormalities in human malignant tumors. Proc Natl Acad Sci U S A 98:12683–12688.
Guiducci C, Cerone MA, Bacchetti S. 2001. Expression of mutant telomerase in immortal telomerase-negative human cells results in cell cycle deregulation, nuclear and chromosomal abnormalities and rapid loss of viability. Oncogene 20:714–725.
Gunderson KL, Steemers FJ, Lee G, Mendoza LG, Chee MS. 2005. A genome-wide scalable SNP genotyping assay using microarray technology. Nat Genet 37:549–554.
Hiyama E, Hiyama K, Yokoyama T, Ichikawa T, Matsuura Y. 1992. Length of telomeric repeats in neuroblastoma: Correlation with prognosis and other biological characteristics. Jpn J Cancer Res 83:159–164.
London WB, Castleberry RP, Matthay KK, Look AT, Seeger RC, Shimada H, Thorner P, Brodeur G, Maris JM, Reynolds CP, Cohn SL. 2005. Evidence for an age cutoff greater than 365 days for neuroblastoma risk group stratification in the Children's Oncology Group. J Clin Oncol 23:6459–6465.
McClintock B. 1938. The production of homozygous deficient tissues with mutant characteristics by means of the aberrant mitotic behavior of ring-shaped chromosomes. Genetics 23:315–376.
Meeker AK, Argani P. 2004. Telomere shortening occurs early during breast tumorigenesis: A cause of chromosome destabilization underlying malignant transformation? J Mammary Gland Biol Neoplasia 9:285–296.
Meeker AK, Gage WR, Hicks JL, Simon I, Coffman JR, Platz EA, March GE, De Marzo AM. 2002. Telomere length assessment in human archival tissues: Combined telomere fluorescence *in situ* hybridization and immunostaining. Am J Pathol 160:1259–1268.
Narath R, Ambros IM, Kowalska A, Bozsaky E, Boukamp P, Ambros PF. 2007. Induction of senescence in MYCN amplified neuroblastoma cell lines by hydroxyurea. Genes Chromosomes Cancer 46:130–142.
O'sullivan JN, Finley JC, Risques RA, Shen WT, Gollahon KA, Moskovitz AH, Gryaznov S, Harley CB, Rabinovitch PS. 2004. Telomere length assessment in tissue sections by quantitative FISH: Image analysis algorithms. Cytometry A 58:120–131.
Ohali A, Avigad S, Ash S, Goshen Y, Luria D, Feinmesser M, Zaizov R, Yaniv I. 2006. Telomere length is a prognostic factor in neuroblastoma. Cancer 107:1391–1399.
Ohyashiki JH, Iwama H, Yahata N, Ando K, Hayashi S, Shay JW, Ohyashiki K. 1999. Telomere stability is frequently impaired in high-risk groups of patients with myelodysplastic syndromes. Clin Cancer Res 5:1155–1160.
Onitake Y, Hiyama E, Kamei N, Yamaoka H, Sueda T, Hiyama K. 2009. Telomere biology in neuroblastoma: Telomere binding proteins and alternative strengthening of telomeres. J Pediatr Surg 44:2258–2266.
Poon SS, Martens UM, Ward RK, Lansdorp PM. 1999. Telomere length measurements using digital fluorescence microscopy. Cytometry 36:267–278.
Scheel C, Schaefer KL, Jauch A, Keller M, Wai D, Brinkschmidt C, van Valen F, Boecker W, Dockhorn-Dworniczak B, Poremba C. 2001. Alternative lengthening of telomeres is associated with chromosomal instability in osteosarcomas. Oncogene 20:3835–3844.
Slack A, Chen Z, Tonelli R, Pule M, Hunt L, Pession A, Shohet JM. 2005. The p53 regulatory gene MDM2 is a direct transcriptional target of MYCN in neuroblastoma. Proc Natl Acad Sci U S A 102:731–736.
Srivatsan ES, Murali V, Seeger RC. 1991. Loss of heterozygosity for alleles on chromosomes 11q and 14q in neuroblastoma. Prog Clin Biol Res 366:91–98.
Staaf J, Lindgren D, Vallon-Christersson J, Isaksson A, Goransson H, Juliusson G, Rosenquist R, Hoglund M, Borg A, Ringner M. 2008. Segmentation-based detection of allelic imbalance and loss-of-heterozygosity in cancer cells using whole genome SNP arrays. Genome Biol 9:R136.
Steemers FJ, Chang W, Lee G, Barker DL, Shen R, Gunderson KL. 2006. Whole-genome genotyping with the single-base extension assay. Nat Methods 3:31–33.
Stewenius Y, Gorunova L, Jonson T, Larsson N, Hoglund M, Mandahl N, Mertens F, Mitelman F, Gisselsson D. 2005. Structural and numerical chromosome changes in colon cancer develop through telomere-mediated anaphase bridges, not through mitotic multipolarity. Proc Natl Acad Sci U S A 102:5541–5546.
Swiggers SJ, Kuijpers MA, de Cort MJ, Beverloo HB, Zijlmans JM. 2006. Critically short telomeres in acute myeloid leukemia with loss or gain of parts of chromosomes. Genes Chromosomes Cancer 45:247–256.
Ulaner GA. 2004. Telomere maintenance in clinical medicine. Am J Med 117:262–269.
Ulaner GA, Huang HY, Otero J, Zhao Z, Ben-Porat L, Satagopan JM, Gorlick R, Meyers P, Healey JH, Huvos AG, Hoffman AR, Ladanyi M. 2003. Absence of a telomere maintenance mechanism as a favorable prognostic factor in patients with osteosarcoma. Cancer Res 63:1759–1763.
von Zglinicki T. 2002. Oxidative stress shortens telomeres. Trends Biochem Sci 27:339–344.
Wesbuer S, Lanvers-Kaminsky C, Duran-Seuberth I, Bolling T, Schafer KL, Braun Y, Willich N, Greve B. 2010. Association of telomerase activity with radio- and chemosensitivity of neuroblastomas. Radiat Oncol 5:66.
Wise JL, Crout RJ, McNeil DW, Weyant RJ, Marazita ML, Wenger SL. 2009. Human telomere length correlates to the size of the associated chromosome arm. PLoS One 4:e6013.
Wu KJ, Grandori C, Amacker M, Simon-Vermot N, Polack A, Lingner J, Dalla-Favera R. 1999. Direct activation of TERT transcription by c-MYC. Nat Genet 21:220–224.

III

Intratumoral diversity of chromosome copy number in neuroblastoma mediated by ongoing chromosome loss from a polyploid state.

Gisela Lundberg[1], Yuesheng Yin[1], Daniel Sehic[1], Ingrid Øra[2], David Gisselsson[1, 3]

[1] Department of Clinical Genetics, Lund University, Skåne University and Regional Laboratories, Lund, Sweden.

[2] Department of Paediatric Oncology, Lund University, Skåne University Hospital, Lund, Sweden.

[3] Department of Pathology, Skåne University and Regional Laboratories, Lund, Sweden.

Corresponding author:

Gisela Lundberg, Department of Clinical Genetics, BMC B13, Sölvegatan 19, 22184 Lund, Sweden. Phone +46-46-2226997, fax +46-46-131061, e-mail gisela.lundberg@med.lu.se

Abstract

Background: Neuroblastomas **(**NBs) are tumours of the sympathetic nervous system accounting for 8-10% of paediatric cancers. NBs exhibit extensive inter-tumour genetic heterogeneity, but their extent of intra-tumour genetic diversity remains unexplored.

Aim: To assess intra-tumour genetic variation in NBs with a focus on whole-chromosome changes and their underlying mechanism.

Materials and Methods: Allelic ratios obtained by SNP-array data from 30 aneuploid primary NBs and NB cell lines were used to quantify the size of clones harbouring specific genomic imbalances. In 12 cases, this was supplemented by fluorescence *in situ* hybridisation to assess copy number diversity in detail. Computer simulations of different mitotic segregation errors, single cell cloning, analysis of mitotic figures, and time lapse imaging of diving NB cells were used to predict the most likely mechanism behind intra-tumour variation in chromosome number.

Results: All cases exhibited higher inter-cellular copy number variation than non-neoplastic control tissue, with up to 66% of tumour cells showing non-modal chromosome copy numbers. Computer simulations indicated that loss of chromosomes from a tetraploid state was more likely to explain numerical aberrations in NB than other mechanisms reported in cancer cells. This was supported by a high frequency of lagging chromosomes at anaphase and polyploidisation events in growing NB cells. The dynamic nature of numerical aberrations was corroborated further by detecting substantial copy number diversity in cell populations grown from single NB cells.

Conclusion: Loss of chromosomes from a tetraploid state is a major route towards prominent intra-tumour genomic diversity in aneuploid NBs.

Background

One of the hallmarks of human solid tumours is genomic instability, arising from aberrations occurring when the normal biological mechanisms that repair, replicate and transmit the genome fails.[1] Faithful segregation of chromosomes to daughter cells during mitosis maintains chromosome stability and a diploid genome. Disrupted control of this system may lead to chromosomal mis-segregation and an ensuing pattern of chromosomal instability (CIN) with respect to the copy numbers of individual chromosomes. CIN has also been less frequently used to describe the presence of structural aberrations mainly in blood cancers[2,3] and in inherited syndromes with increased risk of cancer.[4] However, the mechanisms that contribute to structural complexity, on the one hand, and numerical changes, on the other hand, are largely distinct. Structural rearrangements can be caused by abnormal DNA repair pathways that lead to errors in end-joining of double-stranded DNA. Structural rearrangements may also occur through telomere-mediated events, where abnormally short telomeres are recognized as DNA breaks capable of rearranging when DNA-repair pathways are activated.[5] In contrast, alteration in chromosome number has been reported to result from abnormalities in mitotic spindle assembly checkpoint function[6], centrosome duplication[7], kinetochore function[8], and microtubule stability.[9]

Numerical chromosome changes (aneuploidy) are commonly observed in solid tumours[10-15]. If aneuploidy is a cause or a consequence of cancer remains to be proven. Different lines of evidence[16-19] are now emerging for aneuploidy being a series of on-going chromosome aberration events, which contributes to tumour malignancy and might play a key role in generating metastatic disease. Finally, and probably most importantly, multiple genes and pathways regulating chromosome segregation have been found mutated in human cancer cells, implicating that such mutations are inductors of aneuploidy in tumours.

A high degree of aneuploidy is often associated with poor prognosis, particulary in adult cancers.[20] One well known exception from this is the childhood cancer NB, where a near triploid karyotype is typically interconnected with a better clinical outcome.[21] NBs are tumours of the sympathetic nervous system, accounting for 8-10% of all paediatric cancers. It typically presents during infancy or toddler years. It is the most frequently occurring extra-cranial solid tumour in children and about 90% of children with the disease are diagnosed within the first 5 years of life.

NBs exhibit extensive inter-tumour genetic heterogeneity, and are traditionally sub-divided into three clinical-genetic subtypes,[22] based on the pattern of somatic chromosome alterations. Type 1 tumours are characterised by a hyperdiploid to near-triploid chromosome number with no/few structural aberrations, and absence of *MYCN* amplification. Type 2A tumours have near-diploid or near-tetraploid karyotypes dominated by structural rearrangements, most prominently 17q gain and 11q deletions, still with absence of *MYCN* amplification. In contrast, type 2B tumours are signified by amplification of *MYCN,* often in conjunction with 1p deletion and 17q gain in a near-diploid or near-tetraploid background. While type 1 NBs typically occur in children <18 months of age and have an excellent prognosis, type 2A and B tumours occur in older children and are associated with a less favourable outcome. Accordingly, numerical chromosome aberrations / aneuploidy are most prevalent and most pronounced in type 1 NBs. However, less dramatic aneuploidy, often limited to a few trisomies and monosomies, can also be found in the other subtypes. Of the 273 NB cases reported in the Mitelman Database of Chromosome Aberrations and Gene Fusions in Cancer (http://cgap. nci.nih.gov/Chromosomes/Mitelman), 174 have a non-diploid or non-tetraploid karyotype, implying that more than 60% of NBs are aneuploid.

We have previously reported that telomere length abnormalities are frequently present in NB and have linked these to structural chromosome instability.[23] However, the mechanisms

underlying numerical aberrations/aneuploidy in NB remains largely unexplored. Neither has it been thoroughly assessed whether individual cells or cellular subpopulations present in the same tumour vary in copy number in a fashion similar to adult tumours exhibiting CIN. Such intercellular variation may be of importance for tumour progression and chemotherapy resistance on the basis of clonal evolution, and could also have a role in explaining regional variation in biology and morphology within the same tumour. The aim of the present study was to perform a first survey of the prevalence and extent of intra-tumour diversity in NBs with respect to numerical aberrations and to deduce the most likely route to aneuploidy in this tumour type. For this purpose we used a combination of bio-informatic and experimental techniques. Our results show that intra-tumour copy number diversity is present in the vast majority of aneuploid NBs and that a continuous process of chromosome loss from a tetraploid state is the most likely underlying mechanism in NBs with chromosome numbers in the hyperdiploid to hypotetraploid range.

Materials and Methods

Tissue samples and cell lines

Frozen tumour material was obtained from the biobanks of the Departments of Clinical Genetics and Human Genetics at Lund University, (Lund, Sweden) and the Academic Medical Center (Amsterdam, The Netherlands), respectively. Only tumours classified as primary NBs were included, after having undergone histopathological review. All patients were treated according to the European protocol active at the time. The follow-up time ranged from 91 days (dead of the disease) up to 18 years. Written consent was given by the parents for documentation, biological studies and analysis of medical data. The study was approved by the ethics review board of the participating institutes. Established NB cell lines were obtained, from LGC Standards (Teddington, UK) and DSMZ (Braunschweig, Germany). All analysed NB cases were sub-divided into clinical-genetic subtypes according to Brodeur [22] as follows. Type 1: non-*MYCN* amplified hyperdiploid to near triploid tumour dominated by whole chromosome changes. Type 2A: non-*MYCN* amplified near diploid or near tetraploid tumour dominated by structural chromosome changes. Type 2B: *MYCN* amplified near-diploid or near-tetraploid tumour.

Single nucleotide polymorphism (SNP) array analysis

For high-resolution detection of genomic imbalances in cell lines and frozen tumour tissue, 300 ng of DNA extracted using standard methods (DNeasy Blood & Tissue Kit, Qiagen, Valencia, CA) and was then hybridized to Illumina HumanCNV660 Omni BeadChips (Illumina Inc., San Diego, CA) according to the manufacturer's specifications. Allele specific fluorescent signals were first normalized using a proprietary algorithm in the Illumina BeadStudio software (Illumina Inc). Normalized allelic intensity values were thereafter

exported and subjected to an additional normalization step using the tQN-software[24]. The tQN software was also used to estimate B-allele frequencies (BAF) for each SNP based on a set of reference genotype clusters. For identification of imbalances, the BAF segmentation software was used, in which BAF-values are transformed into mirrored BAF (mBAF) values followed by removal of non-informative homozygous SNPs [25]. BAF segmentation also applies segmentation on the mBAF data to define regions of allelic imbalance. For each resulting segment, a copy number estimate was given as the median log2 ratio of all SNPs present within the defined segment. Segments with mBAF values >0.55 were classified as being in allelic imbalance. Segments with log2 ratio >0.073 were classified as genomic gains, those with log2 ratios <0.080 as genomic losses, and those with log2 ratios between these boundaries as copy number neutral genomic imbalances. Segments were fused if the interspersed genomic distance was <1 Mb and the difference in mBAF values between the segments was <0.1. Constitutional copy number variants were excluded from the final data by comparison to the Database of Genomic Variants (http://projects.tcag.ca/variation/; last access Aug. 1 2011).

mBAF values were also used to estimate the proportion of sampled DNA containing the respective genomic imbalances, calculated according to Staaf et al. [25]. This approach has previously been shown to accurately predict the proportion of cells carrying genomic imbalances in tumours with known ploidy levels[25,26]. The chosen mBAF threshold of 0.56 for calling allelic imbalances allowed detection of hemizygous losses present in clones exceeding 20% of and single copy gains (e.g. trisomies) in clones exceeding 25% of sampled cells. The minimum and maximum mBAF values within each abnormal segment were used build confidence intervals for clone sizes, i.e. the proportion of tumour cells containing the abnormality in question. Clone size spans were calculated as the difference in tumour cell content between the most and least prevalent genomic aberrations. Segments corresponding to

genomic imbalances and their estimated tumour cell content are listed in Supplementary Data File S1.

Touch preperations

Frozen tumour material was immediately placed on dry ice and a 2-3 mm piece carved from each biopsy using a scalpel. The cut off piece was then picked up using sterilized tweezers and gently pressed against a microscopy slide. The amount of imprinted cells was validated via phase-contrast microscopy. Prior to the *fluorescence in situ hybridisation* (FISH) procedure the slides were placed in fixative, one part glacial acetic acid and three parts methanol, for ten minutes and then dried in room temperature. The slides were then kept in the freezer at -20° C. As a normal control, post-mortem anonymized adrenal tissue, having undergone the same procedure of freezing and thawing was used.

FISH

Cell culture, fixation and chromosome preparation were performed according to standard methods as previously described. [27] FISH on tumour cell imprints and cell line wells were used to assess copy number diversity in detail, primarily with respect to whole chromosome copy numbers. For this purpose, centromere-specific probes for chromosomes 1, 2, 4, 7, 11, 12, 17 and 18 were obtained (Abbott lLaboratories, Abbott Park, IL), these being the chromosomes showing the most diversity in the SNP-array data. Probes for 1p, 11q and 17q (Abbott Laboratories) were also obtained since these regions are commonly affected by structural changes in NB. FISH was performed according to standard procedures as previously described.[27] The number of signals in each cell was manually scored in digital images acquired by a CCD camera coupled to an epi-fluorescence microscope. For each

specimen, including the normal fibroblast, at least 200 nuclei were analyzed. A normal fibroblast sample served as a technical control for the overall hybridization efficiency for each centromere probe used and this was found to be close to 100%.

In silico simulations

The stochastic models used to simulate mitotic chromosome segregation errors have been previously described. [20] In brief, whole chromosome copy number distributions from NBs were tested against the four previously described main types of aberrant mitosis in tumours, including (1) loss of chromosomes from the tetraploid level, (2) sequential sister chromatid non-disjunction, (3) tripolar mitosis coupled to sister chromatid non-disjunction, and (4) tripolar mitosis coupled to incomplete cytokinesis. Whole chromosome copy number profiles from NBs containing numerical chromosome aberrations were obtained from two independent datasets. The first was the Mitelman Database of Chromosome Aberrations and Gene Fusions in Cancer (http://cgap.nci.nih.gov/ Chromosomes/Mitelman; Dec. 18 2011) providing abnormal karyotypes from 273 NBs. Excluding karyotypes from recurrent tumours, from adults (>18 years of age), karyotypes with no numerical changes, incomplete karyotypes (inc), and karyotypes with markers (mar) or ring chromosomes (r), there remained 52 cases with high-quality karyotypes from pediatric primary NBs (Supplementary Data File S2). For clinical-genetic classification, the presence of double minutes (dmin) or hsr (homogeneously staining regions) in the karyotype was assumed to be equivalent to *MYCN* amplification. The second dataset was based on SNP array (Illumina HumanCNV660 and Omni BeadChip) analysis of >100 NBs, as described above, accessible through the R2 Microarray Analysis and Visualization Platform (http://hgserver1.amc.nl/cgi-bin/r2/main.cgi?&species=hs; Dec. 14

2011) from which the 68 cases containing whole chromosome copy number aberration were extracted (Supplementary Data File S3).

To compare the whole chromosome copy number profiles (i.e. the relative frequencies of monosomies, disomies, trisomies, tetrasomies, pentasomies and higher polysomies) expected from each type of abnormal mitosis to empirical data, a set of R-based algorithms (R.app GUI 1.33 5582 Leopard build 32-bit, R Foundation for Statistical Computing, 2009) were constructed where chromosomes were assumed to segregate normally or abnormally, independently of each other in a fashion according to the specific type of aberrant mitosis being simulated [20]. Each individual tumour was compared to each model by simulating monoclonal expansion from 10,000 virtual pre-neoplastic cells with either a normal diploid (sequential sister-chromatid non-disjunction; the two types of tripolar mitosis) or a normal tetraploid karyotype (loss from tetraploidy; the two types of tripolar mitosis). Each of these original 10,000 cells with a balanced chromosome complement were then set to evolve step-wise according to its specific type of chromosome segregation deficiency until a chromosome number had been reached that corresponded to that of the case being evaluated. Cells that obtained nullisomies (0 copies of a chromosome) were eliminated by replacement with random sampling from the remaining population. The resulting dataset from 10,000 virtual tumours with the same chromosome number was used to calculate the expected prevalence of the specific copy number distribution (i.e. the distribution of monosomies, disomies, trisomies etc.) found in the tumour being evaluated. Performing such simulations for all tumours present in a specific clinical-genetic subtype also generated an overall expected relative distribution of chromosome copy numbers according to each of the abnormal mitotic processes tested. This parameter was used together with the expected prevalence values of observed copy number distributions to assess which type of mitotic aberration best predicted the chromosome aberrations found in each clinical-genetic subtype.

Scoring of mitotic segregation errors

Cell lines were cultured on chamber slides and washed in phosphate buffered saline (PBS). The slides were fixed in -20° C methanol and dried at room temperature. Cell nuclei and chromosomes were counter-stained with DAPI. Using a fluorescence microscope, anaphase bridges, lagging chromosomes and multipolar mitoses were scored as previously described. [28]

Single-cell cloning

One *MYCN* amplified cell line (GI-MEN) and one non-amlified cell line with multiple segmental aberrations (SK-N-AS) were chosen for single-cell cloning due to their steady growing patterns. hTERT transduced BJ cells (BJ-5ta) were used as a stable karyotype control. A suspension of 10 ml containing 100 cells was prepared from each line. The suspension was diluted in steps and transferred into a 96 well plate, incubated for growth in standard medium. The following day, each well was examined using a inverted light microscope. Wells containing only one cell were marked with a permanent marker and monitored every second day until approximately 1000 cells were present. The cells were then trypsinized and placed in chamber slides for approximately one week, then harvested according to methods previously described.[27] At least 200 nuclei in three clones from each cell line were analysed by FISH.

Time lapse imaging

To further investigate the process of tetraploidy development in NB cell lines, time-lapse imaging was performed using the Nikon Eclipse Ti camera (Nikon Instruments Europe B.V. Laan van Kronenburg 2, 1183AS Amstelveen, The Netherlands). The cell line GI-MEN was used, as it was the cell line showing most mitotic aberrations. The total time between frames was 5 minutes.

Statistical analysis of empirical data.

Averages of normal like distributions were compared using two-tailed Student's t-test. Fisher's exact test, two-tailed, was used for nonparametric tests (STATISTICA version 20.0.0, IBM, 2011, CA).

Results

Extensive intercellular diversity in NB tumours and cell lines

To make a first survey of intra-tumour genetic diversity in NB, we used allelic ratios (mBAF values) obtained by SNP array analyses to approximate the prevalence of tumour cells harbouring each detected allelic imbalance (Figure 1A). This will well approximate the proportion of cells carrying genomic imbalances down to a prevalence of approximately 20%.[25,26] From a larger cohort of approximately 100 NB tumours and cell lines analysed by SNP-array, we consecutively selected the 10 cases of each clinical-genetic subtype having the highest quality SNP array profile as quantified by baseline variation at the diploid level (Figure 1B). The tumour cell content of the detected aberrations in primary tumours varied from approximately 100% down to 18% (Supplementary Data File S1). Overall, all cases showed at least one aberration present in >50% of tumour cells (exemplified in Figure 2A-C).

The specific allelic imbalances showing the highest clonal prevelence (present in >90% of the cells) varied extensively between cases and included duplication of 17q sequences (ITCC13, ITCC29), deletion of 1p31p36 (NRC11), duplication of 6q15q27 (NRC7), duplication within 19q13 (NRC14), duplication of 2q32q24 (ITCC38), duplication of 15q22q26 (ITCC36), and uniparental disomy for chromosome 21 (ITCC44). Specific allelic imbalances detected at a prevalence <30%, included 1-4 extra copies of 17q sequences (NRC8, NRC13, ITCC2, ITCC38), duplication of 3p14pter (ITCC2), deletion of 10q23q26 (ITCC174), and monosomies of chromosomes 3 and 10 (ITCC31). As expected, the cell lines showed a trend towards more aberrations with high prevalence but differences were not significant, and prevalence ranged from 97% down to 27% in the cell lines.

Because it can be assumed that all primary tumour samples were contaminated to some degree by non-neoplastic cells, the absolute prevalence estimates cannot be used for valid assessment of intratumour genetic diversity. We therefore chose to quantify diversity as the prevalence span between the most and least frequent genomic imbalance in each case (Figure 2A-C). By this approach, all analysed cases exhibited some degree of intratumoural clonal variation (Table 1), ranging from 5% to 72%. Including all types of aberrations, the prevalence span was narrower ($p<0.05$) for Type 1 tumours (mean 21%) compared to tumours belonging to Types 2A (50%) and 2B (39%; Figure 2D). The difference was even more pronounced when only primary NB tumours were compared (means 20% in type 1 vs. 60% and 58% in 2A and B; $p<0.001$). We then compared the spans of whole chromosome changes within each case with those of structural aberrations (Figure 2E). There was a significantly narrower span for numerical aberrations in general (mean 21%) than for structural aberrations (mean 36%; $p<0.05$ irrespective of inclusion of cell lines), indicating that the narrower span in Type 1 tumours compared to Types 2A and B was due to the manifold higher prevalence of whole chromosome changes in the former type as compared to the high prevalence of structural changes in the latter types. Indeed, the total prevalence span correlated positively to the number of structural aberrations (Pearson $r=0.55$) and negatively to the number of numerical aberrations ($r= -0.48$). Furthermore, an average of 78% of the detected numerical aberrations were within the same prevalence level (estimated from minimum and maximum mBAF values; Supplementary Data File S1as the majority of aberrations in present in the same case, most likely corresponding to the majority clone. In contrast, only 52% of the structural changes were confined to the majority clone ($p<0.01$ with either inclusion or exclusion of cell lines). In summary, SNP array-based estimates of intratumour diversity revealed a difference between tumours dominated by whole chromosome changes (Type 1)

and those dominated by structural aberrations (Types 2A and B), with a clear clonal hierarchy being more common in the latter two.

Prevalence span estimation from SNP array data is expected to reveal clear clonal population strata within a tumour biopsy or cell line, if such are present. However, it cannot discern clones with a prevalence <20% and thus gives little information on cell-to-cell variation. Furthermore, it cannot be expected to discern a background of stochastic variation in copy-number centred around the modal chromosome numbers of a major clone (Figure 3). For example, if the stemline of a hyperdiploid NB is characterised by trisomies of 5 chromosomes, stochastic variation leading to smaller clones with a random blend of monosomies and tetrasoimes would not be readily detected as it cannot be discerned from contaminating cells with a normal karyotype. Also, if the rate of newly formed copy number aberrations would be approximately the same for the five different trisomic chromosomes, the neoplastic population would falsely be interpreted as a homogenous clone with 51 chromosomes. Hence, while the SNP array analysis found little evidence for significant genome diversity in Type 1 NBs it did not strictly exclude stochastic or near stochastic variation at the cellular level.

In order to assess intercellular copy number in detail, we selected a subset of the tumours analysed by SNP array for further investigation by interphase FISH (Figure 4A). To be able to assess the intratumoural diversity of whole chromosome numbers we used centromere probes for chromosome 1,2,4,7,11,12,17 and 18, these being the chromosomes showing the most heterogeneity in SNP array data. For each case, FISH experiments were tailored to cover chromosomes / genome segments with aberrations showing both high and low clonal prevalence by SNP array analysis. For comparison, we also used probes for 1p, 11q and 17q, being the segments commonly affected by structural aberrations in NB. Compared to normal

control adrenal tissue, all cell lines and all but one of the tumours (NRC4) showed elevated inter-cellular copy-number variation for the majority of the analysed chromosomes/segments, with up to 75% and 73% of tumour cells showing non-modal copy numbers in primary tumours and cell lines, respectively (Figure 4; Table 2). Assessment of whole chromosome numbers showed an average of 16.5% of cells with non-modal copy numbers compared to 48% for chromosome segments (1p, 11q and 17q). Even though 17q tended to show the overall highest prevalence of cells with non-modal copy numbers (mean 55%), there was high variability between cases and no statistical difference compared to 1p and 11q. Neither was there any overall significant difference in the prevalence of cells with non-modal copy number when whole chromosomes and chromosome segements were compared.

When SNP array data were used to calculate the average prevalence of cells with non-modal copy numbers for the FISH-analysed cases, there was no clear difference between the two methods (Figure 4B). Consistent with the SNP array data, there was a trend for whole chromosomes to have similar fractions of cells with non-modal copy numbers, while structural changes showed dispersed data (mean spans 17% and 34% respectively; $p=0.02$). FISH analysis showed broad numerical distributions for cells with non-modal copy numbers (Figure 4F), inconsistent with the bimodal euploid/aneuploid scenario expected if all numerical aberrations were confined to a single genetically homogeneous clone (Figure 3B). Instead, there was typically a presence of multiple small sub-populations with non-modal chromosome numbers, as predicted from near-stochastic variation around the modal value (Figure 3C). Thus, intra-tumour diversity appeared to be present for both numerical and structural chromosome aberrations in NB, even though the system of clonal hierarchies resulting from these two types of aberrations were distinct as indicated by SNP array data.

Chromosome loss from a tetraploid intermediate best predicts evolution of numerical changes

The distinct sub-clonal stratification of structural changes found in NB by SNP array analysis is a common finding in cancer. [29] In several tumours, including NB, abnormal mitotic chromosome segregation such as anaphase bridging caused by telomere dysfunction has been suggested to be a major underlying mechanism.[30] However, the mechanism causing variation in chromosome number has been little investigated in NB. To connect our findings of a near-stochastic variation in chromosome number in NB with possible mitotic errors, we first used a bio-informatics / statistical approach (Figure 5). By this method, the specific pattern of chromosome copy numbers (monosomies, disomies, trisomies, tetrasomies etc.) found in a cohort of tumour cases by cytogenetics or genomic arrays is compared to patterns expected from different types of mitotic error previously reported in tumour cells.[20] These mitotic errors include (1) chromosome loss from the tetraploid level, (2) sequential sister chromatid non-disjunction, and (3) multipolar mitosis. For evaluation of each reported tumour karyotype/SNP array profile, 10,000 virtual euploid tumour stem lines are created and allowed to evolve according to each different model of mitotic segregation error, until a chromosome number identical to that of the reported tumour is reached. Details of simulations are provided in legend to Figure 5 and in Materials and Methods.

For comparison of chromosome copy number patterns in NB with those expected from the respective types of chromosome segregation errors, we extracted high-quality genomic data from one cytogenetic and one SNP array-based dataset, resulting in 52 and 68 cases of NB with whole chromosome aberrations, respectively (details provided in Materials and Methods). We first compared chromosome copy number profiles from these cases with those expected from the various types of chromosome segregation without any restrictions on cell survival imposed by chromosome number, except for elimination of cells with nullisomies.

Under these conditions, none of the tested scenarios were able to replicate the overall distribution of copy number profiles in NB. More than >90% of observed copy number distributions showed an expected prevalence close to 0 (range 0-0.0001) and the overall observed copy number distributions poorly matched those expected from the simulations ($p<0.0001$; Chi Square test).

In a second round of simulations, we took into account the fact that monosomies are very rare in NB genomes, being present in only around 12% of cases in our dataset, with no case showing >1 monosomy. Algorithms were then adjusted to impose a negative impact on cell survival from monosomy, replacing tumour stem lines with at least one monosomy with a randomly sampled stem line from the entire set of 10,000 stem lines. Renewed simulations showed that most types of mitotic segregation error still poorly predicted the observed copy number distributions (Figures 6 and 7). The type of mitotic error least compatible with the observed copy number distributions were multipolar mitosis from a diploid state (mean expected prevalence ≈0 for both cytogenetic and SNP array data, with a distinctly different expected distribution at $p<0.0001$ by Chi Square test for both datasets), followed by multipolar mitosis from a tetraploid state (mean expected prevalence 14% and 19% for cytogenetic and SNP array data, respectively; $p<0.0001$ for both), sequential sister chromatid separation from a diploid state (16% and 18%; $p<0.0001$ for both), and sequential sister chromatid separation from a tetraploid state (16% and 17%; $p<0.0001$ for both). In contrast, loss of chromosomes from the tetraploid level produced copy number distributions with higher prevalence values (27% and 33%) and an overall distribution of copy numbers profiles that was not significantly different from the observed ones ($p>0.05$ for both datasets). There were no differences between the clinical-genetic subtypes of NB, all of which showed copy number profiles best predicted by chromosome loss from the tetraploid state (Figures 6 and 7). This was consistent with our SNP array subclonality analysis, showing no difference in

clonal population structure between subtypes. However, it should be noted that the simulations showed highly similar expected copy number profiles for cases with only a few whole chromosome changes. Our findings that loss from tetraploidy best predicts the scenario of numerical changes in NB is therefore most valid for cases with >50 chromosomes.

Evolution of whole chromosome changes is an ongoing process

To experimentally validate whether a process of continuous chromosome loss was present in NB cells, as predicted by the simulations, we analysed chromosome segregation patterns at mitosis in established NB cell lines. All cell lines showed different types of aberrations during mitosis such as anaphase lagging (up to 17%), anaphase/telophase bridges (12%) and, less commonly, multipolar mitoses in up to 3% of cell divisions (Table 3; Figure 8A). In contrast, control fibroblasts subjected to the same type of analysis showed cell division anomalies in only 1% of mitoses, all of which consisted of anaphase bridges (data not shown). On average, chromosome loss through lagging was the most common type of aberration (8% of cells compared to 5% for bridges and 1% for multipolar mitosis), indicating that chromosome loss is a common and ongoing process in growing NB cells.

To further validate that chromosomal instability was an ongoing phenomenon that could generate tumour cell sub-populations with different chromosome numbers, we created single cell clones from two cell lines, GI-MEN AND SK-N-AS, that were allowed to expand for 15-20 mitotic generations and from a control fibroblast cell line expanded for the same number of generations. To compare numerical variation between single cell clones and their respective populations of origin, we performed FISH with centromere probes for chromosome 11, 17 and 18 (Figure 8B). As expected, the single-cell clones tended to show less copy number

diversity than their respective original cell populations (Tables 4 and 5), but it could not be concluded that any specific chromosome or genomic segment had more or less instability than that of another. However, all chromosomes showed a significantly higher degree of copy number heterogeneity compared to the single cell clones made from the control group of fibroblasts. The heterogeneity was different from that of the original cultures in the matter that copy numbers were more homogenously distributed around the modal numbers (Figure 8B). This supported that chromosomal copy number variation was an ongoing phenomenon in NB cells.

Because our simulations suggested that tetraploidisation was a key step in the evolution of numerical changes in NB, we finally investigated whether this regularly occurs in growing NB cells, using the triploid-tetraploid GI-MEN cell line as a model. Two of the main routes towards tetraploidisation are fusion of two diploid cells and mitosis with cytokinetic failure, respectively, both leading to cells with a duplicated chromosome complement.[31] We performed phase contrast time-lapse microscopy of growing GI-MEN cells to assess the presence of either of these routes (Figure 8C and Supplementary Video S1). No event of cell fusion was observed within the total time frame of 6 days of time lapse imaging of >100 cells. In total 52 cell divisions were followed from prophase through telophase. Of these, 6% failed to undergo cytokinesis, indicating that, besides chromosome loss through various mechanisms, also polyploidisation through failed cell division can occur regularly in NB cells.

Modelling NB genome evolution as a dynamic process

Taken together, our results indicated that loss from the tetraploid state is the most likely route towards aneuploidy in NB and that this is an on-going process in NB cells. Based on this, we constructed a dynamic model of whole chromosome number changes in NB, by simulating

growth from a diploid pre-tumour population with a certain probability to undergo chromosome loss or whole genome duplication / polyploidisation at each mitosis (Figure 9A). Based on extended FISH-based cell division analysis of GI-MEN the probability of chromosome loss was set to 4 x 10^{-2} per chromosome per mitosis(combined lagging and loss from non-disjunction; data not shown) and the frequency of polyploidization to around 6%. Based on our simulation data we also imposed negative selection on cells having obtained nullisomies or monosomies. Based on available cytogenetic data (Mitelman Database of Chromosome Aberrations and Gene Fusions in Cancer; http://cgap.nci.nih.gov/Chromosomes/Mitelman) we also imposed negative selection on highly polyploidy cells (>92 chromosomes) as stem lines with such chromosome numbers occur only in approximately 2.5% of NBs (7 of 273 cases).

Allowing populations of 10,000 pre-tumour cells to evolve over 500 mitotic generations, identical results were produced by 10 independent simulation experiments: cells losing chromosomes from a diploid state were rapidly out-competed by the descendants of other cells that underwent tetraploidisation at an early stage (Figure 9B, G= 1-10). This resulted in a growing population dominated by cells in the hypotetraploid range, gradually shifting through triploidy down towards hyperdiploidy (Figure 9B, G=50-100). When reaching diploidy, a population shift, similar to that at early generations, occurred that again shifted the population to a hypotetraploid state. Most of the generation time for the population was spent at a peri-triploid state (Figure 9C), during which most of the extrapolated net tumour growth took place (Figure 9D). A control cell population not able to undergo whole genome duplication but otherwise grown under identical conditions, showed an accumulation of hypodiploid cells, existing in a dynamic equilibrium with diploid cells, reflecting a balance between the rate of chromosome loss and the survival advantage of cells without monosomies; as expected no hyperdiploid cells formed in this population. Taken together, our dynamic model showed that

a combined negative selection against cells with excessive chromosome loss (nullisomy and monosomy) combined with a capacity for whole genome duplication will consistently result in a dominance of tumour cells with chromosome numbers in the peri-triploid range, similar to the distribution found in most highly aneuploid NBs, particularly in Type 1 tumours.

Discussion

In the present study we show that intra-tumour diversity of large-scale genomic imbalances is a major feature of most NBs, irrespective of clinical-genetic subtype. These results were arrived at by two independent methods, i.e. SNP array and FISH analyses. Although diversity was observed for both structural and numerical chromosome aberrations, the former were distributed in clear-cut clonal hierarchies while the latter type of aberrations showed near-stochastic variation. Mathematical simulations indicated that this stochastic distribution most likely reflected a process of chromosome loss from a tetraploid state, which was supported by experimental data showing frequent chromosome loss and polyploidisation in NB cell lines. Taken together, our data converged into a complex dynamic model for aneuploidy development in NB, most relevant to tumours with chromosome numbers in the hyperdiploid-hypotetraploid range (Figure 10). To our knowledge, this is the first report of intra-tumour chromosome number variation and its underlying mechanisms in NB.

Our *in silico* approach for estimating the most likely mechanism behind numerical aberrations in NB has several limitations. For example, it assumes that only one route of mitotic error is present in each tumour, which is likely to be an oversimplification.[28] Furthermore, the *in silico* modelling yielded informative results only after negative selection against stem lines with monosomies were introduced based on extrapolation from their scarceness in cytogenetic and SNP array data. Finally, none of the applied models took into account the variable degree of positive and negative selection for different numerical aberrations, which is most probably present in NB as their pattern is clearly non-random.[32,33] However, similar analyses have been performed previously and were shown to correlate well to experimental data on cell division errors in tumour cells. [20] A similar type of analysis has also been performed for acute

childhood leukemia,[34] using the frequencies of uniparental disomies to validate different scenarios behind hyperdiploidy. However, that approach does not allow an equally fine-tuned distinction between the different scenarios of mitotic segregation errors and was therefore not applied in the present study. For example, randomised segregation through multipolar mitosis from a diploid state cannot be distinguished from loss of chromosomes from the tetraploid level. Even though we found our simulation data on chromosome segregation errors to be consistent with experimental findings of chromosome lagging and polyploidisation, it should be stressed that (1) the loss-from-tetraploidy model provides only the best fit out of a few available models and there may be other mechanisms behind aneuploidy hitherto unknown that fit the data better, (2) the models only showed significant differences for tumour stem lines with >50 chromosomes and that the mechanism behind the creation of moderately hyperdiploid karyotypes was not resolved by the present study, and (3) individual NBs even if having >50 chromosomes, may still obtain aneuploidy by a different route, as our approach evaluated only which single scenario that best fit the overall genomic data.

Our *in silico* simulations yielded data comparable to cytogenetic and SNP array results only when strong selection against monosomic cells were introduced in the algorithms. Consistently, there was a very low prevalence of mosomies in the genomic profiles reported by SNP array and cytogenetics, and FISH analysis did not show a monosomic modal number for any of the whole chromosomes assessed in cell lines or primary tumours in the present study, except for chromosome 17 in SK-N-AS. Nevertheless, the loss from tetraploidy model suggested here stipulates that monosomies are continuously produced in growing tumour cells, which is consistent with our FISH data showing monosomic sub-populations for most of the assessed chromosomes. The lack of monosomies in tumour stem lines could perhaps be explained by monosomic cells lacking the necessary genomic material for survival through the next cell cycle. If so, whole genome duplication through failed mitosis or other

mechanisms may confer sufficient extra genomic material to allow growth even in a context in which chromosome copies are continuously lost through genomic aberrations. The necessity to have such genomic "buffering capacity" to balance an inherent chromosomal instability could potentially explain why aneuploid NBs typically have chromosome numbers in the hyperdiploid to triploid range. However, a cell population subjected to constant whole chromosome loss will sooner or later reach a point when a high rate of monosomies are generated, in turn leading to reduced growth capacity if monosomy is associated with reduced cellular survival. The reaching of such a critical point could, in theory, explain why the typically highly aneuploid Type 1 (infants with stage 1 or 4s) NBs show an excellent prognosis and may even spontaneously regress.[35,36] However, tumours having numerical aberrations in combination with amplification of *MYCN* or other structural chromosome changes generally do not share this favourable course of disease. [21] Possibly, this is due to a lower overall rate of chromosome loss in these tumours. However, as long as there is no stable *in vitro* system for Type 1 NBs available for comparison of mitotic segregation errors to Types 2A and 2B, this hypothesis cannot be further tested.

The thought of intra-tumoural diversity of chromosome numbers based on cell division anomalies in NB is not new. Kaneko and Knudsen [37] discussed tumour ploidy in the context of abnormal mitosis already in 2000. Their study was focused mainly on ploidy as a prognostic factor and the equality between the numbers of chromosome 1 and the ploidy level of the tumour. However, they also suggested a theoretical model for the development of near-triploid NBs based on tripolar division of a tetraploid cell, assuming asymmetrical 2-3-3 amphitelic distribution of the eight chromatids from the tetrasomic chromosomes. Later studies have so far failed to show experimentally the significance of this mechanism in human tumour cells. Tripolar mitoses may either circumvent the spindle assembly checkpoint,

leading to a high frequency of non-disjunction events and near-random distribution of chromatids to daughter cells.[38] Alternatively, the spindle assembly checkpoint can be satisfied and chromosomes will segregate amphitelically to the daughter cells in a tripolar fashion, but chromosomes will never the less be asymmetrically distributed because of cytokinetic failure, leading to one daughter cell with chromosome gains and another with chromosome losses.[26] Taken together, these data suggest that the scenario proposed by Kaneko and Knudsen is not a typical outcome of tripolar cell division. Furthermore, the data of the present study fails to support this hypothesis in its original form, as our experimental observations show that the generation of numerical aberrations appears to be an ongoing process rather than a stable state based on a single event. Furthermore, our mathematical simulations of copy number distributions resulting from tripolar mitoses were poorer predictors of the actual scenario in NB than those based on continuous loss from the tetraploid level. However, it should be noted that the Kaneko-Knudsen model is consistent with our findings in the sense that it suggests an early tetraploid cell from which chromosomes are lost to create aneuploid tumour cells.

Chromosomes can be lost from a tetraploid cell through a broad set of different mechanisms.[31] Although chromosome lagging at anaphase was the most common type of cell division error found in NB cells in the present study, it does not exclude other mechanisms of origin. Neither does our study provide evidence explaining the high frequency of anaphase lagging in NB cells. Multipolar cell divisions were found in some of the NB cell lines in the present study. It has been well demonstrated that multipolar cell divisions may re-orient to a pseudo-bipolar configuration before anaphase, which nevertheless shows a propensity for chromosome lagging due to merotelic spindle-kinetochore attachments.[7] However, not all cell lines in the present study exhibited multipolar mitoses, while all of them still showed a high frequency of anaphase chromosome lagging. Centrosome disturbances, which are generally believed to be the main cause of multipolar mitoses, were evaluated in NBs by Fukushi et al.[39]

Although a connection could be established with ploidy divergence in a sub-group of infant NBs, they did not find the general connection to aneuploidy expected if extra centrosomes and spindle multipolarity was a major mechanism behind numerical aberrations in NB. Taken together, this makes centrosome disturbances a poor candidate behind the high frequency of lagging chromosomes in NB cells. However, we also found a high frequency of anaphase bridges, in accordance to a previous report showing critically short telomeres and chromosome fusion in NB.[23] Although this type of cell division anomaly has been intimately connected to structural chromosome aberrations,[40] it has also been shown to result in loss of whole chromosomes.[41,42] Another most recent study by Pampalona et al.[43] has demonstrated a connection between telomere deficiency and tetraploidisation. This suggests that telomere dysfunction may contribute to aneuploidy in NB by causing chromosome loss and tetraploidisation in parallel. That telomere dysfunction is a common feature in many cancers has previously been shown by numerous papers,[44-46] albeit they do not have to be critically shortened to have a clinical impact.[23,47] Whether telomere deficiency also has a role for the generation of aneuploidy in NB remains to be studied further.

In conclusion, we find that aneuploid NBs typically exhibit prominent intra-tumour genomic diversity with respect to both numerical and structural aberrations, which may have a role in the chemotherapy resistance in some of these tumours. For numerical aberrations, this diversity can to some extent be explained by errors of chromosome segregation at mitosis.

Legends to Figures

Figure 1. Basic principles and material for survey of diversity by SNP array analysis. *(A)* A monoclonal cellular proliferation with ongoing genomic instability (left panel) will result in a genetically heterogeneous population, where specific genetic aberrations (denoted by circles) will be present at different prevalences. By SNP array analysis, these prevalence values can be approximated from mBAF data for genomic aberrations that lead to allelic imbalances (right panel; details in Materials and Methods). The detected prevalence levels will to some extent reflect the temporal development of genetic aberrations because early aberrations (black and red circles) will tend to have higher prevalence values than later genetic abnormalities. However, the relationship between prevalence and time of occurrence cannot be strictly relied upon, as it will be confounded by variable growth rates for different subclones (exemplified by blue, green, and yellow circles). *(B)* Cases selected for survey of genomic diversity by SNP-array, subdivided according to clinical-genetic subtype.

Figure 2. Intratumoral genome diversity by SNP array analysis. *(A-C)* Representative examples of prevalence estimates from mBAF data for the allelic imbalances present in three NBs. The prevalence specified as abnormaliy content (AC) for each aberration is plotted on the y-axis, while the type of aberration is specified along the x-axis. Segments affected by aberrations are specified according to cytogenetic nomenclature; + and - indicate gain and loss of a single copy, respectively. ITCC35 is a Type 1 NB exhibiting trisomy for seven chromosomes and monosomy for one, all of which are present at similar prevalence. ITCC130 is a type 2A tumour with multiple structural and numerical changes present at different prevalence levels, including 1p deletion, 11q deletion and 17q duplication. ITCC174 is a type

2B *MYCN* amplified NB with structural aberrations confined to three distinct prevalence levels. The prevalence span (s) of each case is denoted on the y axis. *(D)* Mean prevalence spans according to clinical-genetic type and *(E)* aberration type (NUM, numerical/whole chromosome changes; STR, structural changes); errors bars denote standard deviations.

Figure 3. Models of genome diversity. *(A)* Ongoing genomic instability with evolution of distinct subclones during tumour development. Circles of different colours represent cells with different genotypes; light blue circles are cells with a normal karyotype. There will be a high probability for variation in prevalence for genomic changes occurring at different steps during clonal evolution. In the right panel, this is exemplified by trisomies for chromosomes *a* and *b*, where trisomy *a* occurs early in the process and will be present at a high prevalence, while *b* occurs later with presence only in some cells. The relative frequencies (*f*) of copy numbers are denoted on the y axis and the segment copy number on the x axis. *(B)* A single event (such as an unbalanced mitosis or a genetic bottleneck) leading to clonal expansion from a single cell, with no ensuing genetic instability. If trisomies for chromosomes *a* and *b* are present in the cell of origin, their prevalence values will be the same in the resulting cell population. *(C)* A single event followed by genetic instability of a stochastic nature, resulting in near-random variation around a modal value for chromosomes *A* and *B*, both being trisomic in the cell of origin. Prevalence estimates from SNP array analysis will be able to distinguish *A* from *B* and *C*, but not *B* from *C*.

Figure 4. Intratumoral genome diversity by FISH analysis. *(A)* Cases selected for survey of genomic diversity by FISH analysis, subdivided according to clinical-genetic subtype. *(B)* Mean proportion of cells with a non-modal copy number, taking all FISH-analysed

chromosomes into account, with data sub-divided according to clinical-genetic subtypes (1, 2A, 2B). Data from FISH (F) and SNP array analyses are shown side-by-side. FISH data from normal post-mortem adrenal tissue (A) is included as a control. Error bars denote standard deviations. (*C*) FISH analysis of tumour touch preparation (NRC 7), here showing centromere probe 1 in orange and centromere 12 in green, both having a modal copy number of 3. (*D*) FISH analysis of the GI-MEN cell line, here displaying chromosome 18 centromere in blue, 1p in green and 17q in orange. (*E* and *F*) The distribution of chromosome 18 in the adrenal gland, which functioned as control, and case NRC 13.

Figure 5. Models of mitotic instability. *(A)* Schematic overview of the types of mitotic segregation error evaluated for comparison against cytogenetic and SNP array data. Segregation errors were simplified by translating the most common outcome for each type of error into an algorithm: (1) Loss from tetraploidy was modelled as a process that sequentially and randomly creates loss of single chromatids from the tetraploid level.[7] (2) Sister chromatid non-disjunction was set up as a serial process creating one monosomic and one trisomic daughter cell in each step.[26] (3) Multipolar mitosis was modelled as generating three daughter cells with failure of proper sister chromatid separation, leading to a randomised distribution of chromatids to each daughter cell [38] as shown in the figure or amphitelic segregation and cytokinetic failure leading to one daughter cell with chromosome gains and another with losses (not shown). *(B)* Example of modelling loss of tetraploidy for a tumour with a stem line karyotype containing 50 chromosomes with monosomy 1, trisomies 2 and 3, and tetrasomy 4. The chromosome number N=50 is used as the target value for simulations of 10,000 cancer stem lines formed by random loss of chromosomes from a chromosome number of 92 (tetraploid). Each of these virtual stem lines will have a certain copy number (CN) profile (from 0-4), depending on the distribution of losses over its different chromosomes. The

profiles of all 10,000 stem lines are used to generate an overall CN profile for tumours with 50 chromosomes created by loss from tetraplody. This dataset is then used to assess the expected prevalence of the specific CN profile of the original tumour, on the condition that it was created by loss from tetraploidy. To compare observed (cytogenetics/SNP array data) to expected (simulated) data for specific groups of NB cases, overall observed vs. overall expected CN prolifes are also compared by Chi-square test (Figures 6 and 7).

Figure 6. Expected frequencies of observed karyotypes for different types of mitotic instability. NB cases retrieved from the Mitelman Database of Chromosome Aberrations and Gene Fusions in Cancer were subdivided according to clinical-genetic subtype (vertical panels) and according to simulations of three different types of mitotic segregation error. Each blue circle denotes a case, charted according to its chromosome number (x axis) and the expected prevalence of its CN profile (y axis) according to the type of segregation error being simulated. P values reflect the results of Chi square testing of the overall observed distribution (cytogenetics) against the expected distribution (simulations). Monosomic and nullisomic cells were eliminated from all simulations. For multipolar mitosis, only results based on amphitelic segregation and cytokinetic failure are shown because modelling of randomised segregation resulted in prevalence values <1% for all CN profiles

Figure 7. Expected frequencies of observed SNP array profiles for different types of mitotic instability. NB cases analyzed by SNP array were subdivided according to clinical-genetic subtype, analyzed, and annotated as described in Figure 6. Monosomic and nullisomic cells were eliminated from all simulations. For multipolar mitosis, only results based on

amphitelic segregation and cytokinetic failure are shown because modelling of randomised segregation resulted in prevalence values <1% for all CN profiles

Figure 8. Ongoing chromosomal instability in NB cells. *(A)* Visualizing three aberrations during mitosis in GI-MEN, telophase bridging , lagging and a multipolar mitosis. *(B)* The different distributions of chromosome 18 in GI-MEN original culture and the three single-cell based clones derived from it. In the original culture, the modal number was three, whereas in the clones two exhibit a modal copy number of four whereas the last one has a modal copy number of two. (*C*) Time lapse phase contrast microscospy of dividing GI-MEN cells showing a cell (left panel; red arrow) entering mitosis (t = 0 min) up until anaphase (t = 41 min), but then failing to undergo cytokinesis (followed for 24 h post mitosis). Adjacent cells underwent normal cell divisions (right panel; blue arrow). Time is annotated in minutes from maximum mitotic round-up. Total time for video monitoring was 48 h 35 min. See Supplementary Video S1 for full time lapse session.

Figure 9. Dynamic modelling of NB genome evolution. *(A)* A virtual population of 10,000 cells with a normal diploid genome were set to evolve until 500 mitotic generations, with a probability *p* of losing a chromosome at each mitoses, the probability *t* to undergo whole genome duplication (typically tetraploidisation) through mitotic failure, and the probability *1-p-t* to undergo an error-free mitosis. The input values of *p* and *t* were obtained from experimental studies of GI-MEN. Cells with ≤1 copies of any chromosome (*n*) or a chromosome number (*N*) >92 were excluded from future generations. Net growth was estimated as the fraction of cells at each time point having the possibility of undergoing mitosis, i.e. cells without nullisomies, monosomies or high polyploidy (N>92). (*B*)

Chromosome number evolution over 200 mitotic generations (G) for the entire population where the bars (y axis) denote the number of cells (N) having a certain chromosome number (x axis). For each generation, results are shown for a test population (Pop1; left panel) under conditions described in *A* and a control population (Pop2; right panel) where whole genome duplication cannot take place. Already at G=10, Pop1 is dominated hypotetraploid cells, as cells with chromosome losses down to the monosomic level are outcompeted by those having undergone whole genome duplication. The dominance is then shifting to near-triploid cells (G=50, G=100). At G=200 a hyperdiploid population co-exists with a hypotetraploid one as cells with chromosome losses down to the monosomic level are again outcompeted by others having undergone whole genome duplication. The full simulation is presented in Supplementary Video S2. (*C*) Mean chromosome number (mean N) for the entire Pop1 (red line) over 500 generations show a fluctuation around the triploid level, while the control population (Pop2, blue line) is stably near-diploid. (*D*) Estimated net growth rate for Pop1 (red line) fluctuates in parallel to mean chromosome number and overall exceeds that of Pop2 (blue line), the latter accumulating a high fraction of cells with monosomies which are not expected to enter mitosis.

Figure 10. Suggested model for aneuploidy development in NB. A diploid pre-tumour cell undergoes tetraploidisation followed by/or in combination with chromosome loss until a copy number profile allowing clonal expansion is obtained; the present data do not fully exclude that this first step occurs through a single event even though later copy number changes appear to occur in a step-wise fashion. Chromosomes are continuously lost during clonal expansion leading to a population with copy number diversity, the composition of which is further modified by endogenous selection against cell with monosomies and nullisomies, as

well as exogenous unknown factors. Further subclonal development unto a higher ploidy level may also occur through repeated whole genome duplications.

Acknowledgement

This study was supported by the Swedish Children's Cancer Foundation, the Swedish Cancer Society, the Swedish Research Council, the Swedish Medical Society, the Lund University Hospital Donation Funds, the Gunnar Nilsson Cancer Foundation, the Crafoord Foundation, the Erik-Philip Sörensen Foundation, the Lundgren Foundation, the Schyberg Foundation and the Medical Faculty at Lund University.

References

1. **Hanahan D, Weinberg RA. Hallmarks of cancer: the next generation. *Cell.* Mar 4 2011;144(5):646-674.**

2. **Mitelman F, Johansson B, Mertens F. The impact of translocations and gene fusions on cancer causation. *Nat Rev Cancer.* Apr 2007;7(4):233-245.**

3. **Nambiar M, Kari V, Raghavan SC. Chromosomal translocations in cancer. *Biochim Biophys Acta.* Dec 2008;1786(2):139-152.**

4. **Duker NJ. Chromosome breakage syndromes and cancer. *Am J Med Genet.* Oct 30 2002;115(3):125-129.**

5. **Londono-Vallejo JA, Wellinger RJ. Telomeres and telomerase dance to the rhythm of the cell cycle. *Trends Biochem Sci.* Jun 21 2012.**

6. **Cimini D. Merotelic kinetochore orientation, aneuploidy, and cancer. *Biochim Biophys Acta.* Sep 2008;1786(1):32-40.**

7. **Ganem NJ, Godinho SA, Pellman D. A mechanism linking extra centrosomes to chromosomal instability. *Nature.* Jul 9 2009;460(7252):278-282.**

8. **Silkworth WT, Nardi IK, Scholl LM, Cimini D. Multipolar spindle pole coalescence is a major source of kinetochore mis-attachment and chromosome mis-segregation in cancer cells. *PLoS One.* 2009;4(8):e6564.**

9. **Corbett KD, Yip CK, Ee LS, Walz T, Amon A, Harrison SC. The monopolin complex crosslinks kinetochore components to regulate chromosome-microtubule attachments. *Cell.* Aug 20 2010;142(4):556-567.**

10. **Jasmine F, Rahaman R, Dodsworth C, et al. A genome-wide study of cytogenetic changes in colorectal cancer using SNP microarrays: opportunities for future personalized treatment. *PLoS One.* 2012;7(2):e31968.**

11. **Pentenero M, Donadini A, Di Nallo E, et al. Distinctive chromosomal instability patterns in oral verrucous and squamous cell carcinomas detected by high-resolution DNA flow cytometry. *Cancer.* Nov 15 2011;117(22):5052-5057.**

12. **Roylance R, Endesfelder D, Gorman P, et al. Relationship of extreme chromosomal instability with long-term survival in a retrospective analysis of primary breast cancer. *Cancer Epidemiol Biomarkers Prev.* Oct 2011;20(10):2183-2194.**

13. **Thirthagiri E, Robinson CM, Huntley S, et al. Spindle assembly checkpoint and centrosome abnormalities in oral cancer. *Cancer Lett.* Dec 18 2007;258(2):276-285.**

14. **Kuukasjarvi T, Karhu R, Tanner M, et al. Genetic heterogeneity and clonal evolution underlying development of asynchronous metastasis in human breast cancer. *Cancer Res.* Apr 15 1997;57(8):1597-1604.**

15. **Choi CM, Seo KW, Jang SJ, et al. Chromosomal instability is a risk factor for poor prognosis of adenocarcinoma of the lung: Fluorescence in situ hybridization analysis of paraffin-embedded tissue from Korean patients. *Lung Cancer.* Apr 2009;64(1):66-70.**

16. **Baird DM. Mechanisms of telomeric instability. *Cytogenet Genome Res.* 2008;122(3-4):308-314.**

17. **Siegel JJ, Amon A. New Insights into the Troubles of Aneuploidy. *Annu Rev Cell Dev Biol.* Jul 9 2012.**

18. **Mannaert A, Downing T, Imamura H, Dujardin JC. Adaptive mechanisms in pathogens: universal aneuploidy in Leishmania. *Trends Parasitol.* Jul 10 2012.**

19. **Yang C, Shi X, Huang Y, et al. Rapid proliferation of daughter cells lacking particular chromosomes due to multipolar mitosis promotes clonal evolution in colorectal cancer cells. *Cell Cycle.* Jul 15 2012;11(14).**

20. **Gisselsson D. Mechanisms of whole chromosome gains in tumors--many answers to a simple question. *Cytogenet Genome Res.* 2011;133(2-4):190-201.**

21. **Janoueix-Lerosey I, Schleiermacher G, Michels E, et al. Overall genomic pattern is a predictor of outcome in neuroblastoma. *J Clin Oncol.* Mar 1 2009;27(7):1026-1033.**

22. **Brodeur GM. Neuroblastoma: biological insights into a clinical enigma. *Nat Rev Cancer.* Mar 2003;3(3):203-216.**

23. **Lundberg G, Sehic D, Lansberg JK, et al. Alternative lengthening of telomeres-An enhanced chromosomal instability in aggressive non-MYCN amplified and telomere elongated neuroblastomas. *Genes Chromosomes Cancer.* Jan 14 2011.**

24. Staaf J, Vallon-Christersson J, Lindgren D, et al. Normalization of Illumina Infinium whole-genome SNP data improves copy number estimates and allelic intensity ratios. *BMC Bioinformatics.* 2008;9:409.

25. Staaf J, Lindgren D, Vallon-Christersson J, et al. Segmentation-based detection of allelic imbalance and loss-of-heterozygosity in cancer cells using whole genome SNP arrays. *Genome Biol.* 2008;9(9):R136.

26. Gisselsson D, Jin Y, Lindgren D, et al. Generation of trisomies in cancer cells by multipolar mitosis and incomplete cytokinesis. *Proc Natl Acad Sci U S A.* Nov 23 2010;107(47):20489-20493.

27. Lundberg G, Rosengren AH, Hakanson U, et al. Binomial mitotic segregation of MYCN-carrying double minutes in neuroblastoma illustrates the role of randomness in oncogene amplification. *PLoS One.* 2008;3(8):e3099.

28. Gisselsson D. Classification of chromosome segregation errors in cancer. *Chromosoma.* Dec 2008;117(6):511-519.

29. Heim Sverre MF, ed *Cancer cytogenetics.* 3rd ed ed: Hoboken, N.J; 2009.

30. Nicholson JM, Cimini D. How mitotic errors contribute to karyotypic diversity in cancer. *Adv Cancer Res.* 2011;112:43-75.

31. Storchova Z, Kuffer C. The consequences of tetraploidy and aneuploidy. *J Cell Sci.* Dec 1 2008;121(Pt 23):3859-3866.

32. Tonini GP, Romani M. Genetic and epigenetic alterations in neuroblastoma. *Cancer Lett.* Jul 18 2003;197(1-2):69-73.

33. Gisselsson D, Lundberg G, Ora I, Hoglund M. Distinct evolutionary mechanisms for genomic imbalances in high-risk and low-risk neuroblastomas. *J Carcinog.* 2007;6:15.

34. Paulsson K, Morse H, Fioretos T, Behrendtz M, Strombeck B, Johansson B. Evidence for a single-step mechanism in the origin of hyperdiploid childhood acute lymphoblastic leukemia. *Genes Chromosomes Cancer.* Oct 2005;44(2):113-122.

35. Nickerson HJ, Matthay KK, Seeger RC, et al. Favorable biology and outcome of stage IV-S neuroblastoma with supportive care or minimal therapy: a Children's Cancer Group study. *J Clin Oncol.* Feb 2000;18(3):477-486.

36. Hero B, Simon T, Spitz R, et al. Localized infant neuroblastomas often show spontaneous regression: results of the prospective trials NB95-S and NB97. *J Clin Oncol.* Mar 20 2008;26(9):1504-1510.

37. Kaneko Y, Knudson AG. Mechanism and relevance of ploidy in neuroblastoma. *Genes Chromosomes Cancer.* Oct 2000;29(2):89-95.

38. Gisselsson D, Hakanson U, Stoller P, et al. When the genome plays dice: circumvention of the spindle assembly checkpoint and near-random chromosome segregation in multipolar cancer cell mitoses. *PLoS One.* 2008;3(4):e1871.

39. Fukushi D, Watanabe N, Kasai F, et al. Centrosome amplification is correlated with ploidy divergence, but not with MYCN amplification, in neuroblastoma tumors. *Cancer Genet Cytogenet.* Jan 1 2009;188(1):32-41.

40. Genesca A, Pampalona J, Frias C, Dominguez D, Tusell L. Role of telomere dysfunction in genetic intratumor diversity. *Adv Cancer Res.* 2011;112:11-41.

41. Stewenius Y, Gorunova L, Jonson T, et al. Structural and numerical chromosome changes in colon cancer develop through telomere-mediated anaphase bridges, not through mitotic multipolarity. *Proc Natl Acad Sci U S A.* Apr 12 2005;102(15):5541-5546.

42. Pampalona J, Soler D, Genesca A, Tusell L. Whole chromosome loss is promoted by telomere dysfunction in primary cells. *Genes Chromosomes Cancer.* Apr 2010;49(4):368-378.

43. Pampalona J, Frias C, Genesca A, Tusell L. Progressive telomere dysfunction causes cytokinesis failure and leads to the accumulation of polyploid cells. *PLoS Genet.* Apr 2012;8(4):e1002679.

44. Heaphy CM, Subhawong AP, Gross AL, et al. Shorter telomeres in luminal B, HER-2 and triple-negative breast cancer subtypes. *Mod Pathol.* Feb 2011;24(2):194-200.

45. Hong SM, Heaphy CM, Shi C, et al. Telomeres are shortened in acinar-to-ductal metaplasia lesions associated with pancreatic intraepithelial neoplasia but not in isolated acinar-to-ductal metaplasias. *Mod Pathol.* Feb 2011;24(2):256-266.

46. Meeker AK. Telomeres and telomerase in prostatic intraepithelial neoplasia and prostate cancer biology. *Urol Oncol.* Mar-Apr 2006;24(2):122-130.

47. Silvestre DC, Pineda JR, Hoffschir F, et al. Alternative lengthening of telomeres in human glioma stem cells. *Stem Cells.* Mar 2011;29(3):440-451.

A

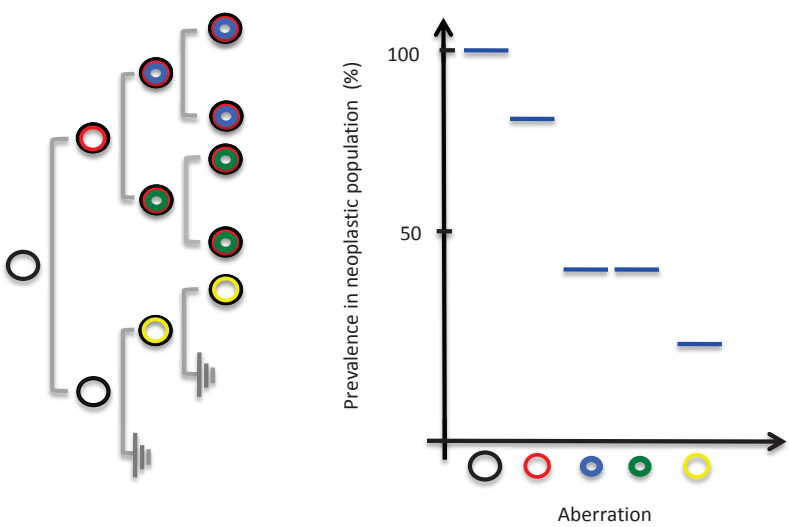
100
50
Prevalence in neoplastic population (%)
Aberration

B

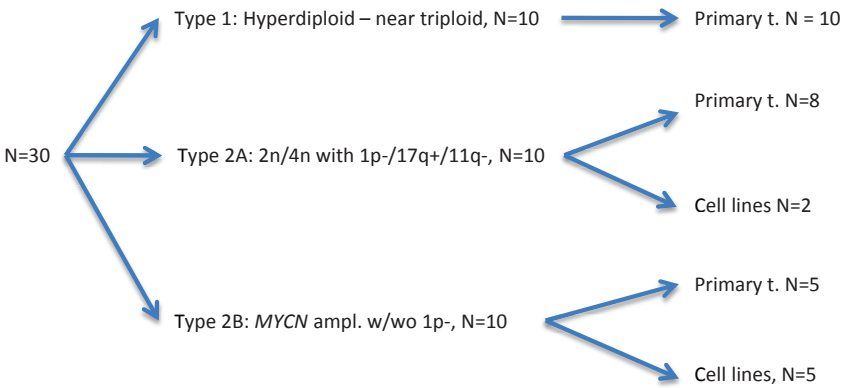
N=30
Type 1: Hyperdiploid – near triploid, N=10
Primary t. N = 10
Type 2A: 2n/4n with 1p-/17q+/11q-, N=10
Primary t. N=8
Cell lines N=2
Type 2B: *MYCN* ampl. w/wo 1p-, N=10
Primary t. N=5
Cell lines, N=5

Figure 1

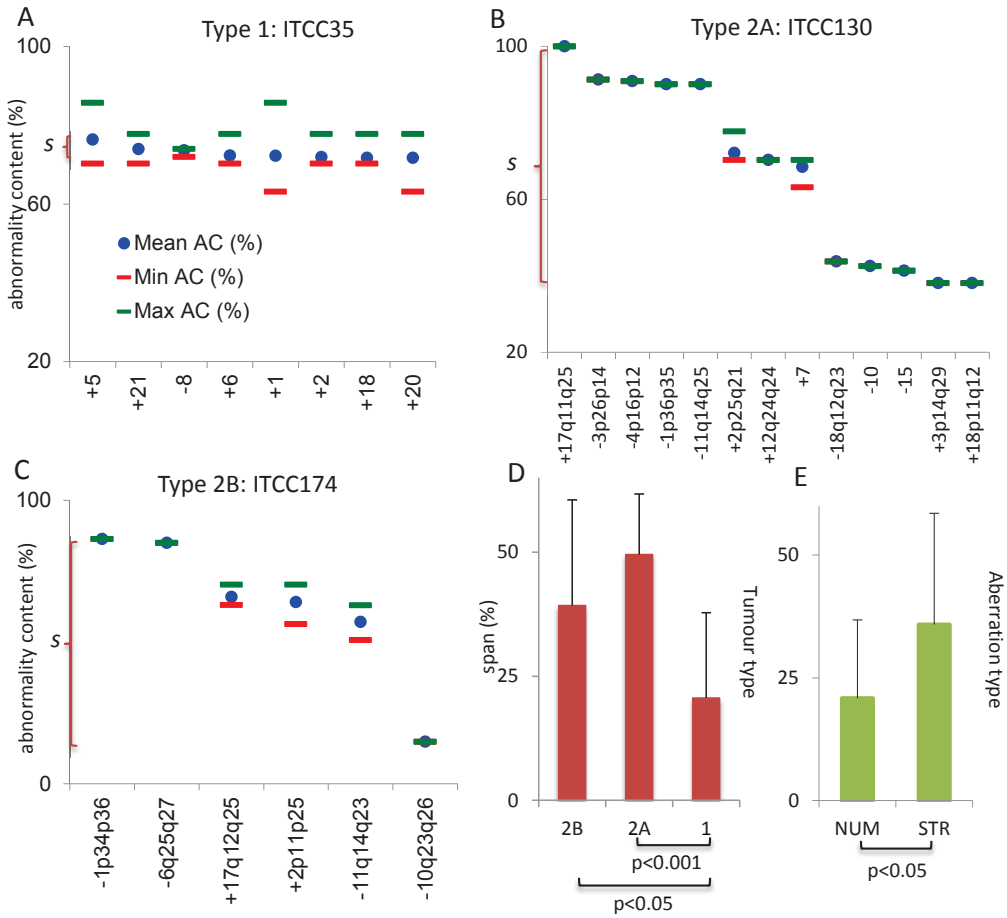
A
Type 1: ITCC35
100
s
60
20
abnormality content (%)
Mean AC (%)
Min AC (%)
Max AC (%)
+5
+21
-8
+6
+1
+2
+18
+20
B
Type 2A: ITCC130
100
s
60
20
+17q11q25
-3p26p14
-4p16p12
-1p36p35
-11q14q25
+2p25q21
+12q24q24
+7
-18q12q23
-10
-15
+3p14q29
+18p11q12
C
Type 2B: ITCC174
100
s
0
abnormality content (%)
-1p34p36
-6q25q27
+17q12q25
+2p11p25
-11q14q23
-10q23q26
D
50
25
0
span (%)
Tumour type
2B
2A
1
p<0.001
p<0.05
E
50
25
0
Aberration type
NUM
STR
p<0.05

Figure 2

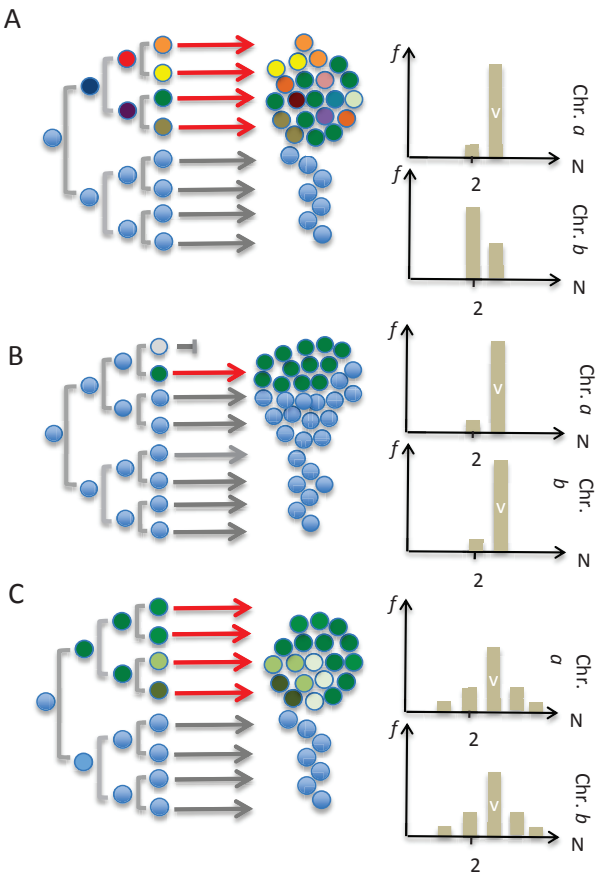

Figure 3

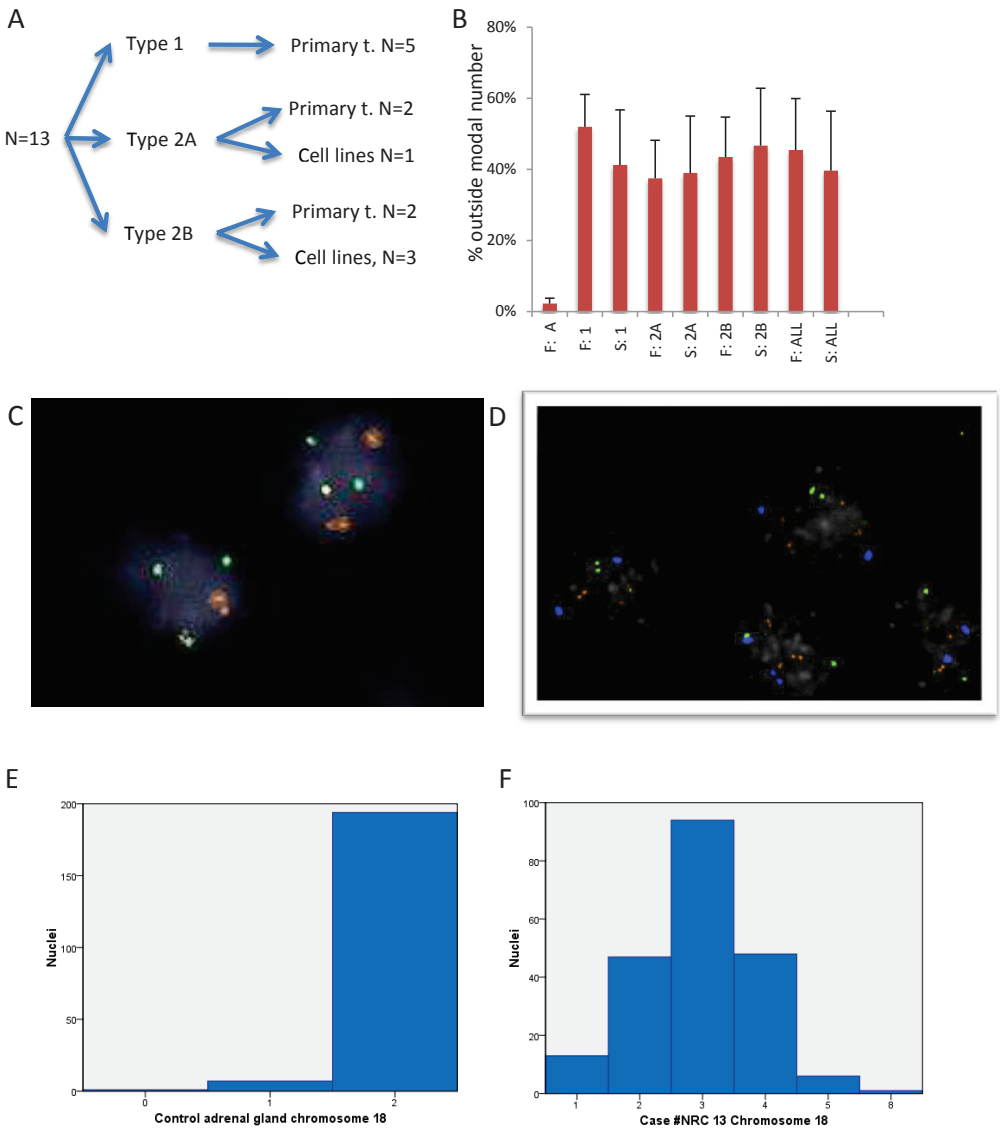
A
N=13
Type 1
Primary t. N=5
Type 2A
Primary t. N=2
Cell lines N=1
Type 2B
Primary t. N=2
Cell lines, N=3
B
% outside modal number
80%
60%
40%
20%
0%
F:: A
F: 1
S: 1
F: 2A
S: 2A
F: 2B
S: 2B
F: ALL
S: ALL
C
D
E
Nuclei
Control adrenal gland chromosome 18
F
Nuclei
Case #NRC 13 Chromosome 18

Figure 4

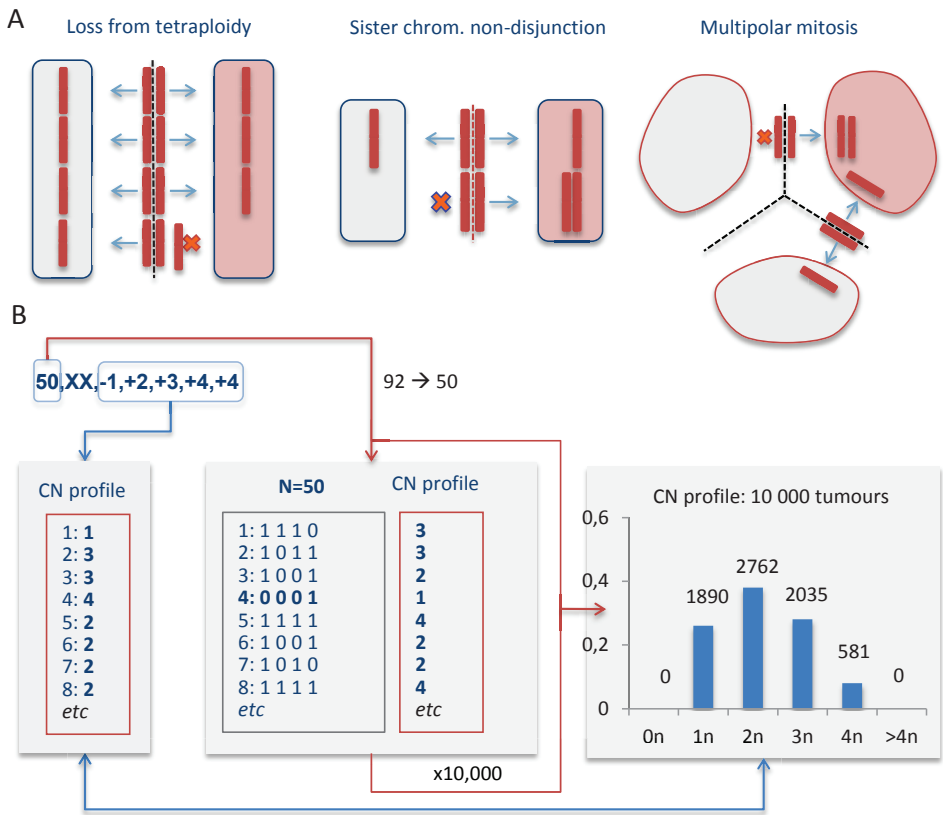
A
Loss from tetraploidy
Sister chrom. non-disjunction
Multipolar mitosis
B
50,XX,-1,+2,+3,+4,+4
92 → 50
CN profile
1: 1
2: 3
3: 3
4: 4
5: 2
6: 2
7: 2
8: 2
etc
N=50
CN profile
1: 1 1 1 0
2: 1 0 1 1
3: 1 0 0 1
4: 0 0 0 1
5: 1 1 1 1
6: 1 0 0 1
7: 1 0 1 0
8: 1 1 1 1
etc
3
3
2
1
4
2
2
4
etc
x10,000
CN profile: 10 000 tumours
0,6
0,4
0,2
0
0
1890
2762
2035
581
0
0n
1n
2n
3n
4n
>4n

Figure 5

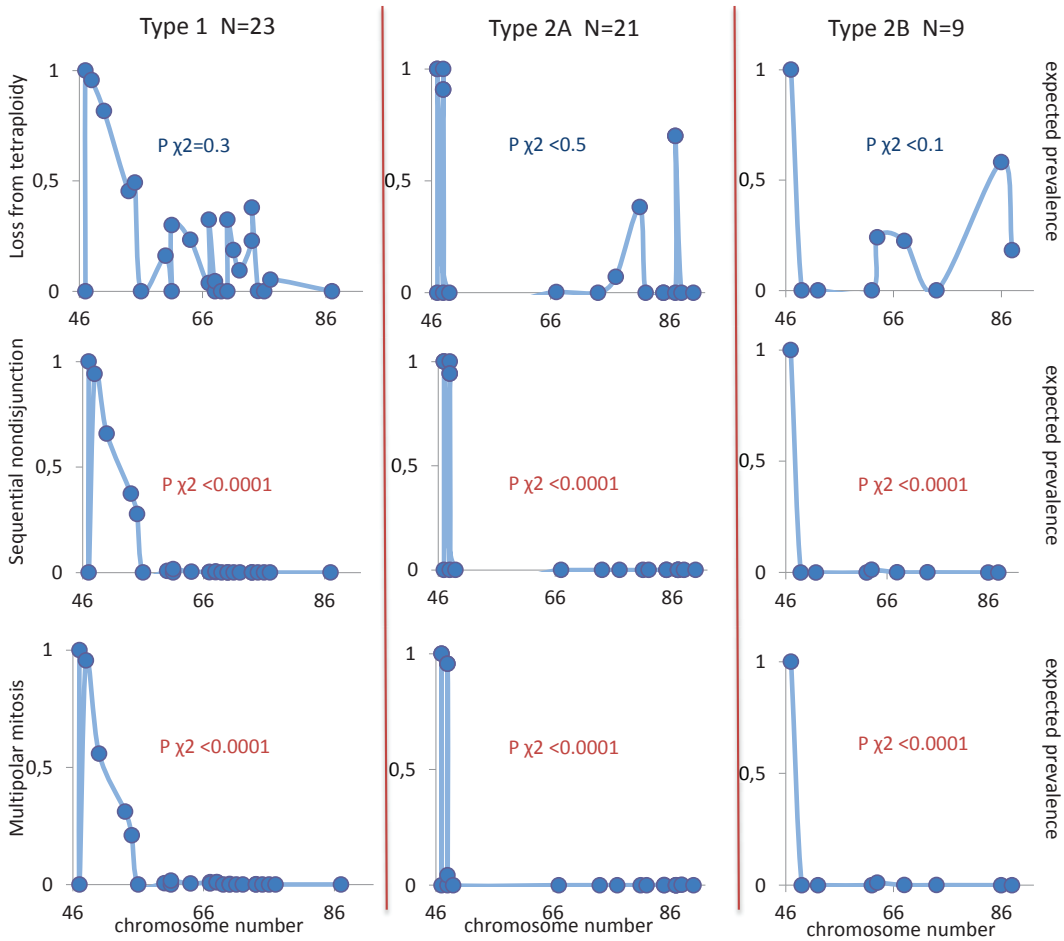
Type 1 N=23
Type 2A N=21
Type 2B N=9
Loss from tetraploidy
Sequential nondisjunction
Multipolar mitosis
expected prevalence
P χ2=0.3
P χ2 <0.5
P χ2 <0.1
P χ2 <0.0001
chromosome number
1
0,5
0
46
66
86

Figure 6

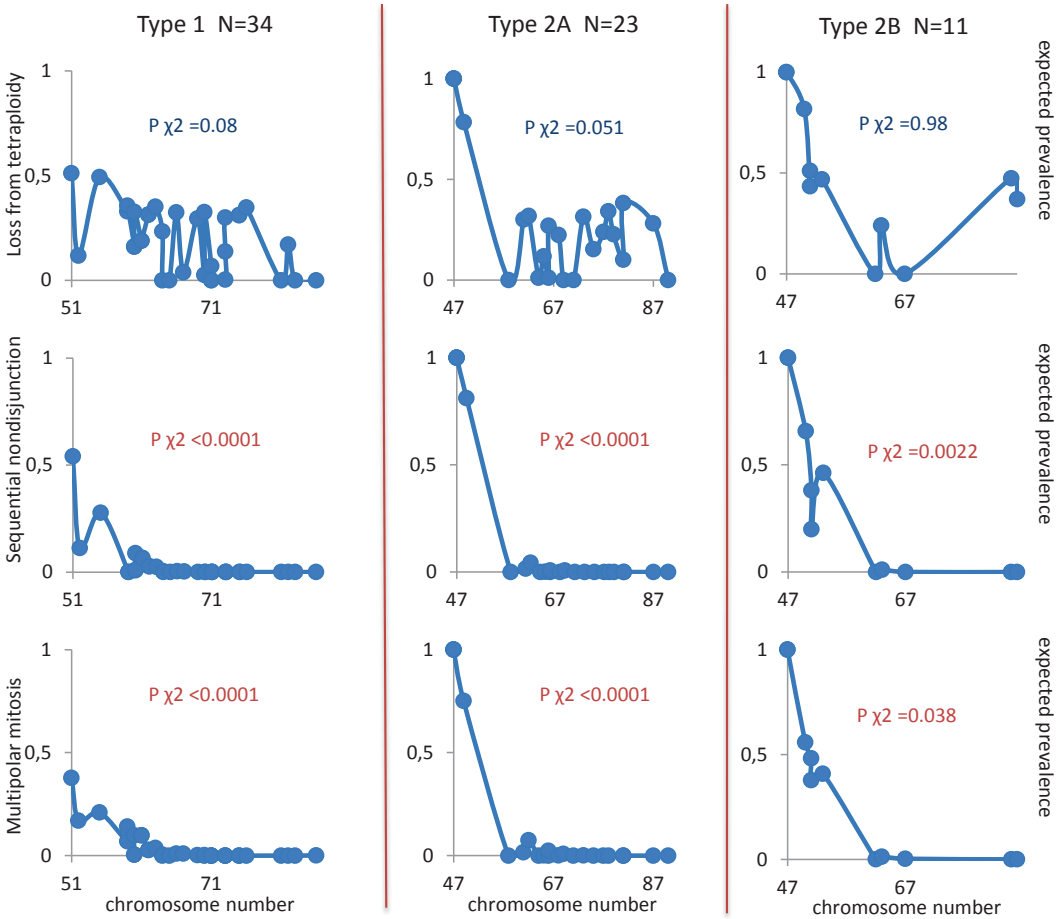
Type 1 N=34
Type 2A N=23
Type 2B N=11
Loss from tetraploidy
Sequential nondisjunction
Multipolar mitosis
P χ2 =0.08
P χ2 =0.051
P χ2 =0.98
P χ2 <0.0001
P χ2 <0.0001
P χ2 =0.0022
P χ2 <0.0001
P χ2 <0.0001
P χ2 =0.038
expected prevalence
chromosome number
1
0,5
0
51
71
47
67
87

Figure 7

A

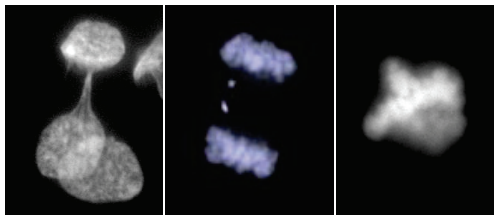

B

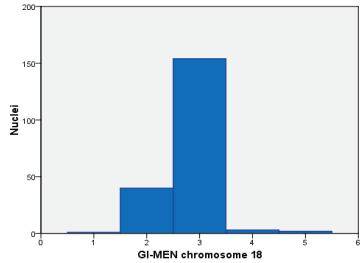
Nuclei
GI-MEN chromosome 18

C

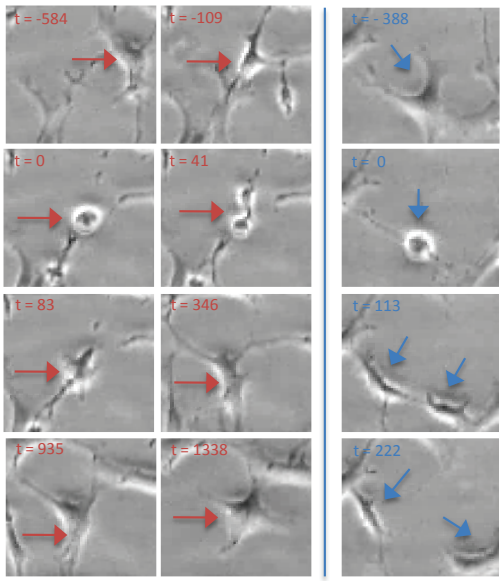
t = -584
t = -109
t = - 388
t = 0
t = 41
t = 0
t = 83
t = 346
t = 113
t = 935
t = 1338
t = 222

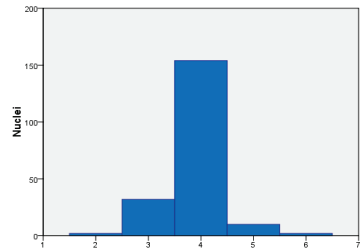
Nuclei
GI-MEN single cell clone A9 chromosome 18

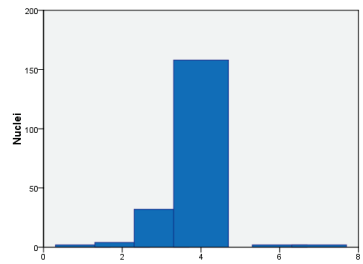
Nuclei
GI-MEN single cell clone D3 chromosome 18

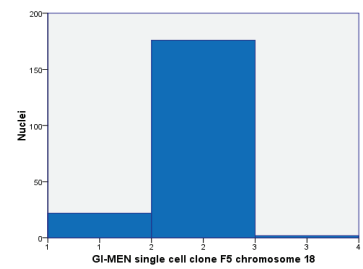
Nuclei
GI-MEN single cell clone F5 chromosome 18

Figure 8

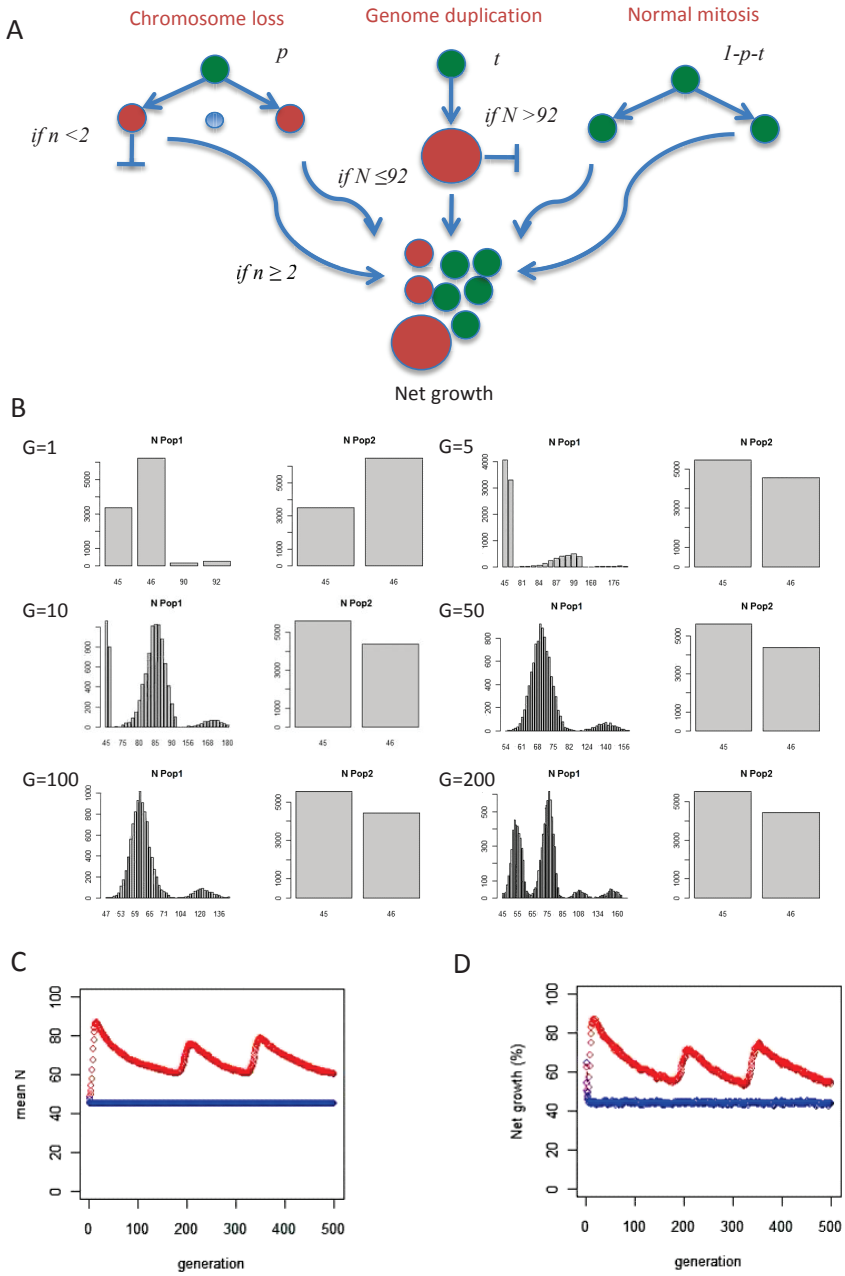
A
Chromosome loss
Genome duplication
Normal mitosis
p
t
1-p-t
if n <2
if N >92
if N ≤92
if n ≥ 2
Net growth
B
G=1
G=5
G=10
G=50
G=100
G=200
N Pop1
N Pop2
C
mean N
generation
D
Net growth (%)
generation

Figure 9

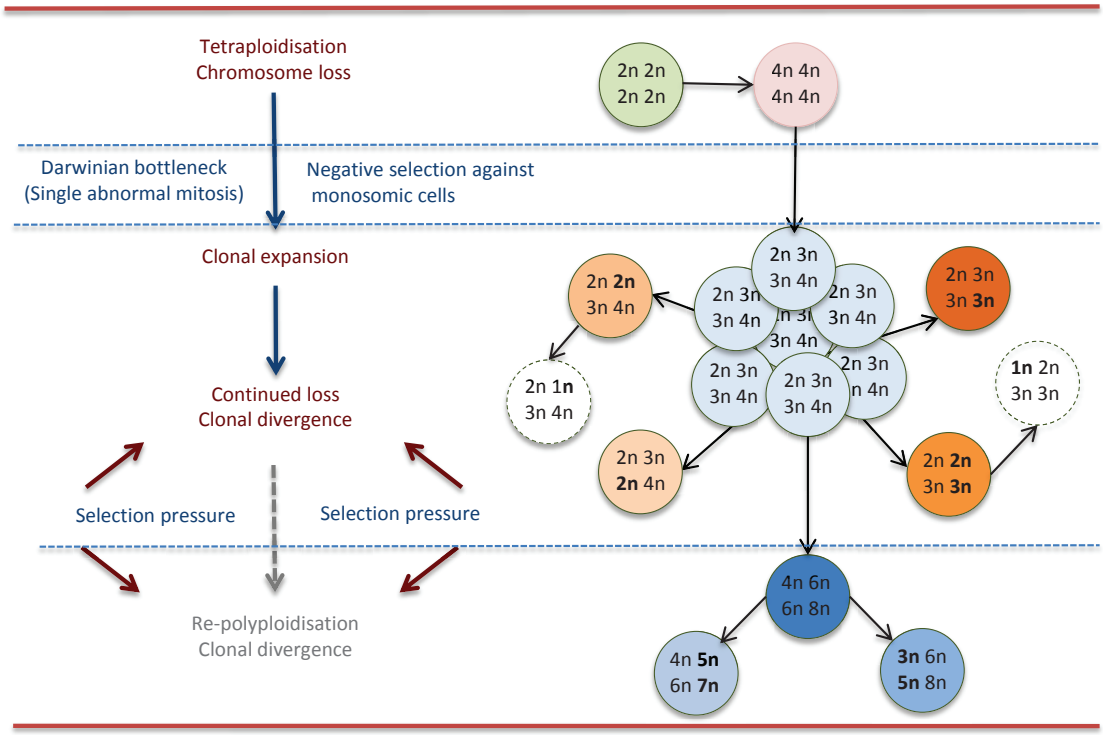
Tetraploidisation
Chromosome loss
Darwinian bottleneck
(Single abnormal mitosis)
Negative selection against
monosomic cells
Clonal expansion
Continued loss
Clonal divergence
Selection pressure
Selection pressure
Re-polyploidisation
Clonal divergence
2n 2n
2n 2n
4n 4n
4n 4n
2n 3n
3n 4n
2n **2n**
3n 4n
2n 3n
3n 4n
2n 3n
3n **3n**
2n 3n
3n 4n
2n 3n
3n 4n
2n 3n
3n 4n
2n 1**n**
3n 4n
1n 2n
3n 3n
2n 3n
2n 4n
2n **2n**
3n **3n**
4n 6n
6n 8n
4n **5n**
6n **7n**
3n 6n
5n 8n

Figure 10

Table 1. Clinical data and genome diversity assessed by spans of clone prevalence

Case[1]	Age (days)	Sex (M/F)[2]	Stage[3]	Time to relapse (days)	Follow-up time (days)	Out-come[4]	Location	Ploidy	Total no. of segments	Numerial changes	Structural changes	Prevalence span (%)
Type 1: Whole chromosome changes												
ITCC35	51	F	4S	-	4686	NED	abdomen	2n-3n	8	8	0	5
NRC1	340	M	3	-	1495	NED	paravertebral-abdominal	3n-5n	15	15	0	10
NRC10	107	M	1	-	5659	NED	adrenal gland	3n-4n	13	13	0	10
NRC3	194	F	2	-	2280	NED	paravertebral-thoracal	3n	7	7	0	13
ITCC44	0	F	2A	-	3195	NED	adrenal gland	2n-3n	12	11	2	15
ITCC111	80	F	4S	-	3897	NED	adrenal gland	2n-3n	11	11	0	16
NRC5	5	M	2B	66	2443	NED	paravertebral-thoracal	2n-3n	10	10	0	20
ITCC9	385	F	2A	160	5871	NED	paravertebral-thoracal	2n-3n	11	11	0	23
ITCC2	41	M	2A	-	4845	NED	paravertebral-thoracal	3n	12	10	2	30
ITCC38	183	M	4S	-	4945	NED	adrenal gland	2n-3n	14	12	2	65
Type 2A: Structural changes, no MYCN amplification												
SK-N-SH	-	-	-	-	-	-	-	2n	5	1	4	26
ITCC130	1339	M	4	515	515	DOD	paravertebral-thoracal	2n	11	0	11	42
ITCC10	281	M	4	-	6450	NED	adrenal gland	2n	6	0	6	45
NRC13	7	M	2	-	2475	NED	adrenal gland	4n	9	6	3	46
NRC14	1815	M	4	494	1573	NED	cervical	4n	9	0	9	48
ITCC36	1364	M	4	91	136	DOD	adrenal gland	2n	10	1	9	50
NRC7	2408	F	3	191	1779	DOD	abdomen	2n	14	10	4	50
ITCC29	304	M	1	676	2884	AWD	paravertebral-thoracal	2n	5	0	5	56
ITCC13	1009	F	4	450	480	DOD	adrenal gland	2n	13	2	10	62
SK-NA-S	-	-	-	-	-	-	-	2n	19	3	16	71

Table 1 – *continued*

Case1	Age (days)	Sex (M/F)[2]	Stage[3]	Time to relapse (days)	Follow-up time (days)	Out-come[4]	Location	Ploidy	Total no. of segments	Numerical changes	Structural changes	Prevalence span (%)
Type 2B: MYCN amplification												
NRC8	721	F	4	-	11	DOC	abdomen	4n	6	4	2	7
NRC4	441	M	4	1182	2389	NED	adrenal gland	2n	4	0	4	19
IMR32	-	-	-	-	-	-	-	2n	10	1	9	23
SKNBE	-	-	-	-	-	-	-	4n	26	6	20	29
NRC11	697	F	4	340	1360	DOD	adrenal gland	2n	4	0	4	35
ITCC31	531	M	4	599	853	DOD	adrenal gland	2n	6	2	4	38
LAN1	-	-	-	-	-	-	-	4n	25	7	18	46
GI-M-EN	-	-	-	-	-	-	-	4n	22	4	18	61
SK-N-FI	-	-	-	-	-	-	-	2n	17	1	16	64
ITCC174	818	M	4	329	400	DOD	adrenal gland	2n	6	0	6	72

[1]NRC, collected from Lund University Hospital, Sweden; ITCC, collected from Academic Medical Center, Amsterdam, the Netherlands. [2]F, female; M, male. 3 [3]According to the International Neuroblastoma Staging System. [4]Status at latest follow-up annotated as: NED, no evidence of disease; DOD, dead of disease; DOC, dead of complications; AWD, alive with disease.

Table 2. Fluorescence in situ hybridization data from primary tumours and cell lines[1]

Genetic type		CEP 1	CEP 2	CEP 4	CEP 7	CEP 11	CEP 12	CEP 16	CEP 17	CEP 18	1p	11q	17q
	Adrenal gland												
	n=	2	2	2	2	2	2	2	2	2	2	2	2
	non-modal (%)	3	1	0.5	3	0	0	2	2	3	0	0	0
	aneusomy (%)	3	1	0.5	3	0	0	2	2	3	0	0	0
1	**NRC 1**												
	n=	4	5			4	4	3		3			
	non-modal (%)	59	56			47	66	49		47			
	aneusomy (%)	97	93			96	97	73		93			
1	**NRC 2**												
	n=	3	3	2	3	3	3			2			
	non-modal (%)	49	44	38	24	45	51			51			
	aneusomy (%)	58	67	38	82	71	56			49			
1	**NRC 3**												
	n=	3					3		2				
	non-modal (%)	55					57		64				
	aneusomy (%)	75					79		64				
1	**NRC 5**												
	n=	3	3				3						
	non-modal (%)	48	63				38						
	aneusomy (%)	79	88				76						
2A	**NRC 7**												
	n=	3					3		3			1	
	non-modal (%)	39					36		31			13	
	aneusomy (%)	82					77		70			90	
2A	**NRC 13**												
	n=									3			5
	non-modal (%)									55			72
	aneusomy (%)									78			94
2A	**SK-N-AS**												
	n=				2	2			1	2	2	1	4
	non-modal (%)				34	14			26	32	16	18	73
	aneusomy (%)				34	14			76	32	16	82	93

Table 2 - *continued*

Genetic type		CEP 1	CEP 2	CEP 4	CEP 7	CEP 11	CEP 12	CEP 16	CEP 17	CEP 18	1p	11q	17q
2A	SK-N-SH												
	n=				3	2			2	2	2		4
	non-modal (%)				27	10			10	25	8		4
	aneusomy (%)				88	10			10	25	8		79
2B	NRC 4												
	n=	2					2			2	1		3
	non-modal (%)	3					4			11	6		50
	aneusomy (%)	3					4			11	94		94
2B	NRC 8												
	n=					4		3					5
	non-modal (%)					66		57					75
	aneusomy (%)					96		57					84
2B	IMR32												
	n=				2	2	3		3	2	2		4
	non-modal (%)				20	36	28		33	4	32		48
	aneusomy (%)				20	36	80		72	4	32		80
2B	GI-M-EN												
	n=					2			2	3	2		2
	non-modal (%)					51			36	23	8		48
	aneusomy (%)					51			36	80	8		48
2B	SK-N-FI												
	n=				2	2				2	2		3
	non-modal (%)				4	15				18	9		58
	aneusomy (%)				4	15				18	9		58

[1] Columns correspond to results for centromere probes (CEP) and probes for chromosome segments 1p, 11q, and 17q. The first row under each specimen denotes the modal number of each particular chromosome or segment, second row is the percentage of nuclei not having the modal copy number and the final row the percentage of nuclei having aneusomi (e.g. non-disomy). Results above the mean aneusomy for all probes in normal adrenal tissue +3 standard deviations (6.5%) are denoted in red, corresponding to a significant prevalence of cells with non-modal chromosome number. [2] SNP array data not available due to difficulties in interpretation of modal values.

Table 3. Mitotic segregation errors

	AB	Lagging	Multipolar
GI-ME-N	7	17	3
SK-N-AS	1	8	0
IMR 32	3	7	0
SK-N-SH	0	2	0
SK-N-FI	12	4	3

[1] Showing the different mitotic errors in percentage of anaphase/ telophase figures for anaphase/ telophase bridges (AB/TB) and lagging, and of all mitotic figures for multipolar mitoses.

Table 4. Single cell clones[1]

	CEP 11	CEP 17	CEP 18
Fibroblasts			
n=	2	2	2
non-modal (%)	0.5	0	0
GI-MEN F5			
n=	5	2	2
non-modal (%)	8	5	12
GI-MEN A9			
n=	6	2	4
non-modal (%)	30	9	23
GI-MEN D3			
n=	5	2	4
non-modal (%)	5	12	21
SK-N-AS C8			
n=	2	1	2
non-modal (%)	11	6	13
SK-N-AS E7			
n=	2	1	2
non-modal (%)	5	6	8
SK-N-AS C5			
n=	2	1	2
non-modal (%)	5	6	8

[1] The first row shows the modal number and the second the percentage of nuclei having a different copy number than that of the modal number. Results above the mean non-modal fraction for all probes in fibroblasts +3 standard deviations (0.77%) are denoted in red, corresponding to a significant prevalence of cells with non-modal chromosome number.

Table 5. Single cell clones from cell lines and fibroblasts[1]

Chromosome examined	GI-MEN vs. single cell	SK-N-AS vs. single cell	Single cells NB vs. fibroblasts
CEP 11	0,7569	0,0192	<0,0001
CEP 17	<0,0001	<0,0001	<0,0001
CEP 18	<0,0002	0,0528	<0,0001
1p	0,0551	<0,0001	
17q	0,0266	<0,0001	

[1] P-values were obtained by Fisher´s exact test, comparing relative numbers of nuclei with non-modal copy numbers of the original cultures to that of the single clones, and comparing the fibroblasts to NB single cell clones (GI-M-EN and SK-N-AS).